HARMONIC VIBRATION ANALYSIS OF LARGE STRUCTURES WITH LOCAL NONLINEARITY

A THESIS SUBMITTED TO
THE GRADUATE SCHOOL OF NATURAL AND APPLIED SCIENCES
OF
MIDDLE EAST TECHNICAL UNIVERSITY

BY

DİREN ABAT

IN PARTIAL FULFILLMENT OF THE REQUIREMENTS
FOR
THE DEGREE OF MASTER OF SCIENCE
IN
MECHANICAL ENGINEERING

FEBRUARY 2009

Approval of the thesis:

HARMONIC VIBRATION ANALYSIS OF LARGE STRUCTURES WITH LOCAL NONLINEARITY

submitted by **DİREN ABAT** in partial fulfillment of requirements for the degree of **Master of Science in Mechanical Engineering Department**, **Middle East Technical University** by,

Prof. Dr. Canan Özgen _____
Dean, Graduate School of **Natural and Applied Sciences**

Prof. Dr. Süha Oral _____
Head of Department, **Mechanical Engineering**

Prof. Dr. H. Nevzat Özgüven _____
Supervisor, **Mechanical Engineering Dept., METU**

Examining Committee Members

Prof. Dr. Kemal Özgören _____
Mechanical Engineering Dept., METU

Prof. Dr. H. Nevzat Özgüven _____
Mechanical Engineering Dept., METU

Prof. Dr. Mehmet Çalışkan _____
Mechanical Engineering Dept., METU

Assist. Prof. Dr. Güçlü Seber _____
Aerospace Engineering Dept., METU

Dr. Ender Ciğeroğlu _____
Mechanical Engineering Dept., METU

Date: 20/02/2009

I hereby declare that all information in this document has been obtained and presented in accordance with academic rules and ethical conduct. I also declare that, as required by these rules and conduct, I have fully cited and referenced all material and results that are not original to this work.

Name, Last name : Diren ABAT

Signature :

ABSTRACT

HARMONIC VIBRATION ANALYSIS OF LARGE STRUCTURES
WITH LOCAL NONLINEARITY

ABAT, Diren
M.S. Department of Mechanical Engineering
Supervisor: Prof. Dr. H. Nevzat ÖZGÜVEN

February 2009, 158 pages

With the rapid development in today's technology, reliability and performance requirements on components of various mechanical systems, which tend to be much lighter and work under much more severe working conditions, dramatically increased. In general, analysis techniques based on simplified model of structural components with linearity assumption may provide time saving for solutions with reasonable accuracy. However, since most engineering structures are often very complex and intrinsically nonlinear, in some cases they may behave in a different manner which cannot be fully described by linear mathematical models, or linear treatments may not be applicable at all. In fact, some studies revealed that deviations in the modal properties of dynamic structures gathered from measured data are due to nonlinearities in the structure. Hence, in problems where accuracy is the primary concern, taking the nonlinear effects into account becomes inevitable.

In this thesis, it is aimed to analyze the harmonic response characteristics of multi degree of freedom nonlinear structures having different type of nonlinearities. The amplitude dependencies of nonlinearities are modelled by using describing function method. To increase the accuracy of the results, effect of the higher order harmonic

terms will be considered by using multi harmonic describing function theory. Mathematical formulations are embedded in a computer program developed in MATLAB® with graphical user interface. The program gets the system matricies from the file which is obtained by using substructuring analysis in ANSYS®, and nonlinearities in the system can easily be defined through the graphical user interface of the MATLAB® program.

Keywords: Structural Nonlinearity, MDOF Nonlinear Systems, Multi Harmonic Analysis, Describing Function, Local Nonlinearity, Nonlinear Dynamics, MDOF Systems.

ÖZ

BÖLGESEL YAPISAL DOĞRUSALSIZLIK İÇEREN BÜYÜK SİSTEMLERİN HARMONİK TİTREŞİM ANALİZİ

ABAT, Diren
Yüksek Lisans, Makina Mühendisliği Bölümü
Tez Yöneticisi: Pr. Dr. H.Nevzat Özgüven

Şubat 2009, 158 Sayfa

Günümüz teknolojisinin gelişimi ile beraber daha hafif olma ve daha ağır çevre koşulları altında çalışma eğiliminde olan çeşitli mekanik sistem bileşenlerinin güvenilirlik ve performans gereksinimleri önemli bir artış göstermiştir. Genel olarak, mekanik yapıların basit modelleri üzerinde doğrusallık varsayımı temel alınarak yapılan analiz yöntemleri makul doğruluklar ile kısa zamanda sonuç verebilmektedir. Fakat tasarlanan çoğu yapı, kompleks olmaları ve gerçekte doğrusal olmamalarından dolayı bir çok durumda doğrusal matematiksel modeller ile tam olarak tanımlanamamakta ya da doğrusallık tanımlamaları hiçbir durumda kullanılamamaktadır. Yapılan çalışmalar, gerçekleştirilen ölçümler ile elde edilen modal parametrelerdeki sapmaların gerçekten de doğrusalsızlıktan kaynaklandığını ortaya çıkarmıştır. Bu nedenle hassasiyetin önem kazandığı problemlerde doğrusal olmayan etkileri hesaba katmak kaçınılmaz olmaktadır.

Bu çalışmada, çok serbestlik dereceli, değişik doğrusalsızlıklar içeren sistemlerin harmonik tepki özellikleri incelenmiştir. Doğrusalsızlıkların genlik bağımlılıkları tanımlayan işlev metodu kullanarak modellenmiştir. Sonuçların hassasiyetini

arttırmak için çok harmonikli tanımlayan işlev teorisi kullanılarak yüksek harmonik etkileri de hesaba katılmıştır. Kullanılan matematiksel denklemler ile MATLAB® platformunda kullanıcı arayüze sahip bir program geliştirilmiştir. Program, sistem matrislerini ANSYS® tarafından oluşturulan dosyadan alabilmekte ve değişik tipte doğrusalsızlıklar kullanıcı arayüzü ile kolayca tanımlanabilmektedir.

Keywords: Yapısal Doğrusalsızlık, Çok Serbestlik Dereceli Doğrusal Olmayan Sistemler, Çok Harmonikli Analiz, Tanımlayan İşlev, Lokal Doğrusalsızlık, Doğrusalsızlık Dinamiği, Çok Serbestlik Dereceli Sistemler.

To:

Diler for her love and continues encouragement …

My family; Nevzat, Güler and Benek for everything else ...

ACKNOWLEDGMENT

I would like to thank my supervisor Prof. Dr. H. Nevzat ÖZGÜVEN for his help and guidance throughout the study.

I am thankful to my company ASELSAN Inc., to my colleagues and especially to Şahap SAKA for letting and supporting of my thesis.

I am grateful to Umut BATU for sharing his comprehensive knowledge and sparing his valuable time.

I want to thank my family Nevzat, Güler and Benek for their continuous encouragement.

I am especially thankful to Diler, for her love, support, patience and encouragement to complete this study.

TABLE OF CONTENTS

NOMENCLATURE

$[C]$	Viscous damping matrix
$\{f\}$	Vector of external forcing
$\{F\}$	Complex amplitude vector of external forcing
F_f	Coefficient of friction damping element
F_p	Preload of the spring element
$[H]$	Structural (hysteretic) damping matrix
i	Unit imaginary number
$[K]$	Stiffness matrix
$[M]$	Mass matrix
n	Degree of freedom
Q	Set of harmonics
$\{s\}$	Internal nonlinear forces vector
$\boldsymbol{S}$	Complex harmonic nonlinear function
x	Displacement vector
$\dot{x}$	Velocity vector
$\ddot{x}$	Acceleration vector
$\{X\}$	Complex amplitude vector of displacements
t	Time
v	Describing function
y_{ab}	Intercoordinate displacement between coordinates a and b

$[\alpha]$	Receptance matrix
β	Coefficient of cubic stifness element
Δ	Nonlinearity matrix
ζ	Phase of harmonic nonlinear function
ϕ_j	Phase of harmonic displacement response
ϕ_{ab}	Phase of intercoordinate harmonic displacement response
ψ	ωt
ω	Frequency of excitation

Subscripts

a, b	General coordinate
ab	Intercoordinate
l	Harmonic order of the internal nonlinear force
m	Harmonic order of the response
p	Number of harmonics in the approximated response
r	Number of harmonics in the approximated nonlinear force

Acronyms

DFM	Describing Function Method
DOF	Degree of Freedom
FEM	Finite Element Method
FD	Frequency Domain
FRF	Frequency Response Function

GUI	Graphical User Interface
HBM	Harmonic Balance Method
MDOF	Multi Degree of Freedom
MHDF	Multi Harmonic Describing Function
MH-NLS	Multi Harmonic Nonlinear Solver
NC	Necessary Coordinates
ODE	Ordinary Differential Equation
PRM	Pseudoreceptance Matrix
TD	Time Domanin
VS	Volterra Series

LIST OF TABLES

TABLES

LIST OF FIGURES

FIGURES

CHAPTER 1

INTRODUCTION

1.1 Introduction

With the rapid development in today's technology, reliability and performance requirements, on components of various mechanical systems which tend to be much lighter and work under much more severe working conditions, are dramatically increased [1]. To meet these requirements, dynamic analysis should be carried out at the design stage which will require constructing an analytical model that can describe the dynamic characteristic of the structure. In general, analysis techniques on a simplified models of structural components with linearity assumption may provide time saving for solutions with reasonable accuracy. However, since most engineering structures are often very complex and intrinsically nonlinear [2], in some cases they may behave in a different manner which cannot be fully described by linear mathematical models, or linear treatments may not be applicable at all. In fact, some studies revealed that deviations in the modal properties of dynamic structures gathered from measured data, are due to nonlinearities in the structure [3]. Hence, in problems where accuracy is the primary concern, taking the nonlinear effects into account becomes inevitable.

Dynamic analysis of structures is based on representing the dynamic properties of a structure through some modelling techniques. Models can be Spatial Models, Modal Models and Response Models. Finite Element Method (FEM) is one of the most frequently used Spatial Modelling technique, which is based on constructing the mathematical model in terms of mass, stiffness and damping matrices and then solving the differential equation of the motion to find the dynamic response of the

structure (Figure 1.1). Another modelling technique which is used to create Modal Model, is based on extracting the dynamic properties of the system from experimentally obtained Frequency Response Function (FRF), by subsequent analysis on that measurements regarding natural frequencies, damping ratios and mode shapes [4]. Response Model, intends to define mathematical model by measuring the response of the structure to a prescribed forcing. All three types of models are based on well defined linear theory, and they are frequently used.

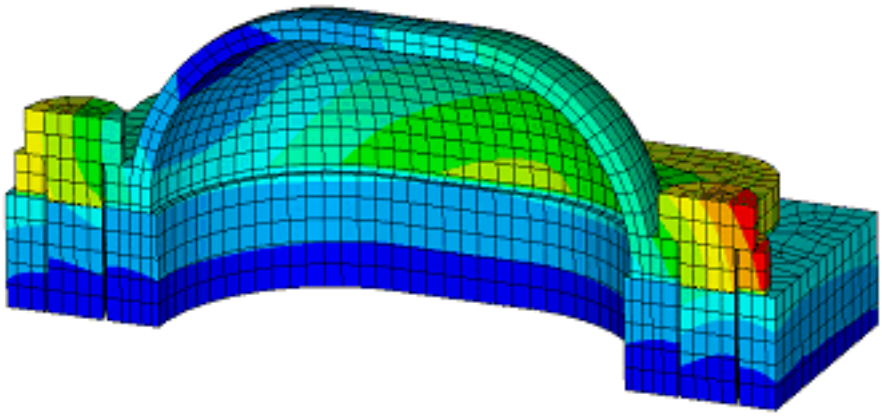

Figure 1.1 Most popular spatial modelling technique, a finite element model

If a structure is constructed with linear mathematical modelling techniques, then, principle of superposition is applicable for the dynamic analysis of that structure. As a conventional rule, superposition principle states that a linear system which responds as $x_1(t)$ to an input $f_1(t)$, and responds as $x_2(t)$ to an input $f_2(t)$, will response to $\xi f_1(t)+\lambda f_2(t)$ (where ξ, λ are constants) as $\xi x_1(t)+ \lambda x_2(t)$ for all $f_1(t)$ and $f_2(t)$ and ξ and λ. Moreover, linearity assumption presumes that, if the excitation is sinusoidal, the response of the structure is purely sinusoidal which means no energy can transfer between different frequencies. From structural dynamics point of view, linearity assumption also claims that global behavior of a system can be predicted from local behavior. If a structure fails to obey superposition behavior, show amplitude or

frequency dependent response characteristics and isolated solutions exist; it is implied that the structure is nonlinear.

There are many sources of nonlinearity in most practical mechanical structures, which can be classified as geometrical, physical, structural or design nonlinearities and constraints [5]. These nonlinearities can exist locally or globally. Global nonlinearity is mainly caused by large amplitude of vibration and/or nonlinear material properties of components such as shock absorbers, vibration isolators, bearings, etc. which have amplitude dependent response characteristics. On the other hand, local nonlinearities can be found in the form of complex stiffness, friction characteristics and looseness in joints (physical nonlinearity); clearance or backlash (structural or design nonlinearity); and nonlinear damping (physical nonlinearity) which are inherently found in structural assemblies formed by many components [6]. As stated before, nonlinear behaviors of structures can not be fully described by linear theory, therefore to obtain accurate results, nonlinear modelling, analysis and solution techniques should be applied.

Basically, there are two main approaches to analyze non-linear structures; time-domain (TD) and frequency domain (FD) techniques. TD analysis is based on successive integration of the equation of motion of a system, which is described as a function of time, to find the steady state response to a well defined excitation [7-8]. Although they yield accurate results, long transients of lightly damped structures, necessity of using small time steps for stiff structures combined with large systems makes the computational effort the primary concern when numerical integration is utilized during the solution. This makes TD analysis a cumbersome task for cases where many design iteration and optimization procedures should be applied. Because of such limitations and drawbacks of TD analysis, alternative and efficient counterpart, approximate FD analysis are developed based on the assumption of steady-state condition which is plausible for many engineering applications. These analyses are mainly concentrated on investigating the response of a system to periodic exitations and discarding the transient response during solution procedure.

1.1.1 Frequency Domain Analysis

With the development of a computational tool, Fast Fourier Transformation, and its utilisation in measuring and data collection devices such as frequency response analysers and data acquisition systems, frequency domain analysis became a primary choice especially in steady state harmonic response analysis. Since all the incidents happening in one load-cycle are represented by average quantities, the solution is generally regarded as "approximate" [9].

Since harmonic forcing is still widely used in vibration simulation and testing, the response of a system to a harmonic forcing is worth investigating. The response of a simple linear system to harmonic forcing reveals several important dynamic parameters that describes the system, namely natural frequencies, damping, phase-lag characteristics, etc. The transfer function concept is used to define FRF of a linear system, which is determined by making several FRF measurements at different frequencies to identify the aforementioned dynamical properties.

The block diagram of a linear system operating at frequency ω, shown in Figure 1.2, implies that, the response of the system under consideration has only frequency dependency and at any frequency, the frequency response function H(ω) (transfer function) of the sytem can be determined by the following equation:

$$H(\omega) = \frac{X(\omega)}{F(\omega)} \tag{1.1}$$

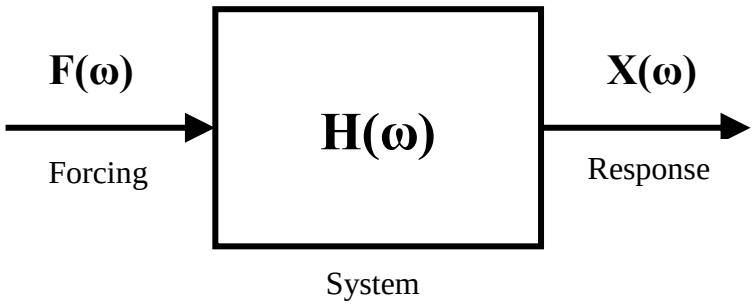

Figure 1.2 Schematic block diagram representation of a linear system operating at frequency ω

However, in nonlinear systems the response characteristics do not only depent on the frequency, but also depend on the amplitude of the response. Response amplitude dependency, makes nonlinear response analysis and system identification procedures a cumbersome task. A similar block diagram representation for such amplitude dependent harmonic response analysis is represented in Figure 1.3.

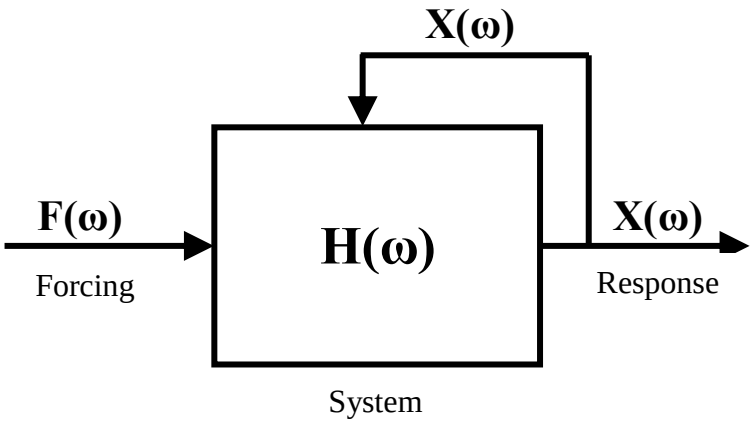

Figure 1.3 Schematic representation of an amplitude dependent nonlinear system operating at frequency ω

The response of a broad type of nonlinear system to a harmonic excitation remains basically harmonic, despite the fact that there is a leakage of energy to frequencies at certain multiples of the excitation frequency. This is the characteristics of nearly all nonlinear systems and response at these higher frequencies is called “higher order harmonic” response.

1.2 Literature Survey

Studies on the vibration analysis of nonlinear structures are divided into two main groups. One of the objective in these studies is to find the harmonic responses of the systems having different kind of nonlinearities which are well defined, quantified and modelled locally or globally. The other group of studies, which generally use the theoretical background on foregoing studies, concentrated on to detect, characterize, localize and quantify the nonlinearities in the systems analysed.

As mentioned before, the former and commonly used nonlinear response analysis method is the numerical integration of the equation of the motion [7-8, 10-12]. In spite of the fact that this method gives very accurate results, long transients because of low damping levels, small time steps for accuracy requirements and large numbers of degrees-of-freedom result in a very costly computational procedure for steady-state response analysis [13].

As an alternative procedure to aforementioned method, to elude its drawbacks, interests have been focused on alternative, approximate frequency-domain methods for determining the steady-state response of structures, particularly to periodic external excitation. The starting point in these methods is to convert the nonlinear ordinary differential equations (ODE) of motion, obtained through some discretization techniques such as Rayleigh-Ritz, Galerkin, assumed modes method, finite element method, etc, into nonlinear algebraic equations by using such tecniques as harmonic balance, describing functions, perturbation method, etc. Finally these equations will be solved simultanously and iteratively.

Describing Function Method (DFM) is commonly used in many branches of engineering, namely, mechanical, electronical, and so on. The main idea underlying in DFM is modeling and studying nonlinear system behavior by replacing each nonlinear element with a (quasi)linear descriptor or describing function whose gain is a function of input amplitude [14]. In other words, DFM aims to find the relation between the response in fundamental harmonics and the excitation, by calculating the average restoring force occurring in one cycle. The theoretical basis of this method is related to the work, method of slowly-varying coeffcients, done by Van der Pol [15]. Bogoliubov and Mitropolsky [16] used a similar approach called method of equivalent linearization.

Watanabe and Sato [17] used first order describing function to linearize the efects of nonlinear stifness in a beam and used their results to develop “nonlinear building block approach” , for coupling nonlinear structures having local nonlinearity.

Budak and Özgüven [18] suggested a new method called “Iterative Receptance Method” for systems where nonlinear spring and damping forces can be expressed as polynomials. They calculated the quasilinear receptance matrix of a nonlinear system which is called “pseudo receptance matrix” (PRM) and thus analyzed harmonic response of structures with symmetrical nonlinearities.

Tanrıkulu, et al. [19] suggested a new approach to obtain fundamental harmonic response analysis of multi degree of freedom (MDOF) systems. They used describing function approach and analyzed three type nonlinearities, which are cubic stiffness, coulomb damping and piecewise linear stiffness.

Later, Kuran and Özgüven [20] developed a modal analysis approach for MDOF nonlinear structures. They extended their work to calculate the higher harmonic terms in the system responses.

In a later work, Cigeroglu and Özgüven [21] used the frequency domain method developed in an earlier study [19] for forced harmonic response analysis of bladed

disks with dry friction dampers. They suggested a nonlinear model for a bladed disk assembly which includes all the blades with blade to blade and/or blade to cover plate dry friction dampers. Single harmonic describing function appraoch was used to analayze the nonlinear MDOF model of a bladed disk system.

Čermelj, Boltežar [22] presented an approximate, FD approach to modelling complex structures with localised nonlinearities for FRF coupling in the frequency domain. They sub-structured these complex structures into its linear and nonlinear parts in the first stage and used harmonic-balance and describing-function-based approximation for the nonlinear part, introducing the multi-coordinate describing function and the multi-coordinate describing-function matrix to form harmonic nonlinear super-model.

Siller and Imregun [23] used the method in [19] and presented an explicit formulation for the frequency response functions for nonlinear MDOF systems. The nonlinear formulation in this work was based on first-order describing functions and focused on cubic stiffness and friction damping nonlinearities. Their technique produces FRFs at selected coordinates only, regardless of the system's size or the type of nonlinearity.

Ferreira and Serpa [24] presented a study on the description and the application of the arc-length method to solve a system of nonlinear equations obtaining as a result the nonlinear frequency response. They considered the fundamental harmonic component by using the describing function approach and investigated the cubic stiffness and gap nonlinearities to illustrate the methodology.

Maliha, et al. [25] obtained a nonlinear multi degree of freedom dynamic model for a spur gear pair on flexible shafts with flexible bearings and they used that model to employ the method developed in previous study [19] for multi harmonic vibration analysis of nonlinear systems with large number of degrees of freedom. The nonlinear elasticity term resulting from backlash is expressed by the describing function theory.

Özer, et al. [26] introduced a new method for type and parametric identification of a nonlinear element in an otherwise linear structure. They used the describing function approach which contains only the first harmonic terms, for representing the nonlinearity in the structure.

Ferreira [13] developed a nonlinear coupling approach to extend the scope of structural dynamic coupling procedures to nonlinear structures. A multi-harmonic analysis was introduced and the describing function methodology was extended to multi harmonic describing function (MHDF) approach to describe the so-called multi harmonic nonlinear receptance coupling approach. The suggested approach couples linear and nonlinear structures with different types of joints by specifying the describing functions for all the nonlinear joints.

Nuij, et al. [27] suggested an extension to higher-order describing functions by introducing the concept of the harmonics generator. The resulting higher-order sinusoidal input describing functions relate the magnitude and phase of the higher harmonics of the periodic response of the system to the magnitude and phase of a sinusoidal excitation.

Aydogan [28] presented a method to identify and to determine the location of cracks in structural parts. The method presented was based on single harmonic describing functions, and capable of detecting and locating the crack even if only the fundamental harmonic is used.

Majed and Raynaud [29] proposed two nonlinear formulations in order to study a structural behaviour that includes the effect of some localized nonlinearities. The former formulation is based on the exploitation of the eigensolutions of the associated conservative linear system and the characteristics of local nonlinearities, whereas the second formulation is using the linearized eigensolutions which are calculated with an iterative process.

Duarte and Machado [30] studied the system constituted by a mass subjected to two types of friction, namely, the viscous and the Coulomb friction. They used DFM to analayse the dynamics of elemental mechanical system and compared their work with standard models.

Atkins, et al. [31] proposed an extension of the classical linear force appropriation method for nonlinear MDOF systems. Writers are focused on weakly nonlinear systems such that, a sinusoidal force will only produce superharmonic components in the response.

Kim, et al. [32] presented a multi-term harmonic balance method (HBM) for nonlinear frequency response calculations of a torsional sub-system containing a clearance type nonlinearity. They investigated the number of harmonic terms that must be included in the HBM response calculations at given sinusoidal excitation and presented analytical predictions for super and sub-harmonic resonances.

Kawamura, et al. [33] proposed an analytical approach for analysing the nonlinear forced vibration of a MDOF system by component mode synthesis method. They divided the system investigated into some components and derived nonlinear modal equation of each component using the free-interface vibration modes. They derived the modal responses of components by solving the modal equations of all components and the conjunction conditions simultaneously. They considered cubic stiffness type nonlinearity.

Several studies [34-38] are also concentrated on analysing the response characteristics of nonlinear systems by using well defined HBM. Moreover, detection and identification of nonlinear systems using HBM is also studied by many researchers [39-40]

Z.K. Peng, et al. [41] developed a new method based on the concept of nonlinear output frequency-response functions, which is derived from the Volterra-series (VS)

theory of nonlinear systems, for the estimation of the nonlinear stiffness and damping parameters of locally nonlinear MDOF systems.

Besides, various studies [42-43] are also using VS theory to analyse the nonlinear systems. The same theory is also used for studies on detection characterization and identification of nonlinear systems [44-45].

1.3 Objective of the Thesis

In this thesis, it is aimed to analyze the harmonic response characteristics MDOF nonlinear structures to different types of nonlinearities. The amplitude dependencies of nonlinearities will be modelled by using DFM. To improve the accuracy of the results, effect of the higher order harmonic terms will be considered as well, by using multi harmonic describing function theory. The mathematical formulations will be embeded in a computer program developed in MATLAB® with graphical user interface. The program will get the system matricies from the file which should be obtained by using substructuring analysis in ANSYS® or manually editted for small size systems. The nonlinearities in the system can easily be defined through the graphical user interface of the MATLAB® program. The substructuring analysis in ANSYS® is described in Appendix B and MATLAB® source code for reading the ANSYS® file is given in the Appendix D.

1.4 Scope of the Study

The outline of the thesis is given below:

In Chapter 2, the nonlinearities used in this thesis will be presented and modeling these nonlinearities via DFM will be discussed.

In Chapter 3, background knowledge on harmonic vibration anlysis of MDOF nonlinear structures will be given and the underlying mathematical background in single and multi-harmonic analysis will be explained.

In Chapter 4, the MATLAB® computer program will be introduced and the basic capabilities of the program will be explained.

In Chapter 5, the program will be verified by comparing the results of some cases studies of the previous works and also the solution of some case studies will be compared with TD solutions.

In Chapter 6, program capabilities and compatibility with standart FEM software will be demonstrated by studying new case studies .

Conclusions and future work will be given in Chapter 7.

CHAPTER 2

MODELING NONLINEARITIES

2.1 Introduction

The descriptive representation of systems by matrices presented a new approach for nonlinear analysis. The system is separated into linear and nonlinear components in such a way that the nonlinearities can also be represented by discrete models (as matrices). The approximate frequency domain linearization methods use techniques, such as DFM, that convert nonlinear differential equations of motion into nonlinear algebraic equations.

However, the approximate linearization methods have some limitations. Methods can only be applied for obtaining a periodic solution of a nonlinear differential equation, because the assumed excitation has a sinusoidal form [13].

2.2 Modeling a System with Nonlinear Components

The mathematical background in the formulations of this section is based on the study of first Budak and Özgüven [18], later Tanrıkulu, et al. [19] and the study that uses the theory of the former study to explain the multi harmonic describing function concept [13].

Consider the differential equation of a nonlinear structure, modeled as an n degrees of freedom discrete system, subjected to an external excitation:

$$M\ \ddot{x} + C\ \dot{x} + i\ H\ x + K\ x + s = f \tag{2.1}$$

In above equation M, C, H and K are the linear mass, viscous damping, hysteretic damping and stiffness matrices of the system, respectively. The vectors x, $\dot{x}$ and $\ddot{x}$ are the displacement, velocity and acceleration vectors, and i stands for the unit imaginary number. Moreover, s represents internal nonlinear forces, whereas f represents external forcing. The nonlinear force vector s is considered to be a function of displacements and its derivatives in a general case ($\{s(x,\dot{x},\ddot{x},...)\}$).

An a^{th} element of the vector $\{s\}$ can be expressed as a sum,

$$s_a = \sum_{b=1}^{n} s_{ab}, \tag{2.2}$$

where s_{ab} represents the nonlinear restoring force element acting between the coordinates a and b for $a \neq b$, and between the ground and the coordinate a for a=b. Note that,

$$s_{ab} = s_{ba}, \tag{2.3}$$

s_{ab} is a function of the inter-coordinate displacement y_{ab} and its derivatives,

$$s_{ab} = s_{ab}(y_{ab}, \dot{y}_{ab}, \ddot{y}_{ab}, ...), \tag{2.4}$$

where

$$\begin{aligned} y_{ab} &= x_a - x_b \quad \text{for } a \neq b, \\ y_{ab} &= x_a \quad \text{for } a = b \end{aligned} \tag{2.5}$$

Assuming that the external excitation is a sinusoidal force, then f can be written as:

$$f = f(t) = \mathrm{Im}\ F\ e^{i\omega t} = \mathrm{Im}(\ F\ e^{i\psi}) \tag{2.6}$$

where, {F} is a harmonic excitation vector operating at frequency ω and generic angle ψ is defined as the product of frequency ω and time t.

When a nonlinear system is subjected to a sinusoidal excitation, the response is generally not exactly sinusoidal, often periodic, having the same period as the excitation and can be represented by Fourier series as:

$$x(t) = \sum_{m=0}^{\infty} x(t)_m = \mathrm{Im}(\sum_{m=0}^{\infty} X_m e^{im\omega t}) = \mathrm{Im}(\sum_{m=0}^{\infty} X_m e^{im\psi}) \tag{2.7}$$

where, subscript m indicates the m^{th} harmonic order and $\{x\}_m$ is the m^{th} displacement response order. Then the complex displacement response amplitude X at coordinate j in the m^{th} harmonic, $(X_j)_m$, can be written as:

$$(X_j)_m = \left|X_j\right|_m e^{i(\phi_j)_m} \tag{2.8}$$

where, $\left|X_j\right|_m$ is the magnitude and $(\phi_j)_m$ is the phase of the complex displacement X_j at harmonic m.

Let the response of the system, $x(t)$, given by Equation (2.7), is approximated by a set, Q_p, of p harmonic terms written as:

$$Q_p = q_1, q_2, q_3, \ldots, q_p \tag{2.9}$$

Here it should be noted that, the even q values in set Q_p are due to nonlinearities with asymmetrical characteristics. If it is confined to symmetrical nonlinearities only, even q values will be neglected.

Then, the approximate response can be defined as:

$$x(t) \approx \tilde{x}(t)_{(q_p)} = \sum_{m=q_1}^{q_p} x(t)_m \tag{2.10}$$

The formulations given above describe the displacements of the main coordinates. On the other hand, the intercoordinate displacement response, between coordinates a and b, $y_{ab,}$ can be expressed as:

$$y_{ab}(t) = x_a(t) - x_b(t) = \sum_{m=0}^{\infty} (y_{ab})_m(t) = \mathrm{Im}\left(\sum_{m=0}^{\infty} (Y_{ab})_m e^{im\omega t}\right) = \mathrm{Im}\left(\sum_{m=0}^{\infty} (Y_{ab})_m e^{im\psi}\right) \tag{2.11}$$

where:

$$\psi = \omega t \tag{2.12}$$

Similarly, the approximate response can be defined as:

$$y_{ab}(t) \approx (\tilde{y}_{ab})_{(q_p)}(t) = \sum_{m=q_1}^{q_p} (y_{ab})_m(t) = \mathrm{Im}\left(\sum_{m=q_1}^{q_p} (Y_{ab})_m e^{im\psi}\right) \tag{2.13}$$

where:

$$\begin{aligned} (Y_{ab})_m &= (X_a)_m - (X_b)_m, \quad (a \neq b) \\ (Y_{ab})_m &= \left|(Y_{ab})\right|_m e^{i(\phi_{ab})_m} \end{aligned} \tag{2.14}$$

2.2.1 Mathematical Formulation for Internal Nonlinear Forces

The internal nonlinear force vector s in Equation (2.1) is response dependent, such that the force related to intercoordinate displacement can be expressed as $s_{ab}(y_{ab})$. By assuming that the variable y_{ab} is in the form shown in Equation (2.13), it can be concluded that, nonlinear function $s_{ab}[(\tilde{y}_{ab})_{(q_p)}]$ is complex and is also a periodic

function of time. Thus, the function $s_{ab}[(\tilde{y}_{ab})_{(q_p)}]$ can also be expressed by a Fourier series. The number of terms considered in the Fourier series of nonlinear function, will be investigated separately, as single harmonic and multi harmonic formulations, in the next sections.

2.2.1.1 Single Harmonic Formulation for Internal Nonlinear Forces

Consider the matrix differential equation of motion of a nonlinear MDOF structure subjected to external sinusoidal excitation:

$$M\ \ddot{x} + C\ \dot{x} + i\ H\ x + K\ x + s = \mathrm{Im}(F\ e^{i\omega t}) = \mathrm{Im}(F\ e^{i\psi}) \quad (2.15)$$

Then the steady-state solution can be represented by a Fourier series as:

$$x(t) = \sum_{m=0}^{\infty} x(t)_m = \mathrm{Im}\left(\sum_{m=0}^{\infty} X_m e^{im\omega t}\right) = \mathrm{Im}\left(\sum_{m=0}^{\infty} X_m e^{im\psi}\right) \quad (2.16)$$

In some cases, where the higher harmonic terms of the response have small amplitudes relative to the fundamental (single) harmonic component, the response to this component is dominated and can be represented by the fundamental component of the Fourier series expansion of x(t) with acceptable numerical error. In such cases, the steady state response $x(t)$ can be formulated as:

$$x(t) = x(t)_1 = \mathrm{Im}(X_1 e^{i\omega t}) = \mathrm{Im}(X_1 e^{i\psi}) \quad (2.17)$$

The response of a general coordinate j, x_j can be written as:

$$x_j \approx (\tilde{x}_j)_1 = (x_j)_1 = \mathrm{Im}((X_j)_1 e^{i\psi}), \quad (2.18)$$

where

$$(X_j)_1 = |X_j|_1 e^{i(\phi_j)_1} \tag{2.19}$$

Again, the same representation as in Equation (2.11) can be presented here, the inter-coordinate displacement response x, between coordinates a and b, $y_{ab,}$ can be expressed as:

$$y_{ab}(t) = x_a(t) - x_b(t) \approx (\tilde{x}_a)_1(t) - (\tilde{x}_b)_1(t) = (\tilde{y}_{ab})_1(t) = (y_{ab})_1(t) = (Y_{ab})_1 e^{i\psi} \tag{2.20}$$

where:

$$\begin{aligned} (Y_{ab})_1 &= (X_a)_1 - (X_b)_1, \quad (a \neq b) \\ (Y_{ab})_1 &= \left|(Y_{ab})\right|_1 e^{i(\phi_{ab})_1} \end{aligned} \tag{2.21}$$

By assuming that the variable y_{ab} is in the form shown in Equation (2.20), it can be concluded that, nonlinear function $s_{ab}[(\tilde{y}_{ab})_1]$ is complex and is also a periodic function of time. Thus, the function $s_{ab}[(\tilde{y}_{ab})_1]$can be expressed by a Fourier series as:

$$s_{ab}[(\tilde{y}_{ab})_1] = \sum_{m=0}^{\infty} (s_{ab})_m = \mathrm{Im}\left(\sum_{m=0}^{\infty} (\boldsymbol{S}_{ab})_m e^{im\psi}\right) \tag{2.22}$$

where:

$$\begin{aligned} (\boldsymbol{S}_{ab})_m &= \left|\boldsymbol{S}_{ab}\right|_m e^{i(\xi_{ab})_m} \\ (\boldsymbol{S}_{ab})_0 &= \frac{1}{2\pi}\int_0^{2\pi} s_{ab}[(\tilde{y}_{ab})_1]d\psi \\ (\boldsymbol{S}_{ab})_m &= \frac{i}{\pi}\int_0^{2\pi} s_{ab}[(\tilde{y}_{ab})_1]e^{-im\psi}d\psi \qquad (m\geq 1) \end{aligned} \tag{2.23}$$

If the nonlinear force $s_{ab}[(\tilde{y}_{ab})_1]$ is assumed to be dominated by the fundamental term like the response itself, the formulation for the approximated nonlinear force can be simplified as:

$$s_{ab}[(\tilde{y}_{ab})_1] \approx (s_{ab})_1 = \mathrm{Im}((\boldsymbol{S}_{ab})_1 e^{i\psi}) \tag{2.24}$$

where:

$$\begin{aligned} (\boldsymbol{S}_{ab})_1 &= \left|\boldsymbol{S}_{ab}\right|_1 e^{i(\xi_{ab})_1} \\ (\boldsymbol{S}_{ab})_1 &= \frac{i}{\pi}\int_0^{2\pi} s_{ab}[(\tilde{y}_{ab})_1]e^{-i\psi}d\psi \end{aligned} \tag{2.25}$$

2.2.1.2 Multi Harmonic Formulation for Internal Nonlinear Forces

When a structure is highly nonlinear, the effects of higher harmonic terms (multiples of the fundamental input frequency), which are the remainder of the Fourier series expansion of response in Equation (2.7), become considerable. Therefore, it is important not to neglect the effects of these terms during the solution procedure.

The steady-state solution to Equation (2.1) can be represented by a Fourier series as:

$$x(t) = \sum_{m=0}^{\infty} x(t)_m = \mathrm{Im}\left(\sum_{m=0}^{\infty} X_m e^{im\psi}\right) \tag{2.26}$$

where:

$$(X_j)_m = \left|X_j\right|_m e^{i(\phi_j)_m} \tag{2.27}$$

The intercoordinate displacement response x, between coordinates a and b, $y_{ab,}$ can be expressed as:

$$y_{ab}(t) \approx (\tilde{y}_{ab})_{(q_p)}(t) = \sum_{m=q_1}^{q_p} (y_{ab})_m(t) = \mathrm{Im}\left(\sum_{m=q_1}^{q_p} (Y_{ab})_m e^{im\psi}\right) \tag{2.28}$$

where:

$$\begin{aligned} (Y_{ab})_m &= (X_a)_m - (X_b)_m, \quad (a \neq b) \\ (Y_{ab})_m &= \left|(Y_{ab})\right|_m e^{i(\phi_{ab})_m} \end{aligned} \tag{2.29}$$

The set, Q_p, for $q_1,\ldots\ldots,q_p$ was given by Equation (2.9).

By assuming that the variable y_{ab} is in the form as in Equation (2.28), it can be concluded that, nonlinear function $s_{ab}[(\tilde{y}_{ab})_{(q_p)}]$ is complex and is also a periodic function of time. $s_{ab}[(\tilde{y}_{ab})_{(q_p)}]$ can be approximated by set, Q_r, of r harmonic terms written as:

$$Q_r = q_1, q_2, q_3, \ldots, q_r \tag{2.30}$$

Again it should be noted here that, if it is confined to symmetrical nonlinearities only, even numbered harmonics will be neglected like the set Q_p given in Equation (2.9).

Accordingly, the approximate nonlinear function $(s_{ab})_{(q_r)}[(\tilde{y}_{ab})_{(q_p)}]$ can be written as:

$$(\tilde{s}_{ab})_{(q_r)}[(\tilde{y}_{ab})_{(q_p)}] = \sum_{m=q_1}^{q_r} (s_{ab})_m = \mathrm{Im}\left(\sum_{m=q_1}^{q_r} (\boldsymbol{S}_{ab})_m e^{im\tau}\right) \tag{2.31}$$

such that:

$$(\boldsymbol{S}_{ab})_m = \left|\boldsymbol{S}_{ab}\right|_m e^{i(\xi_{ab})_m}$$

$$(\boldsymbol{S}_{ab})_0 = \frac{1}{2\pi}\int_0^{2\pi} s_{ab}[(\tilde{y}_{ab})_{(q_p)}]d\psi \qquad (2.32)$$

$$(\boldsymbol{S}_{ab})_m = \frac{i}{\pi}\int_0^{2\pi} s_{ab}[(\tilde{y}_{ab})_{(q_p)}]e^{-im\psi}d\psi, \quad (m\geq 1)$$

2.3 Modeling Nonlinearities with Describing Function

Understanding the dynamic behaviour of a mechanical system needs accurate analytical modelling throughout the design stage. As stated before, many complex mechanical structures are composed of several substructures connected by different kinds of joints and these joints have a considerable effect in the dynamic behaviour of the assembled structures. So, it is important to establish an accurate mathematical model for these joint components.

Most of the studies concentrate on modeling a joint by investigating and identifying its dynamic characteristics [46-52]. The response at the joint caused by an external force is the general procedure for finding the force-response relationship of a joint. The results of these studies are used as an input for further studies, which is the development of an accurate general mathematical model of the joint behaviour by finding the parameters of the identified model. For simple cases, this can be obtained by curve fitting of the experimental force-response relationship. These relationships can be either linear or nonlinear.

Separating the system into linear and nonlinear components facilitated vibration analysis since it allows the nonlinearities to be represented by discrete models. The linear joint models such as springs, viscous dampers and rigid connections, are investigated and well defined in the former studies. On the other hand, the nonlinear joint models, which are amplitude dependent, are represented by local nonlinear coefficients (typically stiffness and/or damping related). The approximate frequency

domain quasi-linearization techniques, such as DFM are widely used to express these amplitude dependent coefficients [13, 18-21, 23].

The theoretical basis of this DFM is related to the Van der Pol method of slowly-varying coefficients [15] and to the method of equivalent linearization proposed by Bogoliubov and Mitroposky [16]. The basic theory of the method depend upon the fact that, when subjected to a harmonic excitation, a wide variety of nonlinear systems exhibit a periodic, oscillatory response that is sufficiently close to a pure sinusoidal. The quasi-linearization technique that DFM is based on simply replaces the system nonlinearity by an approximate linear gain which depends upon the type, amplitude and the frequencies of the input.

In most researches [9, 19, 21, 22, 26, 28, 53] the DFM is used to describe the relation between the fundamental harmonics of the response and the excitation, and in these studies the average restoring force occurring in one cycle is calculated. On the other hand, extensions to multiharmonic responses have been proposed by Kuran and Özgüven [20], Ferreira [13]. Apart from classical harmonic nonlinear vibration analysis, DFM is also widely used in many applications such as impact [54] and control [55-56].

2.3.1 Single Harmonic Describing Function

The notion of single (fundamental) harmonic DFM can be expressed by considering a single degree of freedom system driven by a harmonic excitation which is given by:

$$m\ddot{x} + c\dot{x} + ihx + kx + s = f \sin \omega t \tag{2.33}$$

In above equation, m, c, h and k are the linear mass, viscous damping, hysteretic damping and stiffness values, respectively. x, $\dot{x}$ and $\ddot{x}$ are the displacement, velocity

and acceleration of the mass m, and i stands for the unit imaginary number. s represents internal nonlinear forces, whereas f represents external forcing. The nonlinear force s is considered to be a function of displacements and velocities ($\{s(x,\dot{x},\ddot{x},...)\}$).

The response of the nonlinear system x(t) is assumed to be close enough to a sinusoidal oscillation as:

$$x \approx (X)_1 \sin(\omega t + \theta) = (X)_1 \sin \tau \tag{2.34}$$

where

$$\tau = \omega t + \theta \tag{2.35}$$

In Equation (2.34), $(X)_1$ is complex response amplitude, ω is the excitation frequency and θ is phase angle.

Now it is reasonable to assume that the nonlinear function $s(x,\dot{x})$ is complex and also a periodic function of time, provided that little energy is leaked to frequencies other than the fundamental frequency. Therefore, it can be expressed in a Fourier series as:

$$\begin{aligned} s(x,\dot{x}) \approx v(x,\dot{x})x = (\boldsymbol{S})_0(\omega,(X)_0) + (\boldsymbol{S})_1(\omega,(X)_1)x + i(\boldsymbol{S})_{1_2}(\omega,(X)_1)x \\ +\text{HigherHarmonicTerms} \end{aligned} \tag{2.36}$$

Here, the bias term, $(\boldsymbol{S})_0$ is defined as:

$$(\boldsymbol{S})_0 = \frac{1}{2\pi}\int_0^{2\pi} \boldsymbol{S}((X)_1 \sin\tau, \omega(X)_1 \cos\tau)d\tau \tag{2.37}$$

The remaining real and imaginary parts of the fundamental harmonic are:

$$(\boldsymbol{S})_1 = \frac{\mathrm{i}}{\pi(\mathrm{X})_1}\int_0^{2\pi} \boldsymbol{S}((\mathrm{X})_1 \sin\tau, \omega(\mathrm{X})_1 \cos\tau)\sin\tau \mathrm{d}\tau$$
$$(\boldsymbol{S})_{1_2} = \frac{\mathrm{i}}{\pi(\mathrm{X})_1}\int_0^{2\pi} \boldsymbol{S}((\mathrm{X})_1 \sin\tau, \omega(\mathrm{X})_1 \cos\tau)\cos\tau \mathrm{d}\tau \quad (2.38)$$

$\mathrm{v}(\mathrm{x}, \dot{\mathrm{x}})$ defined in Equation (2.36) can be defined as the optimum equivalent linear complex stiffness representation of the nonlinear function $\mathrm{s}(\mathrm{x}, \dot{\mathrm{x}})$ when the response of the nonlinear system x(t) is close enough to a sinusoidal oscillation. If $\mathrm{s}(\mathrm{x}, \dot{\mathrm{x}})$ is symmetrical around the origin, then $(\boldsymbol{S})_0$ becomes zero. If the nonlinearity is not frequency dependent, then $(\boldsymbol{S})_{1_2}$ becomes zero. Moreover, if the assumption that $\mathrm{s}(\mathrm{x}, \dot{\mathrm{x}})$ is dominated by its fundamental term is valid, then Equation (2.36) can be simplified as:

$$(\mathrm{v}(\mathrm{x}, \dot{\mathrm{x}}))_1 \mathrm{x} = (\boldsymbol{S})_1(\omega, (\mathrm{X})_1)\mathrm{x} + \mathrm{i}(\boldsymbol{S})_{1_2}(\omega, (\mathrm{X})_1)\mathrm{x} \quad (2.39)$$

where $(\mathrm{v}(\mathrm{x}, \dot{\mathrm{x}}))_1$ is called the first-order describing function which can be uniquely defined as:

$$(\mathrm{v}(\mathrm{x}, \dot{\mathrm{x}}))_1 = (\boldsymbol{S})_1 + \mathrm{i}(\boldsymbol{S})_{1_2} \quad (2.40)$$

In nonlinear problems, if the kind of nonlinearity in $\mathrm{s}(\mathrm{x}, \dot{\mathrm{x}})$ is known, the describing function v can be calculated from Equations (2.38) and (2.40).

2.3.2 Higher Harmonic Describing Function

After accepting the hypothesis given by mathematical formulations in Section (2.2.1.2), the elements $(\boldsymbol{S}_{ab})_m$, given by Equation (2.32), of the approximate nonlinear force $(s_{ab})[(\tilde{y}_{ab})_{(q_p)}]$ can be expressed as:

$$(\boldsymbol{S}_{ab})_m = (v_{ab})_m (Y_{ab})_m \qquad (m = q_1, q_2, ..., q_p) \tag{2.41}$$

The corresponding m^{th} harmonic order describing function can be defined as:

$$(v_{ab})_m = \frac{(\boldsymbol{S}_{ab})_m}{(Y_{ab})_m} \tag{2.42}$$

By considering the m harmonics, Equation (2.42) can be written in matrix form as:

$$\begin{Bmatrix} (\boldsymbol{S}_{ab})_{q_1} \\ (\boldsymbol{S}_{ab})_{q_2} \\ \vdots \\ (\boldsymbol{S}_{ab})_{q_p} \end{Bmatrix} = \begin{pmatrix} (v_{ab})_{q_1} & 0 & \cdots & 0 \\ 0 & (v_{ab})_{q_2} & \cdots & 0 \\ \vdots & \vdots & \ddots & \vdots \\ 0 & 0 & \cdots & (v_{ab})_{q_p} \end{pmatrix} \begin{Bmatrix} (Y_{ab})_{q_1} \\ (Y_{ab})_{q_2} \\ \vdots \\ (Y_{ab})_{q_p} \end{Bmatrix} \tag{2.43}$$

Equation (2.43) can be expressed in terms of the general coordinates, {X}, as:

$$\begin{Bmatrix} (\boldsymbol{S}_a)_{q_1} \\ (\boldsymbol{S}_b)_{q_1} \\ (\boldsymbol{S}_a)_{q_2} \\ (\boldsymbol{S}_b)_{q_2} \\ \vdots \\ (\boldsymbol{S}_a)_{q_p} \\ (\boldsymbol{S}_b)_{q_p} \end{Bmatrix} = \begin{pmatrix} (v_{ab})_{q_1} & -(v_{ab})_{q_1} & 0 & 0 & \cdots & 0 & 0 \\ -(v_{ab})_{q_1} & (v_{ab})_{q_1} & 0 & 0 & \cdots & 0 & 0 \\ 0 & 0 & (v_{ab})_{q_2} & -(v_{ab})_{q_2} & \cdots & 0 & 0 \\ 0 & 0 & -(v_{ab})_{q_2} & (v_{ab})_{q_2} & \ddots & 0 & 0 \\ \vdots & \vdots & \vdots & \ddots & \ddots & \vdots & \vdots \\ 0 & 0 & 0 & 0 & \cdots & (v_{ab})_{q_p} & -(v_{ab})_{q_p} \\ 0 & 0 & 0 & 0 & \cdots & -(v_{ab})_{q_p} & (v_{ab})_{q_p} \end{pmatrix} \begin{Bmatrix} (X_a)_{q_1} \\ (X_b)_{q_1} \\ (X_a)_{q_2} \\ (X_b)_{q_2} \\ \vdots \\ (X_a)_{q_p} \\ (X_b)_{q_p} \end{Bmatrix} \tag{2.44}$$

Equation (2.44) can be written in more compact form as:

$$\begin{Bmatrix} (\boldsymbol{S}_a)_m \\ (\boldsymbol{S}_b)_m \end{Bmatrix} = \Delta_m^{ab} \begin{Bmatrix} (X_a)_m \\ (X_b)_m \end{Bmatrix} \qquad (m = q_1, q_2, ..., q_p) \tag{2.45}$$

2.3.3 Multi Harmonic Describing Function

After accepting the conjecture given by mathematical formulations in Section (2.2.1.2), the elements $(\boldsymbol{S}_{ab})_m$, given by Equation (2.32), of the approximate nonlinear force $(s_{ab})_{(q_r)}[(\tilde{y}_{ab})_{(q_p)}]$ can be expressed as:

$$(\boldsymbol{S}_{ab})_m = \sum_{l=q_1}^{q_p} (v_{ab})_{ml} (Y_{ab})_l \qquad (m = q_1, q_2, ..., q_r) \tag{2.46}$$

The Equation (2.46) can be written in matrix format as:

$$\begin{Bmatrix} (\boldsymbol{S}_{ab})_{q_1} \\ (\boldsymbol{S}_{ab})_{q_2} \\ \vdots \\ (\boldsymbol{S}_{ab})_{q_r} \end{Bmatrix} = \begin{pmatrix} (v_{ab})_{q_1 q_1} & (v_{ab})_{q_1 q_2} & \cdots & (v_{ab})_{q_1 q_p} \\ (v_{ab})_{q_2 q_1} & (v_{ab})_{q_2 q_2} & \cdots & (v_{ab})_{q_2 q_p} \\ \vdots & \vdots & \ddots & \vdots \\ (v_{ab})_{q_r q_1} & \cdots & \cdots & (v_{ab})_{q_r q_p} \end{pmatrix} \begin{Bmatrix} (Y_{ab})_{q_1} \\ (Y_{ab})_{q_2} \\ \vdots \\ (Y_{ab})_{q_p} \end{Bmatrix} \tag{2.47}$$

and Equation (2.47) can be expressed as a function of general coordinate {X} as:

$$\begin{Bmatrix} (\boldsymbol{S}_a)_{q_1} \\ (\boldsymbol{S}_b)_{q_1} \\ (\boldsymbol{S}_a)_{q_2} \\ (\boldsymbol{S}_b)_{q_2} \\ \vdots \\ (\boldsymbol{S}_a)_{q_r} \\ (\boldsymbol{S}_b)_{q_r} \end{Bmatrix} = \begin{pmatrix} (v_{ab})_{q_1q_1} & -(v_{ab})_{q_1q_1} & (v_{ab})_{q_1q_2} & -(v_{ab})_{q_1q_2} & \cdots & (v_{ab})_{q_1q_p} & -(v_{ab})_{q_1q_p} \\ -(v_{ab})_{q_1q_1} & (v_{ab})_{q_1q_1} & -(v_{ab})_{q_1q_2} & (v_{ab})_{q_1q_2} & \cdots & -(v_{ab})_{q_1q_p} & (v_{ab})_{q_1q_p} \\ (v_{ab})_{q_2q_1} & -(v_{ab})_{q_2q_1} & (v_{ab})_{q_2q_2} & -(v_{ab})_{q_2q_2} & \cdots & (v_{ab})_{q_2q_p} & -(v_{ab})_{q_2q_p} \\ -(v_{ab})_{q_2q_1} & (v_{ab})_{q_2q_1} & -(v_{ab})_{q_2q_2} & (v_{ab})_{q_2q_2} & \ddots & -(v_{ab})_{q_2q_p} & (v_{ab})_{q_2q_p} \\ \vdots & \vdots & \vdots & \ddots & \ddots & \vdots & \vdots \\ (v_{ab})_{q_rq_1} & -(v_{ab})_{q_rq_1} & (v_{ab})_{q_rq_2} & -(v_{ab})_{q_rq_2} & \cdots & (v_{ab})_{q_rq_p} & -(v_{ab})_{q_rq_p} \\ -(v_{ab})_{q_rq_1} & (v_{ab})_{q_rq_1} & -(v_{ab})_{q_rq_2} & (v_{ab})_{q_rq_2} & \cdots & -(v_{ab})_{q_rq_p} & (v_{ab})_{q_rq_p} \end{pmatrix} \begin{Bmatrix} (X_a)_{q_1} \\ (X_b)_{q_1} \\ (X_a)_{q_2} \\ (X_b)_{q_2} \\ \vdots \\ (X_a)_{q_p} \\ (X_b)_{q_p} \end{Bmatrix} \tag{2.48}$$

Equation (2.48) can be written in a more compact form as:

$$\begin{matrix} (\boldsymbol{S}_a)_m \\ (\boldsymbol{S}_b)_m \end{matrix} = \sum_{l=q_1}^{q_p} \Delta_{ml}^{ab} \begin{Bmatrix} (X_a)_l \\ (X_b)_l \end{Bmatrix} \quad (m = q_1, q_2, \ldots, q_r) \tag{2.49}$$

where:

$$\Delta_{ml}^{ab} = \begin{pmatrix} (v_{ab})_{ml} & -(v_{ab})_{ml} \\ -(v_{ab})_{ml} & (v_{ab})_{ml} \end{pmatrix} \tag{2.50}$$

Accordingly, if the form of nonlinearity $\{ s(x, \dot{x}) \}$ is known, all describing functions, $(v_{ab})_{ml}$ for $m=q_r$ and $l=q_p$ can be found for intercoordinate elements from equation:

$$(v_{ab})_{q_rq_p} = \frac{(s_{ab})_{q_r}((\tilde{y}_{ab})_{(q_p)}) - (s_{ab})_{q_r}((\tilde{y}_{ab})_{(q_{p-1})})}{(Y_{ab})_{(q_p)}} \tag{2.51}$$

and for ground elements:

$$(v_{ab})_{q_r q_p} = \frac{(s_{ab})_{q_r}((\tilde{x}_{ab})_{(q_p)}) - (s_{ab})_{q_r}((\tilde{x}_{ab})_{(q_{p-1})}))}{(X_{ab})_{(q_p)}} \tag{2.52}$$

It should be stated here that, in this study, the higher order terms of the response are calculated by considering multi harmonic describing function theory. Higher order describing function formulation is given just for information and completeness.

2.4 Different Types of Nonlinearities and the Corresponding Describing Functions

The representation of various nonlinear joints models by describing function aprroach will be summarised in this section. This joint models are formed by idealized representation of different nonlinearity models which describe the force and displacement/velocity/frequency relationships. Most common nonlinearities encountered in structural dynamics and their response behaviours are given in Figure 2.1.

2.4.1.1 Cubic Stiffness

This model represents a massless nonlinear spring such that a force applied across the spring is proportional to the cube of the elongation of the spring, y (Figure 2.2). The equation that describes the relation between the force and the response can be written as:

$$s = \beta y^3 \tag{2.53}$$

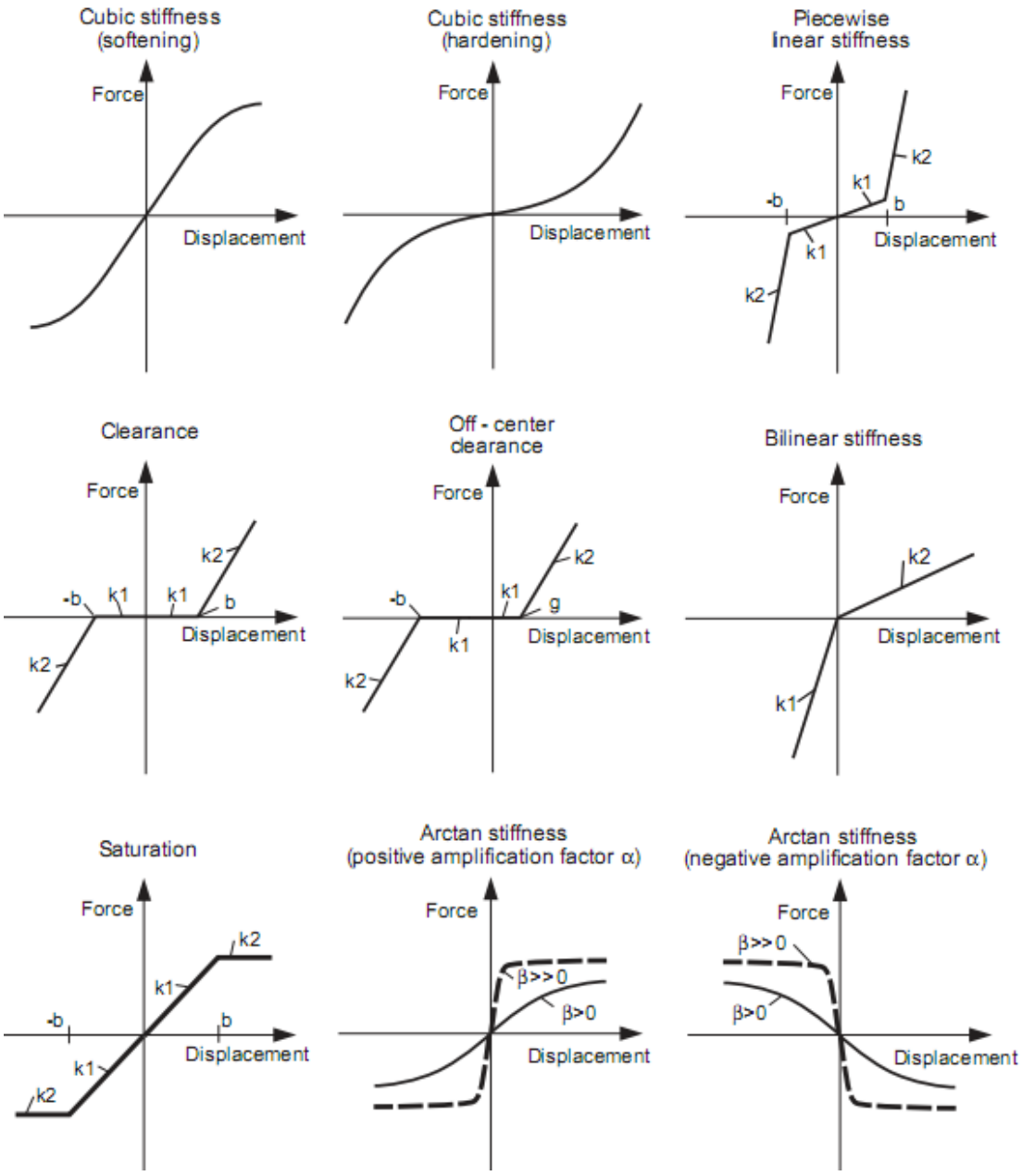

Figure 2.1 Idealized types of various structural nonlinearities [40]

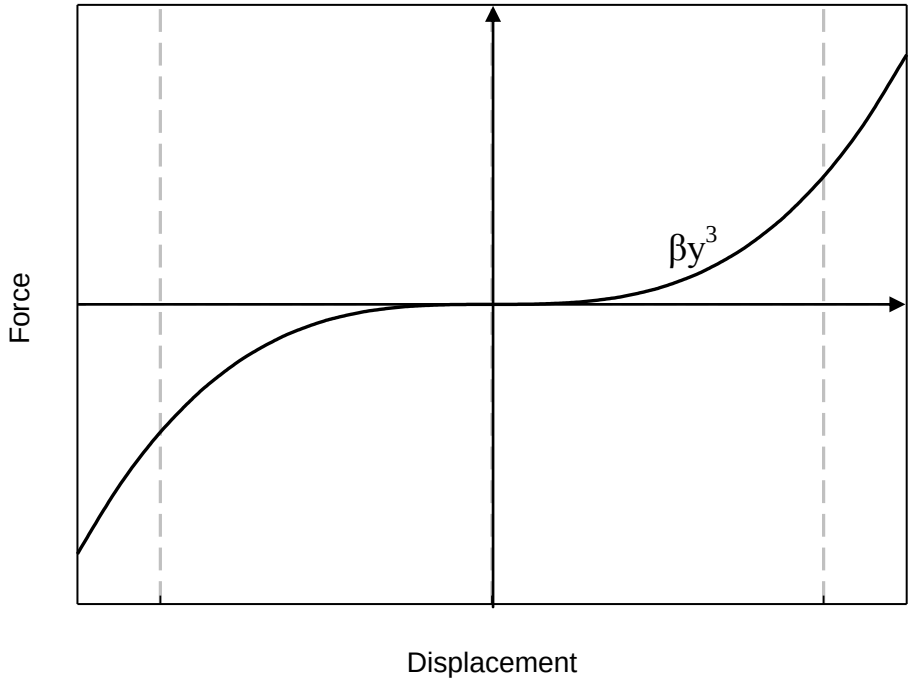

Figure 2.2 Behaviour of a typical hardening cubic stiffness element

It must be emphasized here that, although, the overall stiffness of the nonlinear spring changes with the amplitude y, the stiffness coefficient β defined in equation (2.53) remains constant and is not frequency dependent. Moreover, β can be positive or negative. In cases where $\beta<0$, the effective stiffness decreases as the level of excitation increases. This is why such stiffness elements are regarded as softening springs. The opposite case, where the spring constant $\beta>0$, is referred as hardening spring because as the forcing level increases, also the restoring forcing level increases. Examples of systems with hardening stiffness behaviour are clamped plates and beams, whereas buckling beams and plates are examples of systems having softening stiffness characteristics [6].

The effect of cubic stiffness nonlinearity on system responses is investigated in many studies such as [9, 13, 19-20, 22, 24]. These studies confirm the frequency response distortion characteristics of these systems, such that, for hardening systems as the

level of excitation increases, the resonant frequency shifts up (Figure 2.3). As expected, the resonant frequency shifts down for softening systems.

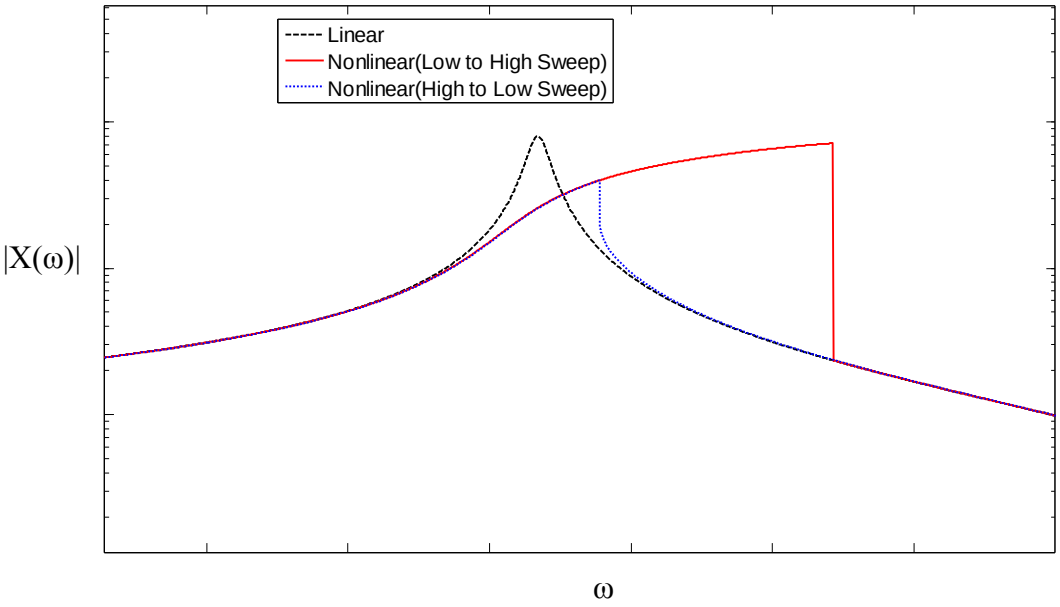

Figure 2.3 Typical response distortion due to (hardening) cubic stiffness nonlinearity

The describing functions of a nonlinear cubic stiffness element having cubic stiffness coefficient β defined in Equation (2.53), can be formulated by considering the first 2 harmonics, first and third for both response and internal nonlinear force, as:

$$
\begin{aligned}
(v_{ab})_{11} &= \frac{3}{4}\beta Y_1^2 \\
(v_{ab})_{13} &= \frac{3}{2}\beta Y_1 Y_3 - \frac{3}{4}\beta Y_1^2 \\
(v_{ab})_{31} &= -\frac{1}{4}\beta Y_1^2 \\
(v_{ab})_{33} &= -\frac{3}{2}\beta Y_1^2 + \frac{3}{4}\beta Y_3^2
\end{aligned}
\qquad (2.54)
$$

The derivation of Equations (2.54) can be found in [13]. It should be stated here that the higher harmonic describing function of cubic stiffness element is given just for information. They will be computed by numerical integration rather than pre-defined formulas during response calculations.

2.4.1.2 Coulomb Friction

Coulomb friction between two surfaces is one of the damping forms which cause nonlinearities in structures. This is why it is generally called as coulomb damping (Figure 2.4). The relationship between the sign of the relative velocity at the interface of the joint and the value of the resulting force can be given as:

$$s = F_f \, \mathrm{sgn}(\dot{y}) \tag{2.55}$$

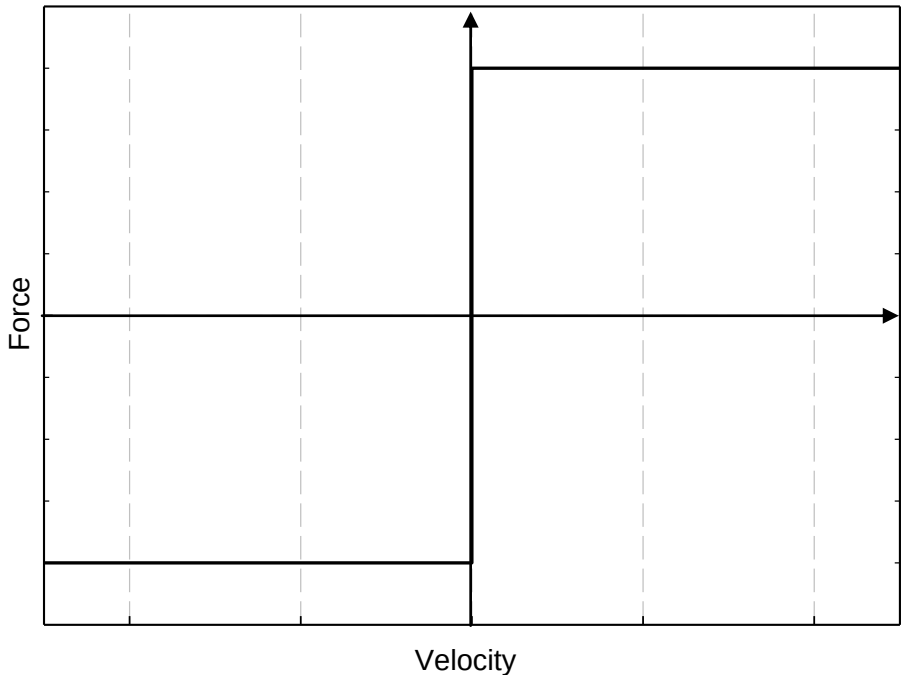

Figure 2.4 Behaviour of Coulomb friction nonlinearity

The Coulomb friction nonlinearity is most evident at low levels of excitation. In extreme situations stick-slip motion may exist. The previous studies [9, 13, 20, 22, and 36] reveal that the response distortion for this case appears at higher damping with lower excitation levels (Figure 2.5). For very small displacements, corresponding to the "stick-slip" stage, the nonlinear force given in Equation 2.55 is usually replaced by a linear elastic force proportional to the current amplitude of motion [9]. The "stick" and "stick-slip" stages will not be included in this work.

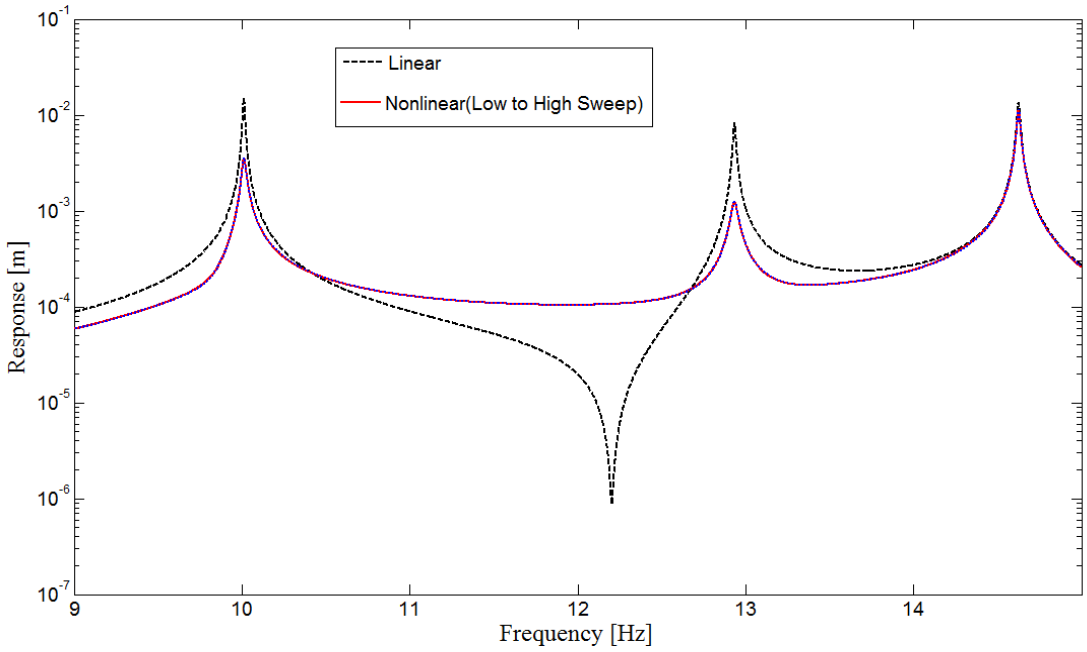

Figure 2.5 Typical response distortion due to Coulomb friction nonlinearity

The describing functions of a coulomb friction damper having friction force F_f, defined in Equation (2.55), can be formulated by considering the first harmonics only, as:

$$(v_{ab})_{11} = i\frac{4F_f}{\pi Y_1} \tag{2.56}$$

2.4.1.3 Piecewise Linear Stiffness

Many structural and mechanical systems with nonlinear material or geometrical properties can be modeled as systems with piecewise linear stiffness (Example: preloaded bearings [6]) (Figure 2.6). Because of this prevalence, there are number of researches that analyze systems with piecewise stiffness nonlinearity [19-20, 40, 57, etc]. This type of nonlinearity can be expressed as a model with a massless nonlinear spring such that force applied across the spring is proportional to the elongation of the spring, but this proportionality constant is different at specified elongation values

(Figure 2.7). The equation that describes the relation between the force and the response can be written as:

$$\begin{aligned} s &= k_1 y, && \text{for } |y| < \delta \\ s &= (k_1 - k_2)\delta + k_2 y && \text{for } |y| \geq \delta \end{aligned} \tag{2.57}$$

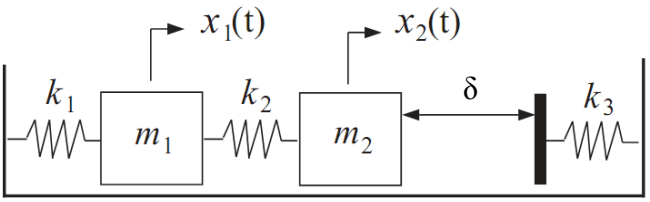

Figure 2.6 An example of a system with piecewise nonlinearity

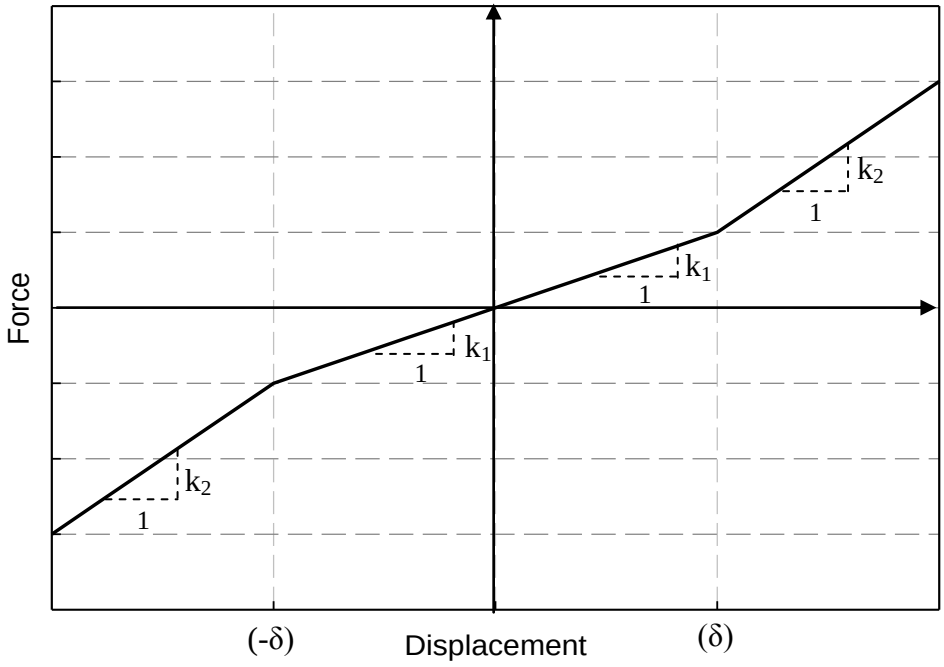

Figure 2.7 Behaviour of a typical piecewise linear stiffness element

It can be deduced that two of the nonlinearities in Figure 2.1 are special cases of this kind of nonlinearity. In fact, for saturation nolinearity, k_2 in Equation (2.56) will be taken as 0, whereas for clearence (backlash) nonlinearity, k_1 will be taken as 0.

The describing functions of a piecewise linear stiffness element having system coefficients k_1, k_2 and δ defined in Equation (2.57), can be formulated by considering the first harmonics only, as:

$$(v_{ab})_{11} = k_1, \qquad \text{for } Y_1 < \delta$$
$$(v_{ab})_{11} = \frac{2(k_1 - k_2)}{\pi}\left[\arcsin(\frac{\delta}{Y_1}) + (\frac{\delta}{Y_1})\sqrt{1-(\frac{\delta}{Y_1})^2}\right] + k_2 \qquad \text{for } Y_1 \geq \delta \tag{2.58}$$

2.4.1.4 Arctan Stiffness

The arctan spring (Figure 2.8) has a softening stiffness characteristic, however, the difference of this kind of stiffness nonlinearity from the cubic stiffness nonlinearity is that the stiffness of the arctan spring converges to $(\pm\rho.\pi/2)$ for large amplitudes, whereas the softening cubic stiffness spring does not converge to a constant value [40]. The equation that describes the relation between the force and the response can be written as [40]:

$$s = \rho \arctan(\kappa y) \tag{2.59}$$

The coefficient ρ is the amplification factor whereas κ is the compression factor. The describing functions of an arctan spring element having system coefficients ρ, and κ defined in Equation (2.59), can be formulated by considering the first harmonics only, as [40]:

$$(v_{ab})_{11} = y + \frac{2\rho}{\kappa(Y_1)^2}\left(\sqrt{\kappa(Y_1)^2 + 1} - 1\right) \tag{2.60}$$

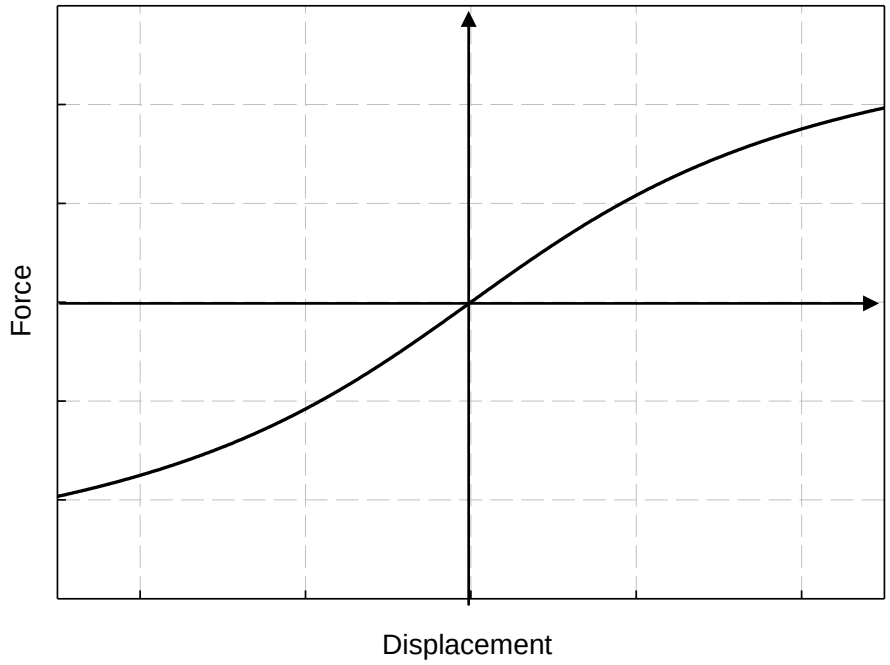

Figure 2.8 Behaviour of a typical arctan stiffness element

2.4.1.5 Preloaded Spring Element

Preloaded spring elements are encountered in many practical mechanical and structural systems either due to intentional pre-compression, unintended manufacturing or heat treatment process. The equation that describes the relation between the force and the response can be written as [58]:

$$\begin{aligned} s &= F_p \frac{|y|}{y} + ky \qquad \text{for} \quad |y| > 0 \\ s &= [-F_p \quad F_p] \qquad \text{for} \quad |y| = 0 \end{aligned} \tag{2.61}$$

where F_p is the preload force value. Typical force-displacement relationship of preload stiffness element is given in Figure 2.10.

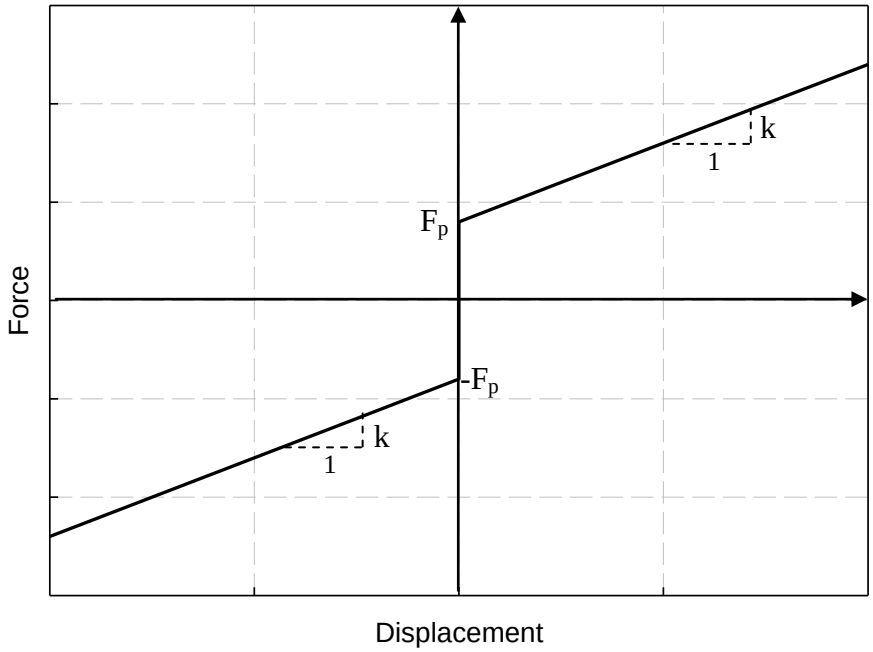

Figure 2.9 Behaviour of a typical preloaded stiffness element

The describing function of a preloaded stiffness element having system coefficients F_p and k defined in Equation (2.61) can be formulated by considering the first harmonics only, as [59]:

$$(v_{ab})_{11} = \frac{4F_p}{\pi Y_1} + k \tag{2.62}$$

CHAPTER 3

HARMONIC VIBRATION ANALYSIS OF MDOF NONLINEAR STRUCTURES

3.1 Introduction

Construction of the ODE of motion of a MDOF system commences with spatial discretization of the system under investigation with various methods such as Ritz, Galerkin, FEM, variational formulations, etc. By discretization, a large system can be represented in a matrix form such that, the elements of the system matrices represent local mass, stiffness and damping coefficients and the matrix indexes of these coefficients represent the distribution of these elements in space. Budak and Özgüven [18] first suggested that nonlinear forces also can be expressed in a matrix form. The theoretical background of this section is again based on the study of Tanrıkulu, et al [19] and a later work of Ferreira [13], for modelling nonlinearities via a common quasilinearization technique, DFM which was presented in Chapter 2. In this chapter, multi harmonic response solution will be presented. Some equations of Chapter 2 may also be given here for completeness.

3.2 Mathematical Formulation

Consider a nonlinear structure under the harmonic external forcing. If the structure is modelled as a discrete system with n degrees of freedom, then the matrix differential equation of motion can be written as:

$$M\ \ddot{x} + C\ \dot{x} + i\,H\ x + K\ x + s(x,\dot{x}) = f \qquad (3.1)$$

Assuming the external excitation is a sinusoidal force then f can be written as:

$$f = \mathrm{Im}(F\ e^{i\psi}) \tag{3.2}$$

As stated in Section 2.2 and expressed by Equation (2.7), the response is generally not exactly sinusoidal, often periodic, having the same period as the excitation and can be represented by Fourier series written as:

$$x(t) = \mathrm{Im}(\sum_{m=0}^{\infty} X_m e^{im\psi}) \tag{3.3}$$

Since the nonlinear forces are response dependent, they can also be assumed to be periodic, having the same period as the excitation and can be represented by Fourier series written as:

$$s(x,\dot{x}) = \sum_{m=0}^{\infty} s_m = \mathrm{Im}(\sum_{m=0}^{\infty} \boldsymbol{S}_m e^{im\psi}) \tag{3.4}$$

If Equations (3.2), (3.3) and (3.4) are substituted, in complex form, into the matrix differential equation of motion (Equation 3.1), the following equation can be obtained by grouping terms with the same frequencies:

$$\left[-m\omega^2\ M + im\omega\ C + i\ H + K\right] X_m + \boldsymbol{S}_m = F_m \tag{3.5}$$

Equation (3.5) can be rewritten by using the receptance definition, as:

$$[\alpha]_m^{-1}\ X_m + \boldsymbol{S}_m = F_m,\ (m = q_1, q_2, q_3, q_4, ..., q_p) \tag{3.6}$$

where:

$$[\alpha]_m = \left[-m\omega^2\ M + im\omega\ C + i\ H + K\right]^{-1} \tag{3.7}$$

is the receptance matrix of the linear part of the structure at frequency mω.

Budak and Özgüven [18] first suggested that nonlinear forces can be expressed in a matrix form. They developed a method for the harmonic vibration analysis of nonlinear structures, which has later been extended by Tanrıkulu, et al. [19] by using describing functions and in these studies the amplitude vector of nonlinear forces are expressed in the form:

$$\boldsymbol{S}_{m} = [\Delta]_{m} \; X_{m} \tag{3.8}$$

where, the elements o the matrix $[\Delta]_{m}$, the nonlinearity matrix, are defined as:

$$\begin{aligned} [\Delta_{aa}]_{m} &= \sum_{b=1}^{n} (v_{ab})_{m} \\ [\Delta_{ab}]_{m} &= -(v_{ab})_{m}, \quad (a \neq b) \end{aligned} \tag{3.9}$$

Later, Ferreira [13] extended the theory behind the Equations (3.8) and (3.9) to express the nonlinear forces by using multiharmonic describing function theory and express Equation (3.8) by using the corresponding describing function Equation (2.49), as:

$$\boldsymbol{S}_{m} = \sum_{l=1}^{m} [\Delta]_{ml} \; X_{l} \tag{3.10}$$

where, the elements o the matrix $[\Delta]_{ml}$, the nonlinearity matrix, are defined as:

$$\begin{aligned} [\Delta_{aa}]_{ml} &= \sum_{b=1}^{n} (v_{ab})_{ml} \\ [\Delta_{ab}]_{ml} &= -(v_{ab})_{ml}, \quad (a \neq b) \end{aligned} \tag{3.11}$$

If the single or higher order describing function theory is used for qualinearization of nonlinear forces, then Equation (3.6) can be rewritten as:

$$[\alpha]_m^{-1} \; X_m + [\Delta]_m \; X_m = F_m \tag{3.12}$$

Equation (3.12) can be extended to an assembled matrix equation by considering all m harmonics, which can be given as:

$$\begin{pmatrix} [\alpha]_1^{-1}+[\Delta]_1 & 0 & \cdots & 0 \\ 0 & [\alpha]_2^{-1}+[\Delta]_2 & \cdots & 0 \\ \vdots & \vdots & \ddots & \vdots \\ 0 & 0 & \cdots & [\alpha]_m^{-1}+[\Delta]_m \end{pmatrix} \begin{Bmatrix} \{X\}_1 \\ \{X\}_2 \\ \vdots \\ \vdots \\ \{X\}_m \end{Bmatrix} = \begin{Bmatrix} \{F\}_1 \\ \{F\}_2 \\ \vdots \\ \vdots \\ \{F\}_m \end{Bmatrix} \tag{3.13}$$

Then, the desired response solution can be obtained from the following equation:

$$\begin{Bmatrix} \{X\}_1 \\ \{X\}_2 \\ \vdots \\ \vdots \\ \{X\}_m \end{Bmatrix} = \begin{pmatrix} [\alpha]_1^{-1}+[\Delta]_1 & 0 & \cdots & 0 \\ 0 & [\alpha]_2^{-1}+[\Delta]_2 & \cdots & 0 \\ \vdots & \vdots & \ddots & \vdots \\ 0 & 0 & \cdots & [\alpha]_m^{-1}+[\Delta]_m \end{pmatrix}^{-1} \begin{Bmatrix} \{F\}_1 \\ \{F\}_2 \\ \vdots \\ \vdots \\ \{F\}_m \end{Bmatrix} \tag{3.14}$$

Equation (3.14) can be written in a more compact form as:

$$\{X\} = [\theta]\{F\} \tag{3.15}$$

where;

$$\theta = \begin{pmatrix} [\alpha]_1^{-1}+[\Delta]_1 & 0 & \cdots & 0 \\ 0 & [\alpha]_2^{-1}+[\Delta]_2 & \cdots & 0 \\ \vdots & \vdots & \ddots & \vdots \\ 0 & 0 & \cdots & [\alpha]_m^{-1}+[\Delta]_m \end{pmatrix}^{-1} \tag{3.16}$$

On the other hand, if multi harmonic describing function theory is used for quasilinearization of nonlinear forces, Equation (3.6) can be rewritten as:

$$[\alpha]_m^{-1} \; X_m + \sum_{l=1}^{m} [\Delta]_{ml} \; X_l = F_m \tag{3.17}$$

By considering m harmonics for the solution and the Equation (2.50), Equation (3.17) can be written in a matrix form as:

$$\begin{pmatrix} [\alpha]_1^{-1}+[\Delta]_{11} & [\Delta]_{12} & \cdots & [\Delta]_{1m} \\ [\Delta]_{21} & [\alpha]_2^{-1}+[\Delta]_{22} & \cdots & [\Delta]_{2m} \\ \vdots & \vdots & \ddots & \vdots \\ [\Delta]_{m1} & [\Delta]_{m2} & \cdots & [\alpha]_m^{-1}+[\Delta]_{mm} \end{pmatrix} \begin{Bmatrix} \{X\}_1 \\ \{X\}_2 \\ \vdots \\ \vdots \\ \{X\}_m \end{Bmatrix} = \begin{Bmatrix} \{F\}_1 \\ \{F\}_2 \\ \vdots \\ \vdots \\ \{F\}_m \end{Bmatrix} \tag{3.18}$$

Then, the desired response solution can be calculated from the equation:

$$\begin{Bmatrix} \{X\}_1 \\ \{X\}_2 \\ \vdots \\ \vdots \\ \{X\}_m \end{Bmatrix} = \begin{pmatrix} [\alpha]_1^{-1}+[\Delta]_{11} & [\Delta]_{12} & \cdots & [\Delta]_{1m} \\ [\Delta]_{21} & [\alpha]_2^{-1}+[\Delta]_{22} & \cdots & [\Delta]_{2m} \\ \vdots & \vdots & \ddots & \vdots \\ [\Delta]_{m1} & [\Delta]_{m2} & \cdots & [\alpha]_m^{-1}+[\Delta]_{mm} \end{pmatrix}^{-1} \begin{Bmatrix} \{F\}_1 \\ \{F\}_2 \\ \vdots \\ \vdots \\ \{F\}_m \end{Bmatrix} \tag{3.19}$$

Equation (3.18) can be written in a more compact form as:

$$\{X\} = [\theta]\{F\} \tag{3.20}$$

where;

$$\theta = \begin{pmatrix} [\alpha]_1^{-1}+[\Delta]_{11} & [\Delta]_{12} & \cdots & [\Delta]_{1m} \\ [\Delta]_{21} & [\alpha]_2^{-1}+[\Delta]_{22} & \cdots & [\Delta]_{2m} \\ \vdots & \vdots & \ddots & \vdots \\ [\Delta]_{m1} & [\Delta]_{m2} & \cdots & [\alpha]_m^{-1}+[\Delta]_{mm} \end{pmatrix}^{-1} \tag{3.21}$$

In Equation 3.15 and 3.20, θ is the response level dependent quasilinear receptance matrix of the structure.

Equations (3.16) and (3.21), require to take the inverse of a large matrix to form $[\theta]$, if the system investigated is a large system. Therefore, the response calculation of a large structure for several frequencies by using Equations (3.16) and (3.21) is numerically costly. However, in case the nonlinearity in a structure is local then the nonlinearity matrix would be highly sparse. Its elements can be considered as modifications to the receptance matrix of the corresponding linear system at the desired frequency. This kind of modification can be applied by using the method developed by Özgüven [61] for the harmonic response analysis of nonproportionally damped linear structures. The method in [61] is extended to nonlinear systems by Tanrıkulu, et al. [19] and Maliha, et al. [25], by considering the equation in which the dynamic stiffness matrix of the linear part can be partitioned as follows (in the following equations the subscript m is dropped for simplicity):

$$\begin{pmatrix} [\alpha_{11}]^{-1} & [\alpha_{12}]^{-1} \\ [\alpha_{21}]^{-1} & [\alpha_{22}]^{-1} \end{pmatrix} \begin{Bmatrix} \{X_1\} \\ \{X_2\} \end{Bmatrix} + \begin{pmatrix} [\Delta_{11}] & 0 \\ 0 & 0 \end{pmatrix} \begin{Bmatrix} \{X_1\} \\ \{X_2\} \end{Bmatrix} = \begin{Bmatrix} \{F_1\} \\ \{F_2\} \end{Bmatrix} \qquad (3.22)$$

where subscript "11" stands for the matrix elements corresponding to the coordinates having nonlinear connection, whereas "22" stands for the matrix elements corresponding to the coordinates having no nonlinear connection.

In Equation (3.22), $[\Delta_{11}]$ matrix includes multi harmonic quasilinear coefficients of the nonlinear coordinates as well. Besides, $\{X_1\}$ includes the multi harmonic responses of the coordinates affected by nonlinearities. Then, quasilinear recepance matrix of the nonlinear system can be found from:

$$\begin{aligned} [\theta_{11}] &= [[I] + [\alpha_{11}][\Delta_{11}]]^{-1}[\alpha_{11}] \\ [\theta_{12}] &= [\theta_{21}]^T = [[I]+[\alpha_{11}][\Delta_{11}]]^{-1}[\alpha_{12}] \\ [\theta_{22}] &= [\alpha_{22}] - [\alpha_{21}][\Delta_{11}][\theta_{12}] \end{aligned} \qquad (3.23)$$

Additional computational time saving can be achieved by avoiding the matrix inversion in Equation (3.7), namely, in the equation which is used to find the receptance matrix of the linear system in large systems. In fact, the receptance matrix of the linear part of the system can be determined through the modal summation, which can be formulated for the m^{th} harmonic as:

$$[\alpha]_m = \sum_{r=1}^{N} \frac{\{\Phi^r\}\{\Phi^r\}^T}{(\omega_r^2 - (m\omega)^2 + i\eta_r\omega_r^2)} \qquad (m = q_1, q_2, q_3, q_4, ..., q_p) \qquad (3.24)$$

where $\{\Phi^r\}$ is the r^{th} modal vector, ω_r is the r^{th} natural frequency of the undamped linear part of the structure and η_r is the r^{th} structural damping proportionality constant.

The receptance of the system can be found by taking reduced number of modal parameters into account by modal truncation such that N << n , which can reduce the computational effort drastically.

Since the nonlinearity matrix is expressed in terms of analytically obtained describing functions defined as a function of unknown response values which is the X vector, the solution requires an iterative procedure.

$$\{X\}_{j+1} = [\theta]_j \{F\} \qquad (j = 1, 2, 3, ...) \tag{3.25}$$

In Equation (3.25), $\{X\}_{j+1}$ is the complex displacement amplitude vector at the $(j+1)^{th}$ iteration step, while $[\theta]_j$ is the quasilinear recepance matrix at the j^{th} iteration step that is obtained by using $\{X\}_j$.

Then, $\{X\}$ can be calculated from the quasilinear receptance matrix obtained by using either Equations (3.16) or (3.21), by updating at every iteration step. Such an iteration procedure is the implementation of the "fixed point iteration method". Iterations are to be repeated until a specified tolerance is reached. The convergence criteria can be specified as:

$$e = \frac{|\{X\}_{j+1} - \{X\}_j|}{|\{X\}_j|} x100 \tag{3.26}$$

The number of iterations can be drastically reduced, if instead of $\{X\}_{j+1}$, the avaraged displacement $\{X^*\}_{j+1}$ is used for the next iteration [19].

$$\{X^*\}_{j+1} = \frac{\{X\}_{j+1} - \{X\}_j}{2} \tag{3.27}$$

Moreover, in case of divergent or numerically unstable solutions, relaxation on the fixed point iteration to obtain a fast convergence, can be applied as [21, 62] :

$$\{X^*\}_{j+1} = (1 - \lambda)\{X\}_{j+1} - \lambda\{X\}_j \qquad (0 \le \lambda \le 1) \tag{3.28}$$

To obtain the multiple solutions due to nonlinearity, computations will be performed in the range of interest from low-to-high and then from high-to-low frequency values. The linear response of the system at a starting frequency is taken as the initial guess for the displacement vector $\{X\}_j$ at that frequency. After that, at other frequencies, the solution obtained at the previous frequency step is taken as the initial guess [19, 21, 62].

CHAPTER 4

COMPUTER PROGRAM: MH-NLS

4.1 Introduction

The theory and the mathematical formulations described in the previous chapters are implemented in MATLAB® environment and an original computer program, called "MH-NLS" (**M**ulti **H**armonic **N**on-**L**inear **S**olver), with a user friendly graphical user interface (GUI) is constructed, in order to analyze the nonlinear response characteristics of MDOF systems. The program is compatible with a popular finite element program, ANSYS®, and takes an output file of that program in the preprocessing stage to form the system matrices in structural dynamic analysis. In this chapter, this program will be introduced by defining its basic features. The user manual of the program is given in Appendix A. The logic of the program is summarized in the flow chart shown in Figure 4.12.

4.2 Program Description

MH-NLS is a MATLAB® based GUI program which computes the harmonic nonlinear response of selected degrees of freedom of a nonlinear MDOF structure. The preprocessing stage of the program mainly consists of:

- Defining the system to be analyzed,
- Selecting the solution parameters and the method,
- Setting the nonlinear connections and variables
- Describing the response coordinates for output.

The output of the program is amplitude of the response and frequency response values of selected coordinates at predetermined forcing level over a frequency range. Program is capable of analyzing systems with following types of:

- Cubic stiffness,
- Coulomb damping,
- Piecewise linear stiffness,
- Preloaded stiffness,
- Arctan stiffness,

Apart from nonlinearities, user can also define linear local viscous dampers between coordinates.

4.2.1 Preprocessing

The preprocessing stage of MH-NLS, like preprocessing stages of other programs such as ANSYS®, PATRAN®, etc., prepares the program for the solution procedure. The starting point of the preprocessing stage is to introduce the system to be analyzed, namely, the mass, stiffness, damping and external forcing matrices of the system. This can be accomplished by simply loading of a text file which is an output of the ANSYS® program. This text file can be created by the ANSYS® program by following the instructions given in Appendix B. The content of a sample file which is created by analayzing the system given in Figure 5.10, is depicted in Appendix C.

Loading operation is realized by a special algorithm which can read and form the system matricies from an output file of ANSYS®. This algorithm is given in Appendix D. The structural damping is modelled as proportional damping and the loss factor of the material is entered as an input before loading operation. Loading operation creates [M], [K], [H] matrices and {F} vector. Then undamped natural frequencies of the system are computed and displayed on the GUI window in order to guide the user for further parameter selections.

Solution parameters such as:

- Lower and upper limits of the frequency range of interest
- Number of frequency points
- Allowable percentage error tolerance
- Maximum iteration number
- Relaxation number for converging and diverging solutions [21]

can be entered through the GUI window.

FRF matrix construction method can also be selected depending on the system size. For systems with small degrees of freedom, MATLAB® gives fast solution with matrix inversion, whereas for large systems, modal summation with limited number of modes is the best choice in obtaining FRF of the linear part of the system for fast solution with reasonable accuracy.

Next preprocessing stage is setting the position and parameters of the nonlinearities in the system. Nonlinearity types given in Section 2.4 can be easily defined by illustrative GUI windows that involve schematic diagrams and describing paramters for different types of nonlinearities (Appendix A).

Although, the external force vector on the system can be modelled in ANSYS® and laoded from the file created, it is also possible to define different force values on different coordinates. It is also possible to switch back again to the force vector loaded from the file for further usage in the solution procedure.

Three types of solution methods are defined in the program, namely:

- Single harmonic solution
- Higher harmonic solution

- Multi harmonic solution.

These three types of solution methods are based on corresponding describing function theories, which are single, higher and multi harmonic describing function theories. The selections other than single harmonic solution needs defining the number of harmonic component used in solution formulation. Single harmonic describing functions are programmed as formulas, whereas higher and multi harmonic describing functions are calculated with pre-defined numerical integration formulations. Because of the numerical integration procedure, higher and multi harmonic solutions are completed in much longer time than single harmonic solution.

The last preprocessing stage is defining the response coordinate and FRF elements to be observed. The response coordinate X, elements of FRF matrix, α_1 and α_2, which can be any number in ranges $1 \leq X \leq n$, $1 \leq \alpha_1 \leq n$, $1 \leq \alpha_2 \leq n$.

In ANSYS®, the nodes are numbered and for each node the x, y, and z DOFs are specified. However in MH-NLS, each DOF is specified with a different number (See Table 4.1) which are also defined in ANSYS output file (given as row number in load vector definition). In specifying coordinates where a nonlinear element is connected or a force is applied and for output coordinate definition, one should use the coordinate numbers used in MH-NLS.

Table 4.1 Renumbering strategy during file loading process

MH-NLS Coordinates	ANSYS® Node Number	DOF components of nodes
1 ←	1	UX
2 ←	1	UY
3 ←	2	UX
4 ←	2	UY

It can be seen from Table 4.1 that, the UY component of the first node in ANSYS® is recognized as the second coordinate of the system by the program. To determine the renumbering of each DOF in defining nonlinearities, forcing and output coordinates, user should use the output file of ANSYS®. The renumbered DOFs are given as row numbers in the load vector defined in the ANSYS® output file (See APPENDIX C).

4.2.2 Solution Algorithm

When the user clicks the solution button in the GUI, program first sets the solution parameters defined by the user. The next step is determining the necessary coordinates (NC) which will be used in the calculation procedure. These coordinates are the ones having nonlinear connection, external forcing and the coordinates for which response and FRF computations will be performed. As stated before in Section 3.2, in systems where the nonlinearities are localized to a few coordinates only, arranging the systems matrices (SM) in such a partitioned way that the NC and all coordinates except NC can be arranged like:

$$SM = \begin{pmatrix} [SM]_{11} & [SM]_{12} \\ [SM]_{21} & [SM]_{22} \end{pmatrix} \tag{4.1}$$

will reduce the computational effort considerably. In Equation (4.1), 1 denotes NC and 2 denotes all coordinates except NC. The SM are symmetric such that:

$$[SM]_{12} = [SM]_{21} \tag{4.2}$$

By using the predetermined NC, the system matrices [M], [K], [H], {F} are reordered. In higher and multi harmonic solutions, further reordering will be performed on higher order FRF matrix. The methodology of this procedure is explained below:

Whether the FRF matrix is constructed with matrix inversion or modal summation, the matrix will be in the form:

$$[\alpha] = \begin{pmatrix} [\alpha]_1 & 0 & \cdots & 0 \\ 0 & [\alpha]_2 & \cdots & 0 \\ \vdots & \vdots & \ddots & \vdots \\ 0 & 0 & \cdots & [\alpha]_m \end{pmatrix} \tag{4.3}$$

The matrix can also be expressed by considering the NC as:

$$[\alpha] = \begin{pmatrix} \begin{pmatrix} [\alpha]_{11} & [\alpha]_{12} \\ [\alpha]_{21} & [\alpha]_{22} \end{pmatrix}_1 & 0 & \cdots & 0 \\ 0 & \begin{pmatrix} [\alpha]_{11} & [\alpha]_{12} \\ [\alpha]_{21} & [\alpha]_{22} \end{pmatrix}_2 & \cdots & 0 \\ \vdots & \vdots & \ddots & \vdots \\ 0 & 0 & \cdots & \begin{pmatrix} [\alpha]_{11} & [\alpha]_{12} \\ [\alpha]_{21} & [\alpha]_{22} \end{pmatrix}_m \end{pmatrix} \tag{4.4}$$

In order to be able to use the Equation (3.23), the matrix in Equation (4.4) should be reordered in such a way that the necessary coordinates of both single and multi harmonic components of the FRF matrix are collected. After obtaining $[\alpha]$ (Equation 4.4), the submatrices $[\alpha]_{11}$ and $[\alpha]_{12}$ which will be used in Equation (3.23) will be in the following form:

$$[\alpha]_{11} = \begin{pmatrix} [\alpha]_{11\ 1} & 0 & \cdots & 0 \\ 0 & [\alpha]_{11\ 2} & \cdots & 0 \\ \vdots & \vdots & \ddots & \vdots \\ 0 & 0 & \cdots & [\alpha]_{11\ m} \end{pmatrix} \tag{4.5}$$

$$[\alpha]_{12} = \begin{pmatrix} [\alpha]_{12\ 1} & 0 & \cdots & 0 \\ 0 & [\alpha]_{12\ 2} & \cdots & 0 \\ \vdots & \vdots & \ddots & \vdots \\ 0 & 0 & \cdots & [\alpha]_{12\ m} \end{pmatrix} \tag{4.6}$$

Since all necessary information for the calculation is presented in $[\alpha]_{11}$ and $[\alpha]_{12}$, the other elements $[\alpha]_{21}$ and $[\alpha]_{22}$ are not necessary for further calculations. The required pseudo-receptance elements of $[\theta]$, $[\theta_{11}]$ and $[\theta_{12}]$, can easily be found by using Equation (3.23). Then the desired response values can be found by using the equation:

$$\begin{bmatrix} \overset{(NCN.m)x(NCN.m)}{[\theta_{11}]} & \overset{(NCN.m)x(n-NCN).m}{[\theta_{12}]} \end{bmatrix} \overset{(n.m)x1}{F} = \overset{(NCN.m)x1}{\{X\}} \tag{4.7}$$

where:

NCN : Number of Necessary Coordinates

m : Harmonic Number

n : Degree of Freedom

Equation (4.7) confirms that the result gives all the harmonic response components of NC.

The formulations given above can handle single and multiharmonic solution; however, different solution algorithm should be used for higher order solution. This situation can be explained by looking at the equation that gives response for higher order solution:

$$\begin{Bmatrix} \{X\}_1 \\ \{X\}_2 \\ \vdots \\ \vdots \\ \{X\}_m \end{Bmatrix} = \begin{pmatrix} [\alpha]_1^{-1}+[\Delta]_1 & 0 & \cdots & 0 \\ 0 & [\alpha]_2^{-1}+[\Delta]_2 & \cdots & 0 \\ \vdots & \vdots & \ddots & \vdots \\ 0 & 0 & \cdots & [\alpha]_m^{-1}+[\Delta]_m \end{pmatrix}^{-1} \begin{Bmatrix} \{F\}_1 \\ \{F\}_2 \\ \vdots \\ \vdots \\ \{F\}_m \end{Bmatrix} \tag{4.8}$$

In Equation (4.8), all $\{F\}$ terms other than $\{F\}_1$ are zero. Moreover, the inverse of the so-called pseudo dynamic stiffness matrix, which is the PRM, has the same diagonal characteristic like itself. As a result, the multiplication of the pseudoreceptance with forcing vector forms a response matrix having zero higher harmonic components. To avoid this situation and find the higher order harmonic terms of the response, Equation (4.8) can be divided into two equations:

$$\{X\}_1 = \left[[\alpha]_1^{-1} + [\Delta]_1 \right]^{-1} \{F\}_1 \tag{4.9}$$

$$\begin{pmatrix} [\alpha]_2^{-1}+[\Delta]_2 & 0 & \cdots & 0 \\ 0 & [\alpha]_3^{-1}+[\Delta]_3 & 0 & 0 \\ \vdots & \vdots & \ddots & \vdots \\ 0 & 0 & \cdots & [\alpha]_m^{-1}+[\Delta]_m \end{pmatrix} \begin{Bmatrix} \{X\}_2 \\ \{X\}_3 \\ \vdots \\ \{X\}_m \end{Bmatrix} = \begin{Bmatrix} \{F\}_2 \\ \{F\}_3 \\ \vdots \\ \{F\}_m \end{Bmatrix} \tag{4.10}$$

Since the terms in the right hand side of Equation (4.10) is zero, the higher order responses can be found by using the iterative formulation by reordering the terms in Equation (4.10).

$$\begin{Bmatrix} \{X\}_2 \\ \{X\}_3 \\ \vdots \\ \{X\}_m \end{Bmatrix}_{j+1} = -\begin{pmatrix} [\alpha]_2 & 0 & \cdots & 0 \\ 0 & [\alpha]_3 & 0 & 0 \\ \vdots & \vdots & \ddots & \vdots \\ 0 & 0 & \cdots & [\alpha]_m \end{pmatrix}\begin{pmatrix} [\Delta]_2 & 0 & \cdots & 0 \\ 0 & [\Delta]_3 & 0 & 0 \\ \vdots & \vdots & \ddots & \vdots \\ 0 & 0 & \cdots & [\Delta]_m \end{pmatrix}_j \begin{Bmatrix} \{X\}_2 \\ \{X\}_3 \\ \vdots \\ \{X\}_m \end{Bmatrix}_j \tag{4.11}$$

The calculations in the solution algorithm are performed with constant frequency increment. For single harmonic solution, both low-to-high and high-to-low frequency sweeps are calculated whereas for higher and multi harmonic solutions only low-to-high frequency sweep calculations are performed because of the calculation time concerns. In addition to the response and FRF plots, results can also be saved to text files for further use.

The converging and diverging relaxation numbers are switched by the program by comparing the error obtained at present and previous steps. After relaxation, the average of the previous and current iteration of the response value will be used for further computations (Equation 3.27). When the convergence criterion is satisfied by the current iteration value, the program stops the iteration and switches to the forward frequency value in the frequency range.

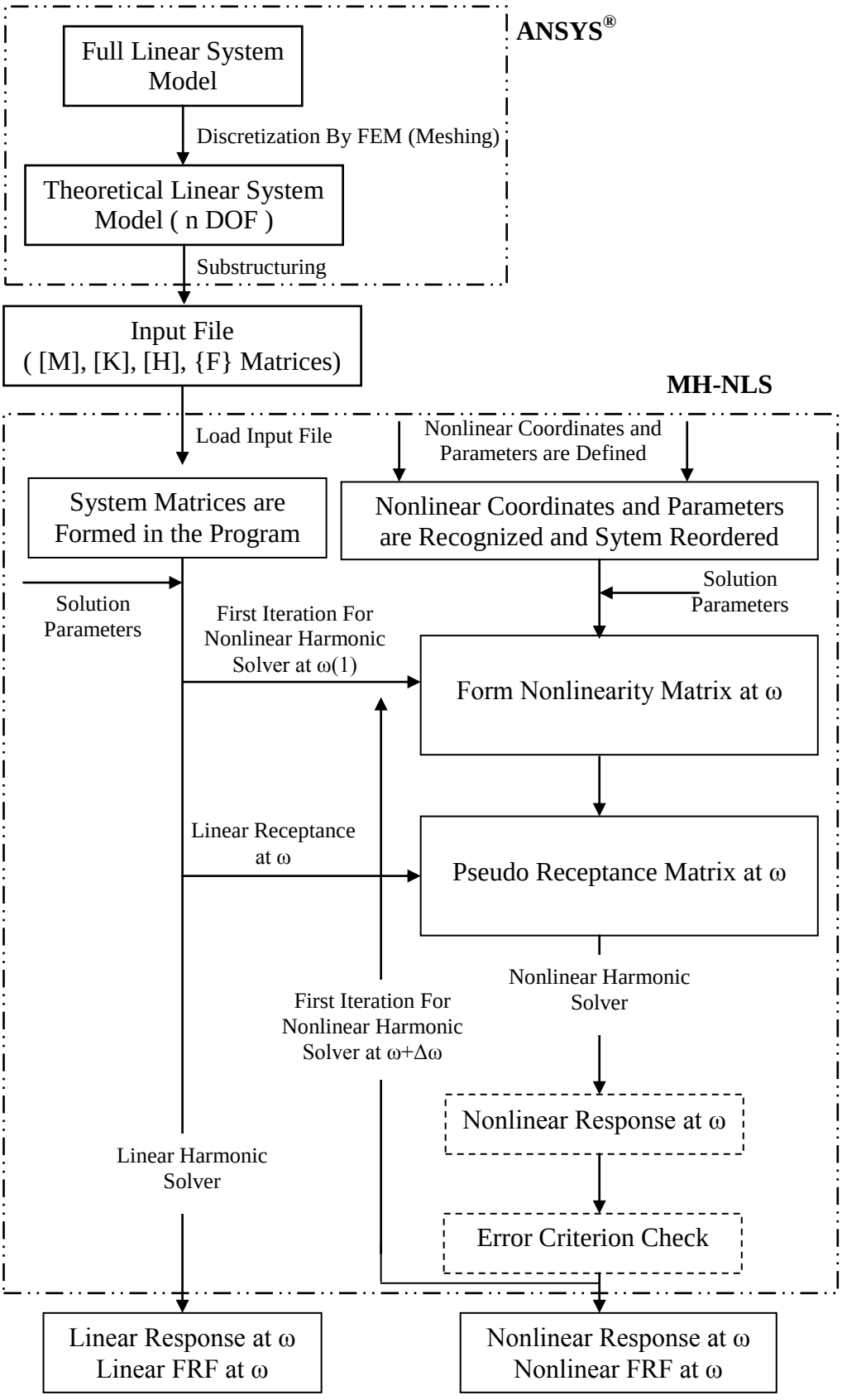

Figure 4.1 Flow diagram of the harmonic nonlinear analysis

4.3 Post Processing

The output of the program is both text files and the plots. For single harmonic solution, response plot is the simply the response to the prescribed harmonic forcing. However, for higher and multi harmonic responses, there will be "harmonic number+1" plots which are the response of all harmonics on the same window, the first harmonic response and the m^{th} harmonic response of the required coordinate ($m=1, 2, \ldots, q_p$) (Figure 4.2 and 4.3).

The plot (Figure 4.4), which gives the FRF for given coordinates i and j and harmonic m in MH-NLS, is simply the i-j^{th} element of m^{th} diagonal (DOF x DOF) sized matrix of PRM (See APPENDIX A).

The solution time for the calculation is displayed on the GUI window.

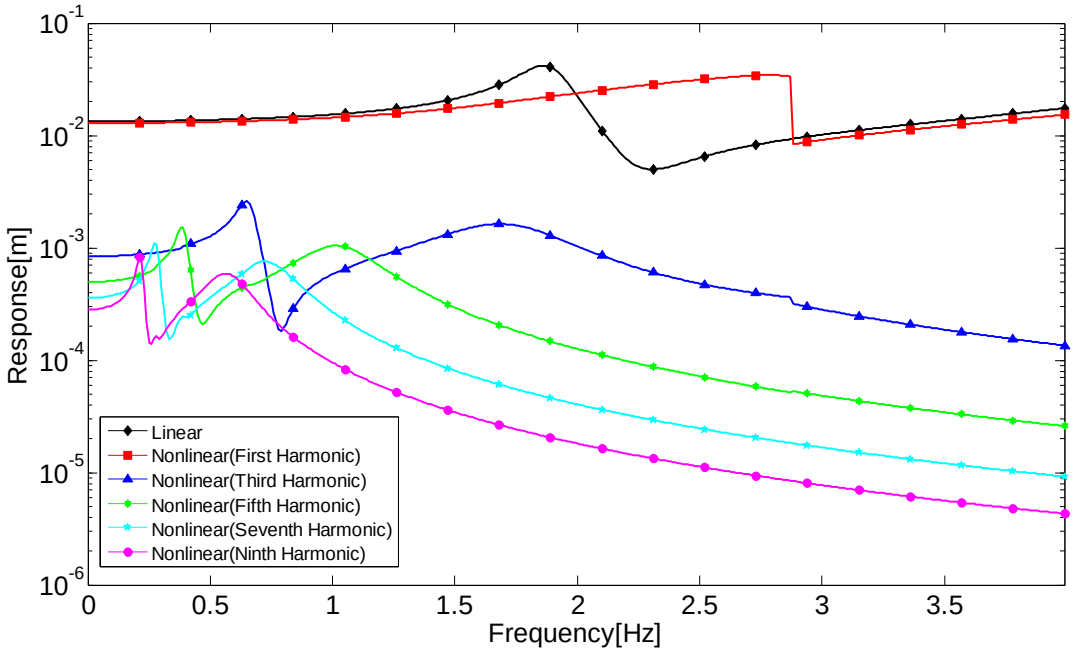

Figure 4.2 A typical response plot of all harmonic components

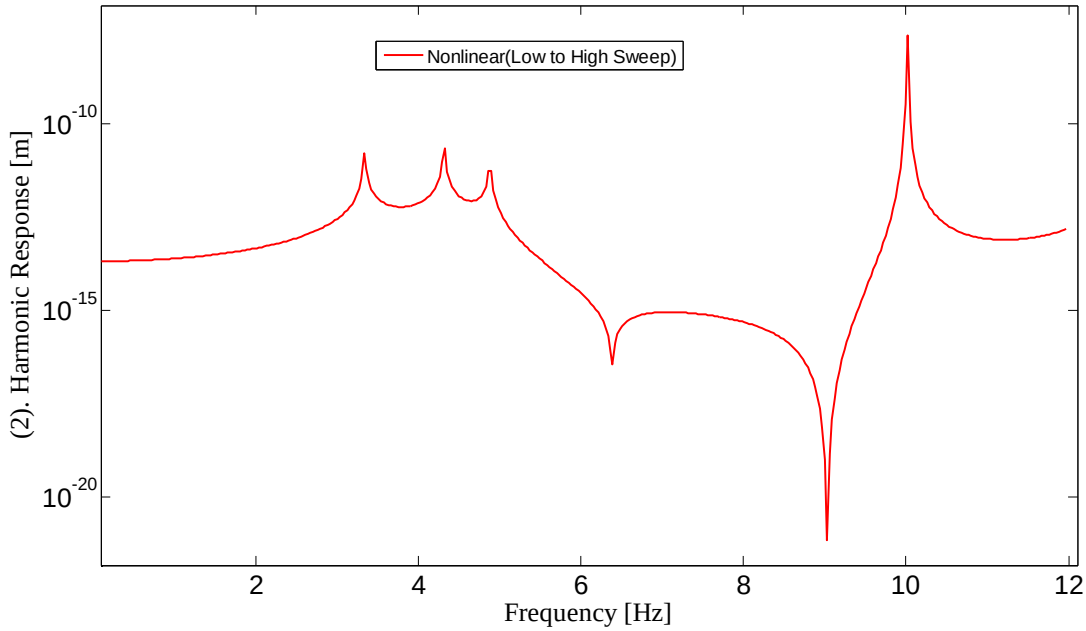

Figure 4.3 A typical response plot of second harmonic component

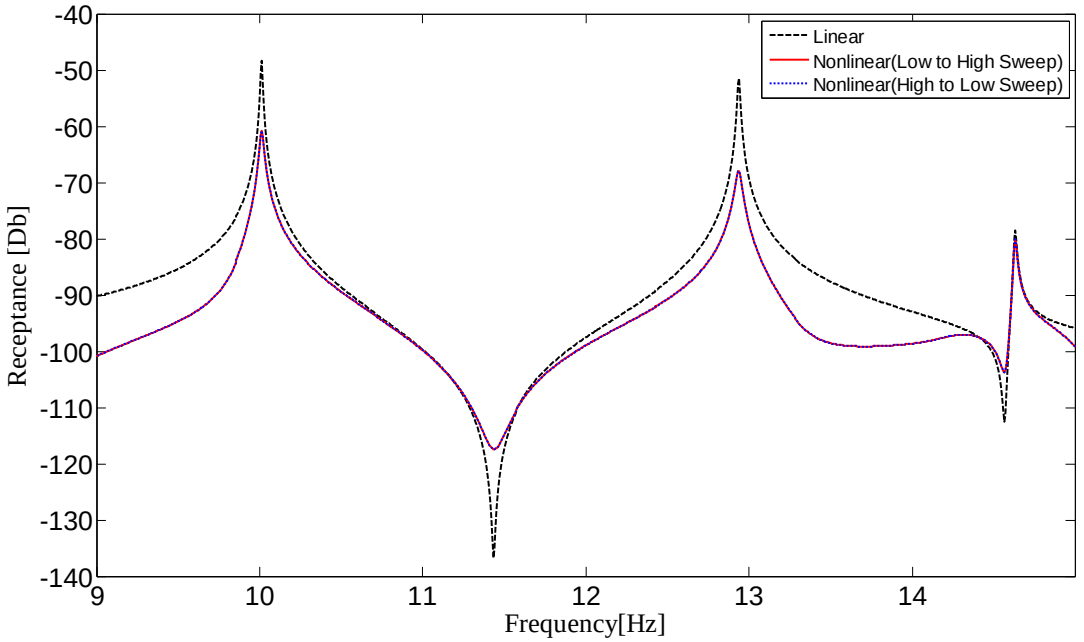

Figure 4.4 A typical FRF plot

CHAPTER 5

VERIFICATION OF THE PROGRAM

In this chapter, case studies to demonstrate the validity of the computer program developed will be given. The results obtained by using the program will be compared with the frequency domain solutions of several case studies found in the literature. Finally, comparison with the time domain integration results will be presented by using further case studies. The case studies corresponding to the problems taken from literature are numbered using letter “L” while case studies corresponding to the time integration comparisons are numbered using letter “T”.

5.1 Comparison of the Program Solutions with Results Given in Literature

For comparison of the program solution with respect to the solutions found in the literature, some case studies of the previous works are solved and the solutions are compared.

5.1.1 Case Study L.1

Siller [9] ignores the multi harmonic effects and concentrates on single harmonic solution. Performed case study L.1, considered as sample case 1 in [9], is a 3-DOF system, consist of 3 masses and each mass is linked to each other and to the ground by linear stiffness and damping elements, creating fully populated linear matrices. The system is excited by a single harmonic force at mass m_2. The diagram of the system is given in Figure 5.1.

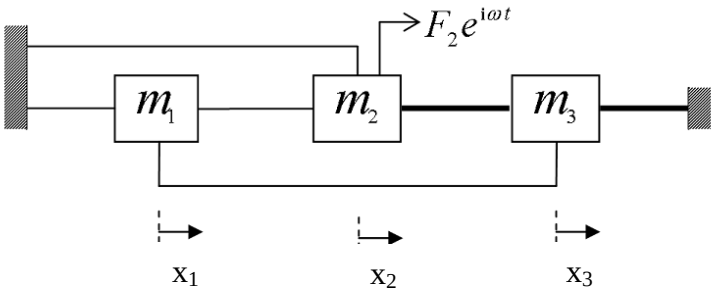

Figure 5.1 Diagram for case study L.1 [9]

The numerical values of all the system coefficients are given below in matrix format:

$$[M]=\begin{pmatrix} m_{11} & 0 & 0 \\ 0 & m_{22} & 0 \\ 0 & 0 & m_{33} \end{pmatrix}=\begin{pmatrix} 31.59 & 0 & 0 \\ 0 & 55.401 & 0 \\ 0 & 0 & 24.212 \end{pmatrix} \text{ kg}$$

$$[K]=\begin{pmatrix} k_{11} & k_{12} & k_{13} \\ k_{21} & k_{22} & k_{23} \\ k_{31} & k_{32} & k_{33} \end{pmatrix}=\begin{pmatrix} 200491.263 & -64920.98 & -36279.371 \\ -64920.98 & 398118.365 & -17503.205 \\ -36279.371 & -17503.205 & 132578.825 \end{pmatrix} \text{ N/m}$$

$$\{F\}=\begin{Bmatrix} F_1 \\ F_2 \\ F_3 \end{Bmatrix}=\begin{Bmatrix} 0 \\ 12 \\ 0 \end{Bmatrix} \text{ N}$$

The system is proportionally damped, where the loss factor is 0.12%

The nonlinearities defined between coordinates are given in Table 5.1. In Figure 5.1, nonlinear connections are indicated as bold lines.

Table 5.1 Nonlinearity definitions for case study L.1

Nonlinear Connections:(DOF1-DOF2)	Cubic Stiffness Coefficient:β (N/m^3)
2-3	7.82e6
3-3(Ground)	1.44e7

The frequency domain solutions of case study L.1 given in [9] are presented in Figure 5.2 and Figure 5.3. Single harmonic solutions of the same system analyzed with MH-NLS are given in Figure 5.4 and 5.5.

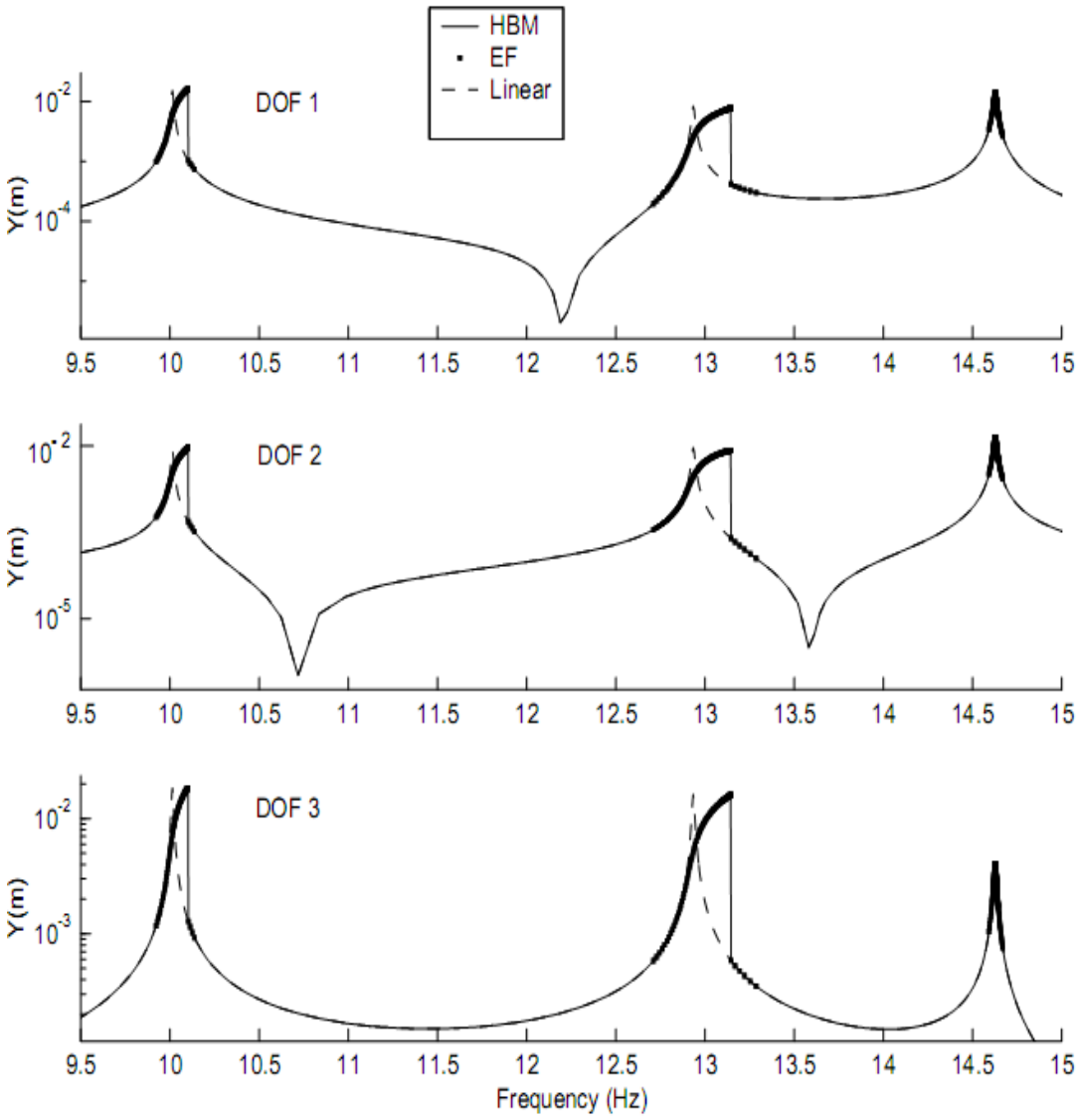

Figure 5.2 Calculated nonlinear response for case study L.1 given in [9]

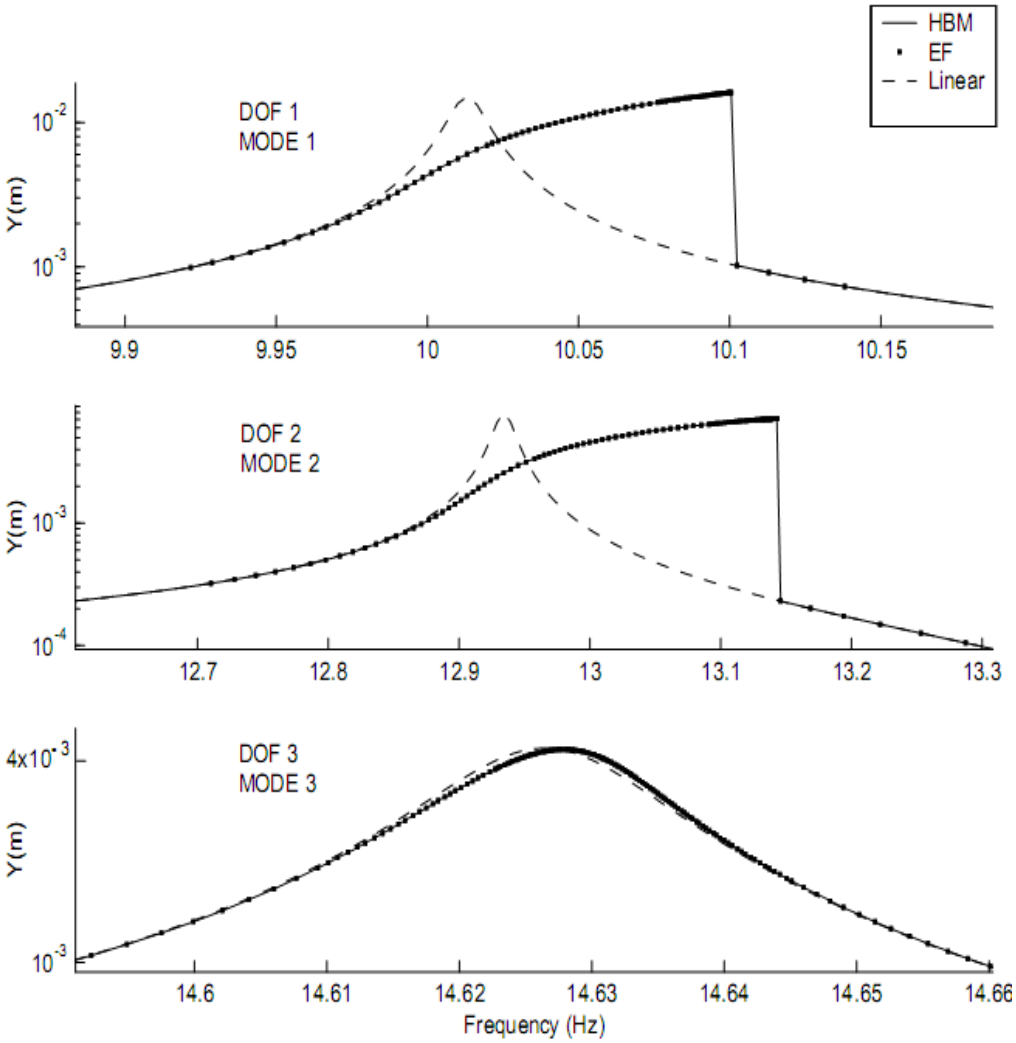

Figure 5.3 Calculated nonlinear response for case study L.1, zoom-in of the individual resonances [9]

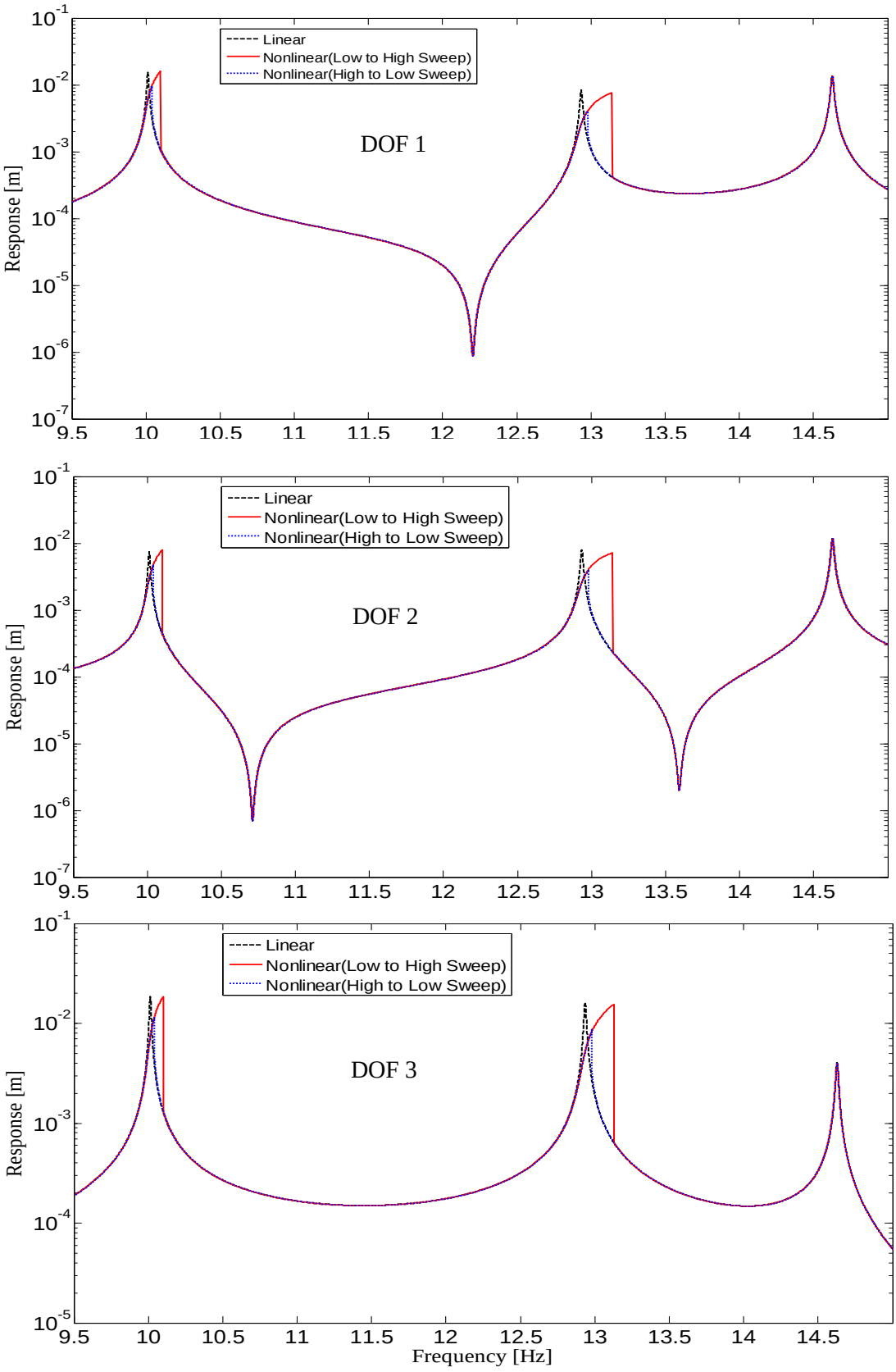

Figure 5.4 MH-NLS solution of case study L.1

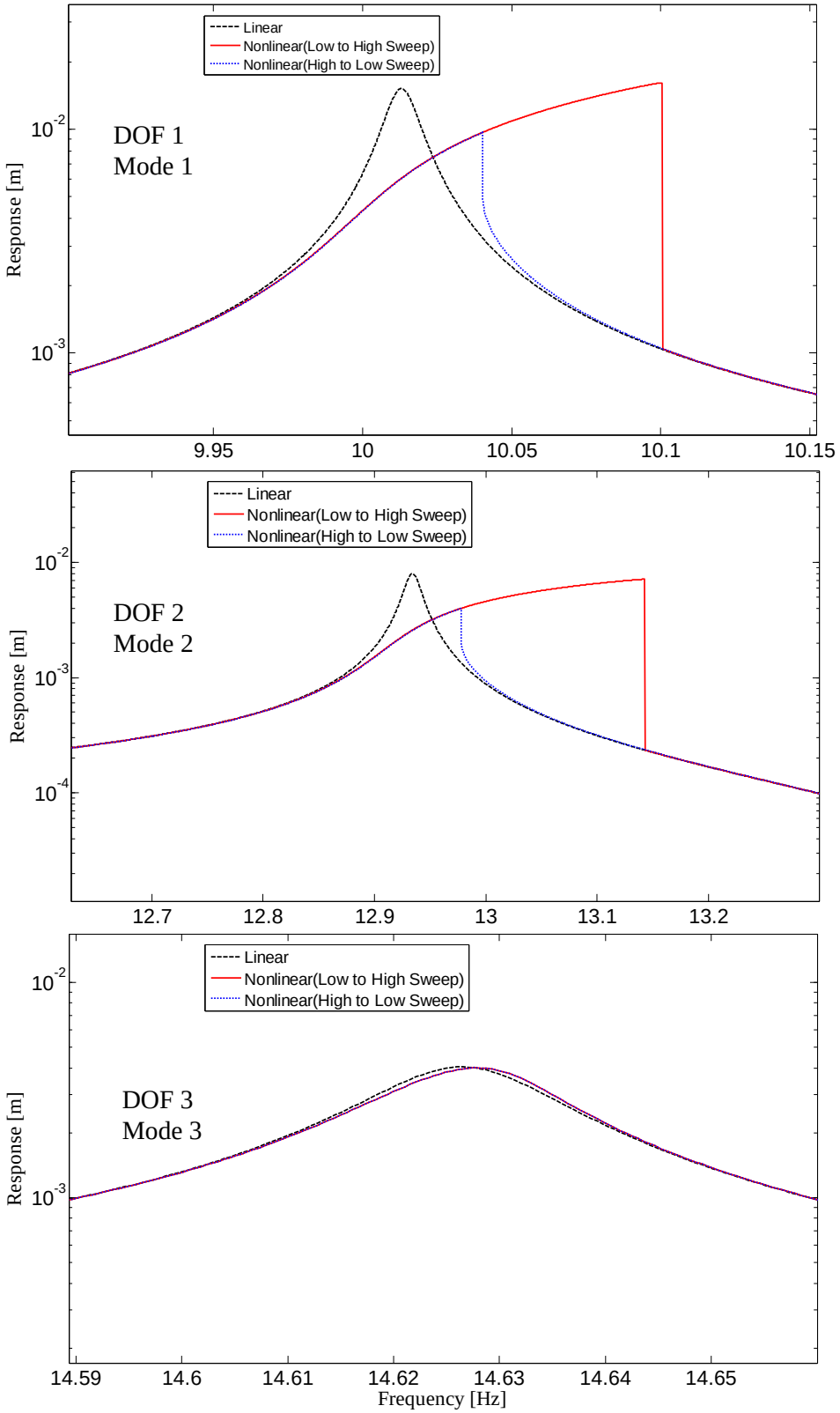

Figure 5.5 MH-NLS solution of case study L.1, zoom-in of the individual resonances

It is clear that the results are showing the same behavior as the results of the previous work [9]. Moreover, multi harmonic solution of the response of DOF 1 given in Figure 5.6 reveals that multi harmonic components have very small amplitudes relative to the fundamental harmonic component. It can be concluded that single harmonic solution gives satisfactory results with reasonable accuracy in this frequency range. Then it can be concluded that single harmonic solution assumption of [9] is valid.

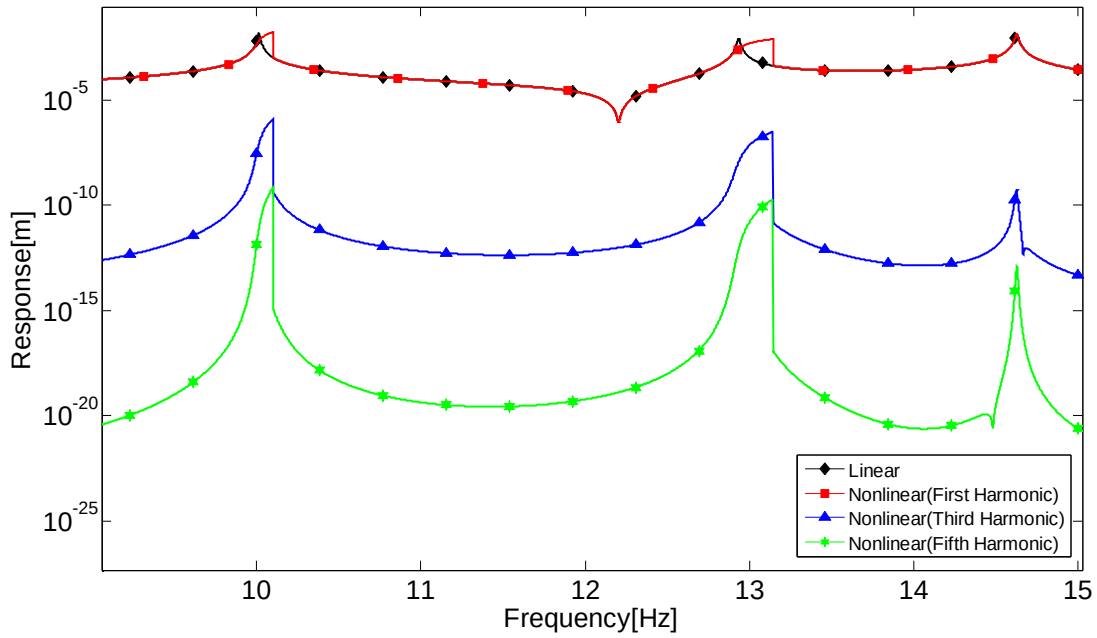

Figure 5.6 MH-NLS multi harmonic solution of DOF 1 of case study L.1, frequency range of interest: 9.5-15 Hz

The multi harmonic effects can more clearly be observed in Figure 5.7 when the frequency range of interest is taken as 0-15 Hz . The frequencies corresponding to the peaks of the third harmonic component between 2.5-6 Hz and the peaks of the fifth harmonic component between 2-3 Hz, are due to the first natural frequency of the undamped part of the system ($\omega_1/3$, $\omega_1/5$) . The multi harmonic components are observable but again have no noticable effect on the total response at corresponding

frequency range since their amplitudes are negligible with respect to the fundamental harmonic component.

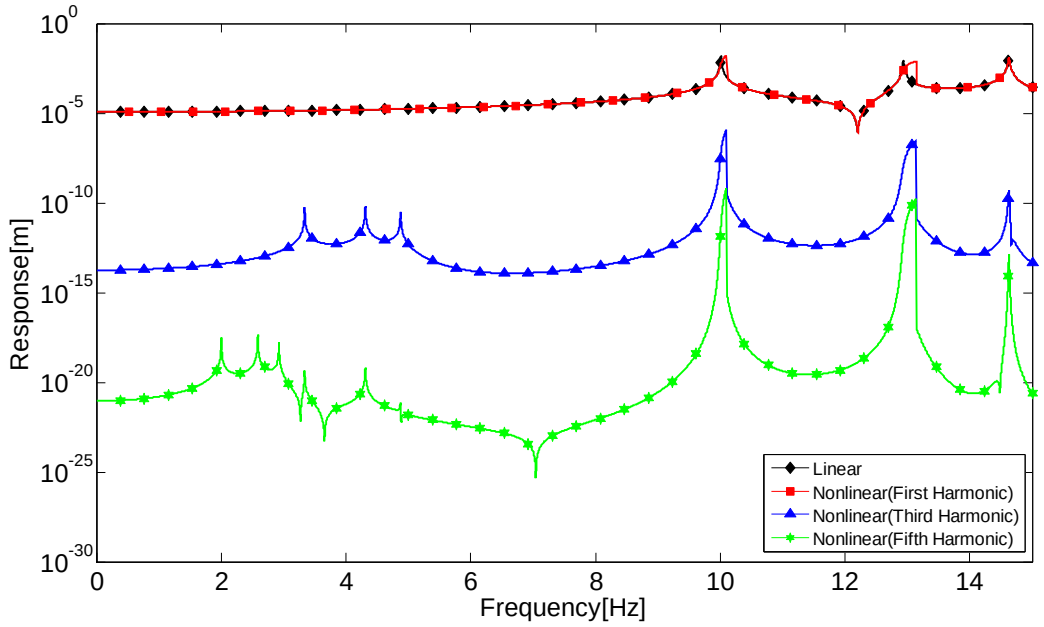

Figure 5.7 MH-NLS multi harmonic solution of DOF 1 of case study L.1, frequency range of interest: 0-15 Hz

During the numerical solution attempts, it is observed that having smaller frequency increments would improve the accuracy of the results by accurately locating the jumping frequency, which also generally corresponds to the resonance frequency. This condition is investigated by several single harmonic solution trials for the second mode corresponding to the first DOF of the case study L.1 using different frequency increment and the results are given in Figure 5.8 and 5.9.

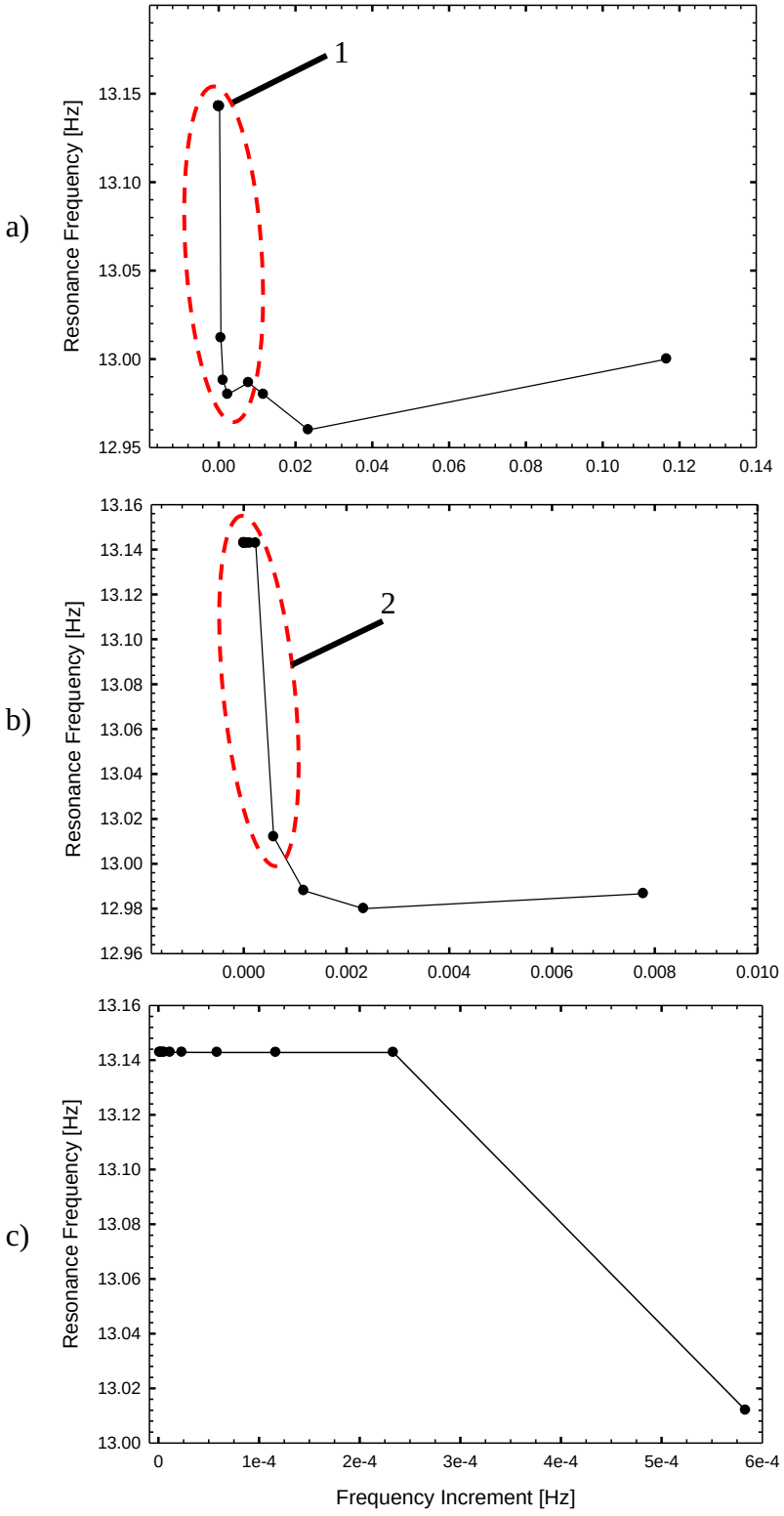

Figure 5.8 The effect of frequency increment at the observed resonance (jump) frequency of mode 2 corresponding to DOF 1, case study L.1

a) Main plot b) Zoom-in ellipse region 1 c) Zoom-in ellipse region 2

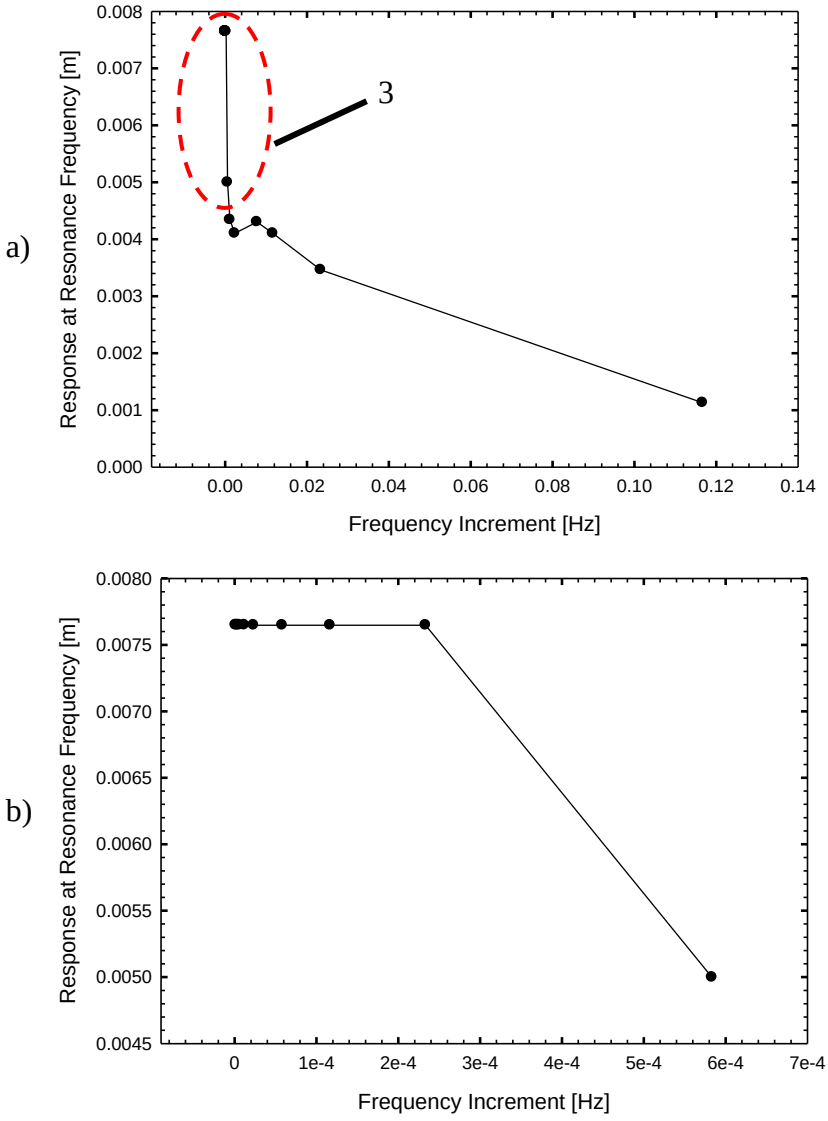

Figure 5.9 The effect of frequency increment on response magnitude at resonance (jump) frequency of mode 2 corresponding to DOF 1, case study L.1

a) Main plot b) Zoom-in ellipse region 3

The results show that, with smaller frequency increment it is more probable to observe the correct jumping frequency. However user should be aware of the fact that smaller frequency increment means more computation time. The opportunity cost between solution time and solution accuracy should be considered before starting the solution.

5.1.2 Case Study L.2

Again the work performed by Siller [9] (sample case 2) is considered. In this case, the system in Figure 5.1 has Colulomb (Friction) damping type nonlinearity. All linear system properties, mass, stiffness, damping and forcing definitions, are same as case study L.1.

The nonlinearities defined between coordinates are given in Table 5.2. Again in Figure 5.1, nonlinear connections are indicated as bold lines.

Table 5.2 Nonlinearity definitions for case study L.1

Nonlinear Connections:(DOF1-DOF2)	Coulomb Friction Force: F_f (N)
2-3	1.25
3-3(Ground)	2.1

The frequency domain solution of the case study L.2 given in [9] is presented in Figure 5.10. Single harmonic solutions of the same system analyzed with MH-NLS and time domain integration results are given in Figure 5.11.

It is clear that the results in Figure 5.11 are showing the same behavior as the results of the previous work [9] but show some discrepancies at some regions (13-14 Hz). But it is clear that the results of MH-NLS are in an excellent agreement with TD integration results, which can be considered as exact solution, at these regions. Solution time comparison of single harmonic FD solution with respect to TD solutions of 3^{rd} DOF is given in Table 5.3.

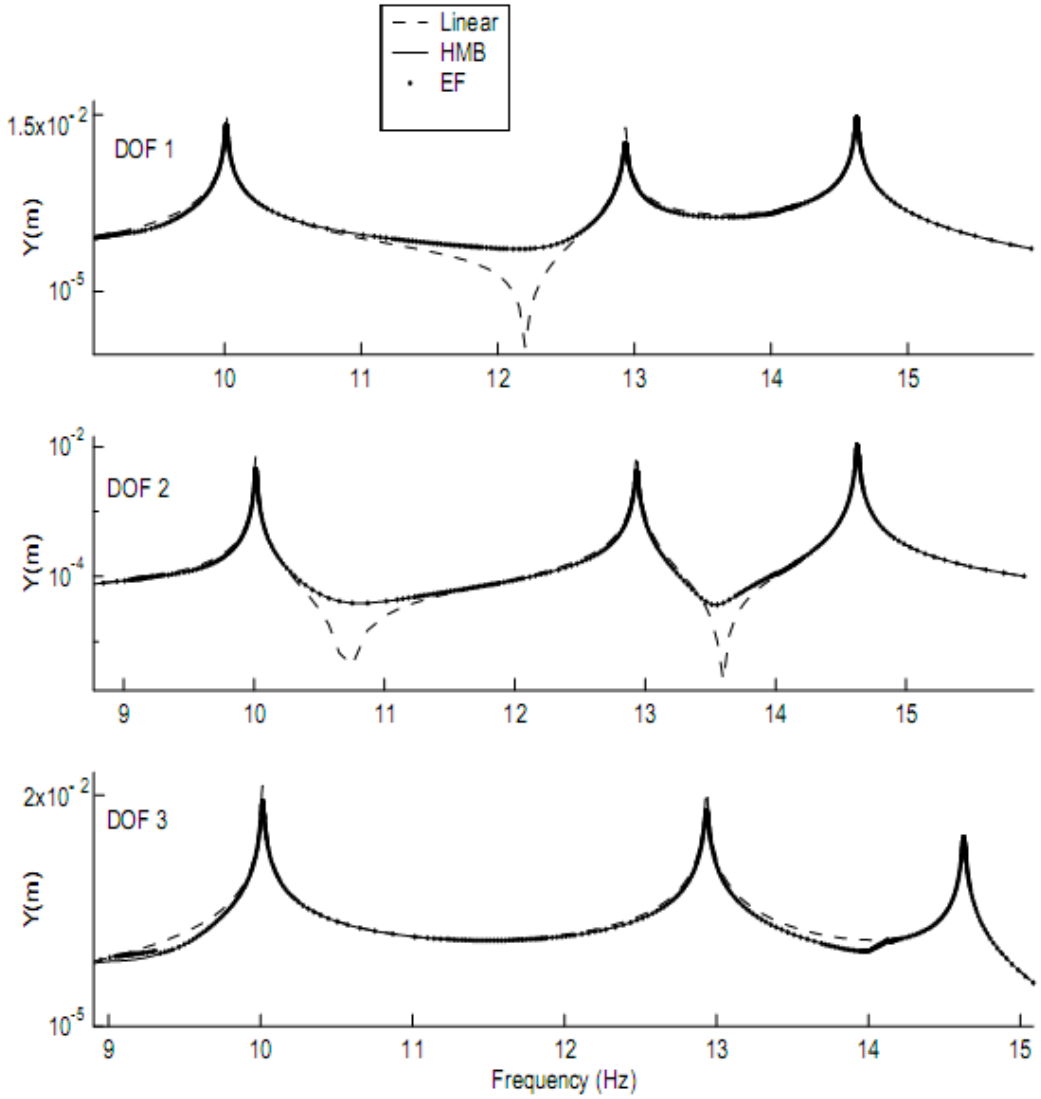

Figure 5.10 Calculated nonlinear response for case study L.2 given in [9]

Table 5.3 Solution Time Comparison for Case Study L.2, times for response calculation of the third DOF

Solution Method	Frequency Increment [Hz]	Solution Time [s]
Single Harmonic	0.006	14
Time Integration (ODE 45) (60 s run for convergence)	0.4	201

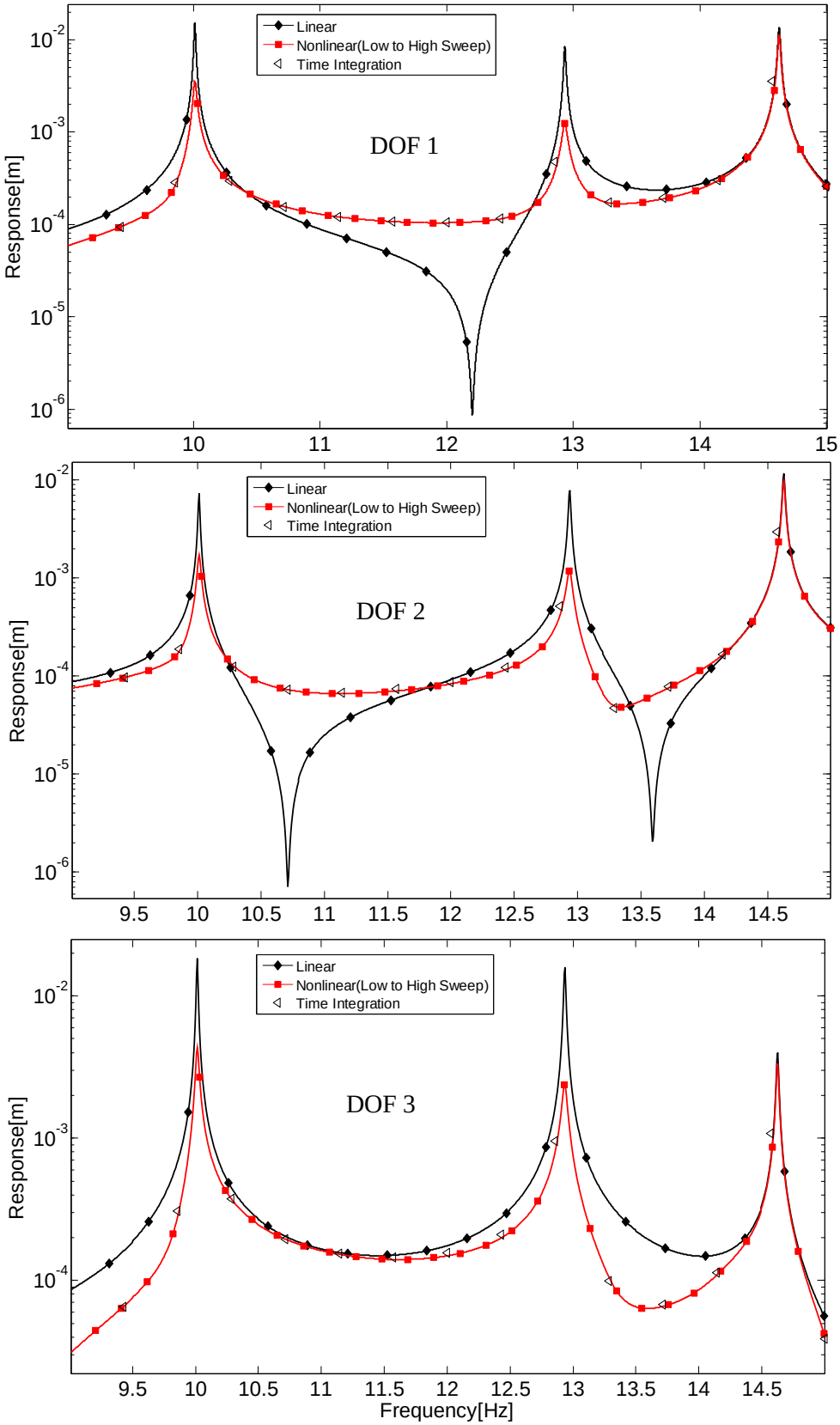

Figure 5.11 Comparison of MH-NLS and TD solutions of case study L.2

5.2 Comparison of the Program Solution with Time Domain Solution

In this section, six different systems will be analyzed by using the program MH-NLS with different kind of nonlinearities and the results will be compared with the time domain integration results. Time domain solutions are obtained by using the ODE integrators of MATLAB®. Integrations are performed by using several integrators like ODE45, ODE113, ODE15s, etc. according to the stiffness characteristics of the problem [64]. Integrations are continued until steady state is reached.

5.2.1 Case Study T.1

Consider the system shown in Figure 5.12. The linear and nonlinear parameters are given as follows:

$$m_1 = 1\,\text{kg}, \quad m_2 = 5\,\text{kg},$$

$$k_1 = k_2 = k_3 = 500\ \text{N/m},$$

$$c_1 = c_2 = c_3 = 5\ \text{Ns/m},$$

$$F_1 = 25\ \text{N}$$

Nonlinearities between coordinates are defined in Table 5.4

Table 5.4 Nonlinearity definitions for case study T.1

Nonlinear Connections: (DOF1-DOF2)	Nonlinearity Type	Nonlinearity Coefficients
1-1(Ground) (s_1^*)	Cubic Stiffness	$\beta = 10^3\ \text{N/m}^3$
2-2(Ground) (s_2^*)	Cubic Stiffness	$\beta = 10^3\ \text{N/m}^3$

The undamped natural frequencies of the system are ω_1=1.894 Hz and ω_2=5.177 Hz. Figure 5.13 shows the variation of multi harmonic solution components of the response (x_1) with respect to the excitation frequency.

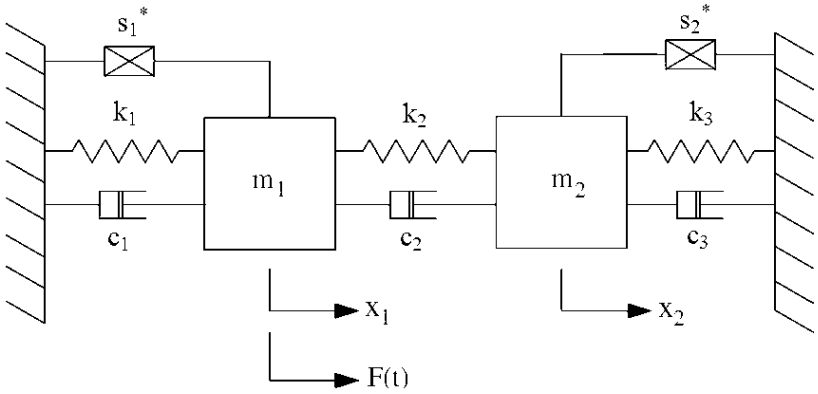

Figure 5.12 A 2-DOF system with 2 nonlinear elements

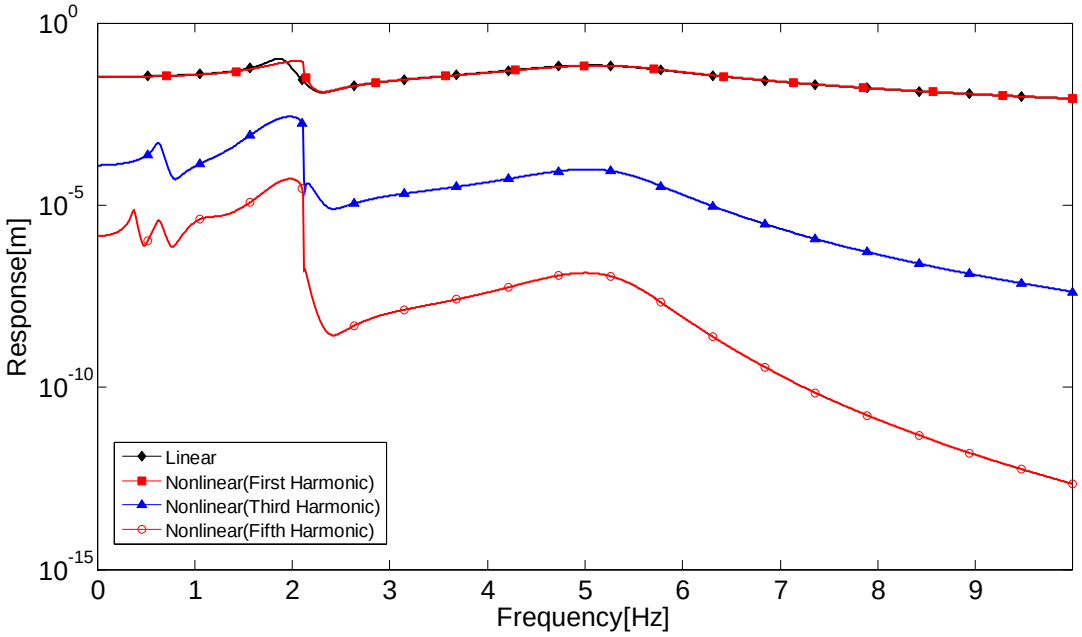

Figure 5.13 Frequency domain (multi harmonic) solutions for case study T.1

Figure 5.14 concentrated on fundamental harmonic response region and compares frequency domain solution with respect to time integration result:

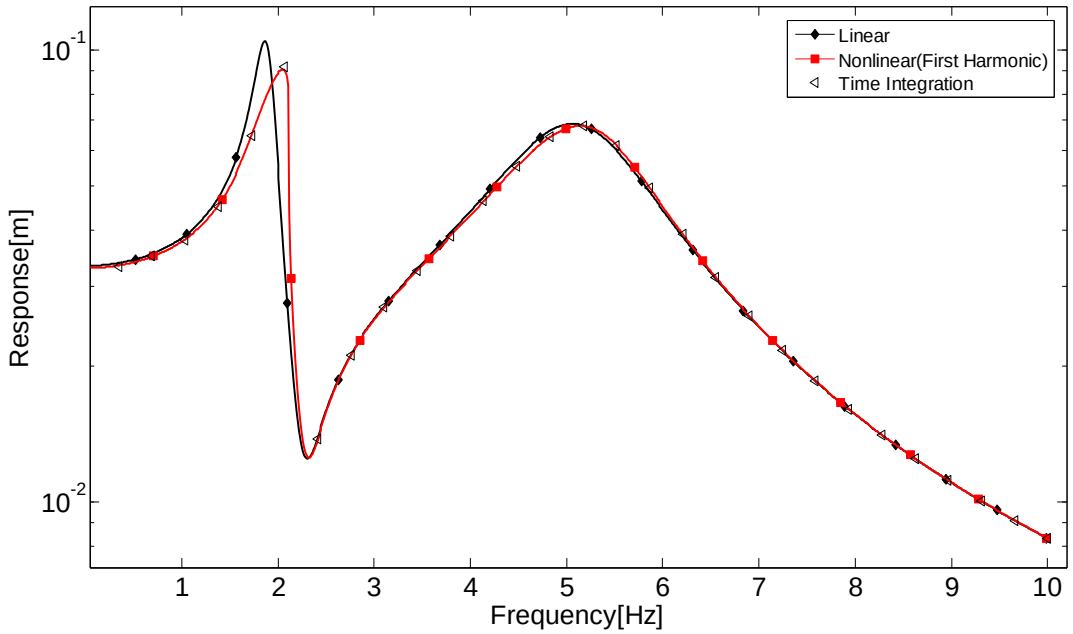

Figure 5.14 Frequency domain (multi harmonic) and time domain integration results for case study T.1-zoom in of the fundamental harmonic response region.

In Figure 5.14, there is an excellent agreement between frequency and time domain results for the frequencies around and beyond resonance where the fundamental harmonic is dominant in response. The power spectral density function estimate of the response obtained from time domain solution when system is harmonically excited at 2 Hz is given in Figure 5.15. The figure confirms that the effect of the third harmonic component is not considerable as it is ~40 times lower than the fundamental harmonic component .

Although, the multi harmonic components have no significant effect on the total response at the frequency range studied, it is interesting to study the peaks in Figure 5.13 worth mentioning. The first peak of the third harmonic component of the response (~0.63 Hz) is due to the first natural frequency of the system (1.895/3 Hz). Similarly, the first peak of the fifth harmonic component of the response (~0.38 Hz) is again due to the first natural frequency of the system (1.895/5 Hz).

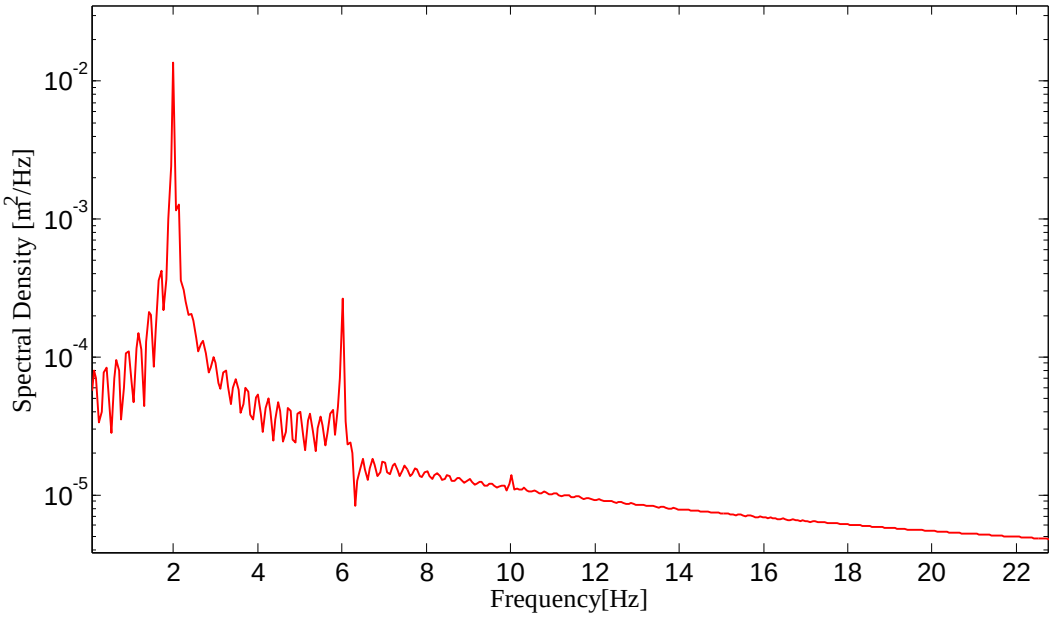

Figure 5.15 Power spectral density function estimate of x_1 for case study T.1 when system is harmonically excited at 2 Hz

5.2.2 Case Study T.2

In this case study, again the system shown in Figure 5.12 is considered. The linear parameters are the same as the ones in case study T.1. Nonlinearities between coordinates are defined in Table 5.5.

Table 5.5 Nonlinearity definitions for case study T.2

Nonlinear Connections: (DOF1-DOF2)	Nonlinearity Type	Nonlinearity Coefficients
1-1(Ground) (s_1^*)	Cubic Stiffness	$\beta = 8x10^5$ N/m^3
2-2(Ground) (s_2^*)	Cubic Stiffness	$\beta = 8x10^5$ N/m^3

Figure 5.16 gives multiharmonic frequency domain solution of x_1 over 0-10 Hz frequency range.

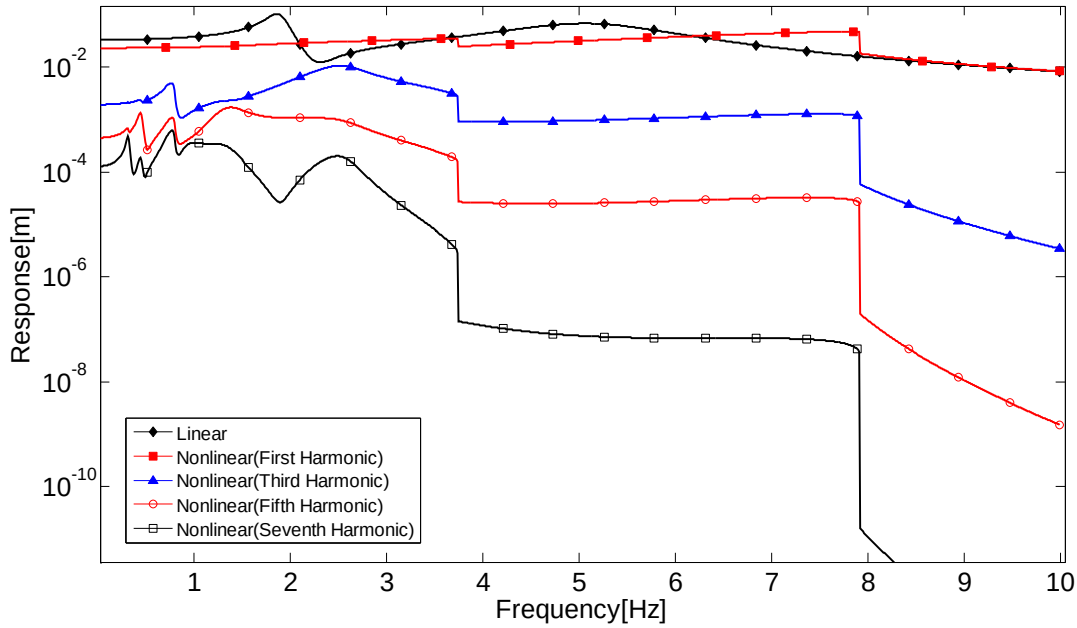

Figure 5.16 Frequency domain (multi harmonic) solutions for case study T.2

The magnified view of Figure 5.16, concentrated on the frequency range 0-4 Hz is given in Figure 5.17:

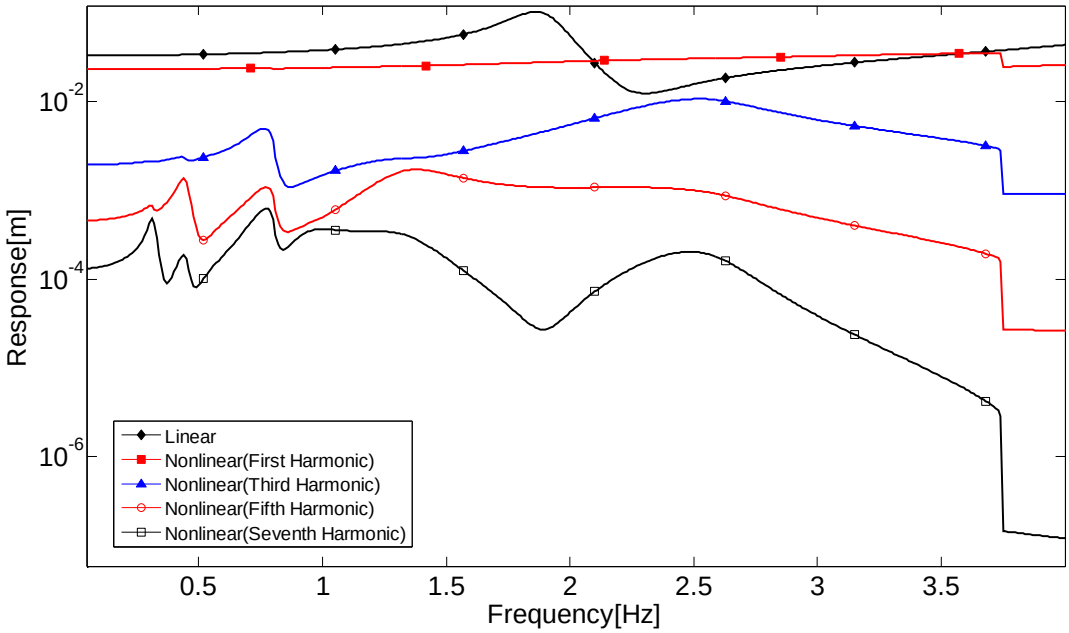

Figure 5.17 Frequency domain (multi harmonic) solutions between 0-4 Hz for case study T.2.

In this case study, multi harmonic components of the solution have some effect on the total response. The first peak of the third harmonic component of the response (~0.63 Hz) is corresponding to the first natural frequency of the undamped system (1.895/3 Hz). At this frequency, multiharmonic response components are very effective. This case can be observed through Figure 5.18 which gives power spectral density function estimate of response when system is harmonically excited at 0.63 Hz. Moreover, the first peak of the fifth and seventh harmonic components of the response (~0.38 Hz, ~0.27 Hz) is again corresponding to the first natural frequency of the undamped system (1.895/5, 1.895/7 Hz).

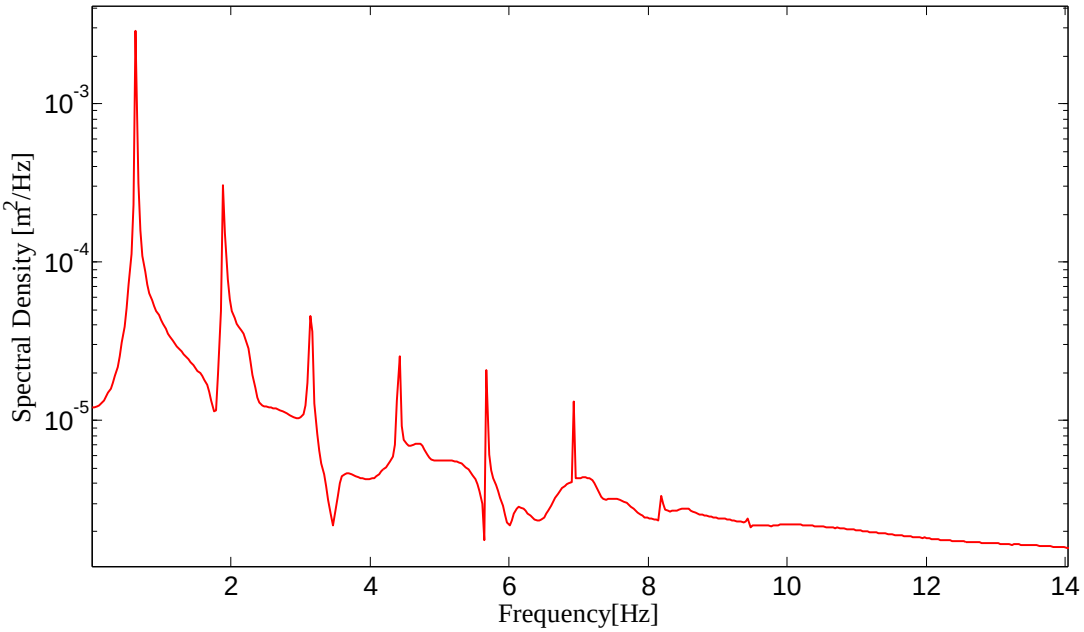

Figure 5.18 Power spectral density function estimate of x_1 for case study T.2 when system is harmonically excited at 0.63 Hz

The first harmonic component and time integration results are compared in Figure 5.19.

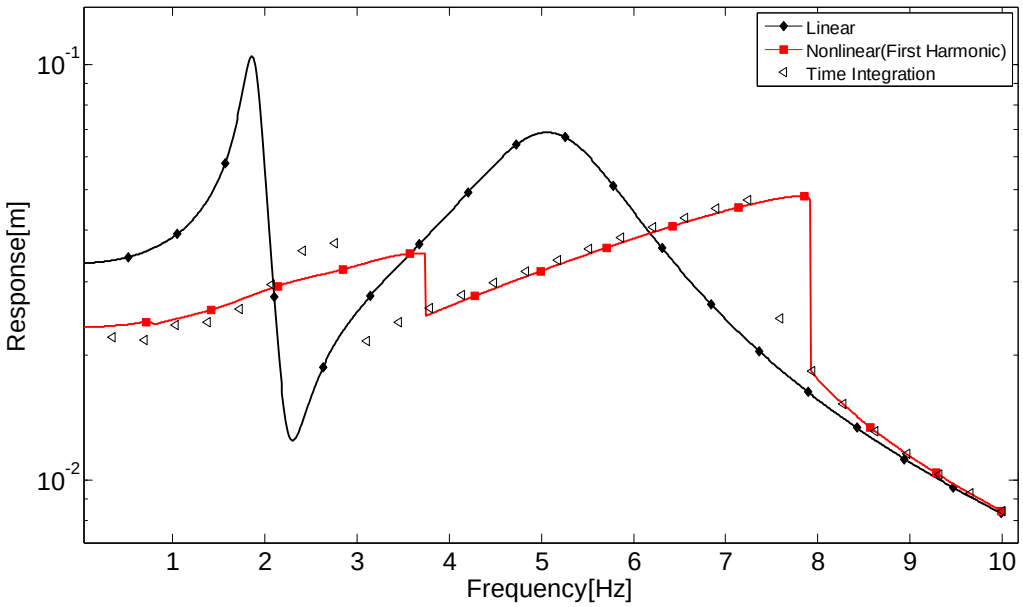

Figure 5.19 Frequency domain (multi harmonic) and time domain integration results for case study T.2.

By considering the amplitude and phase of the harmonic components, the amplitude of the total response is found and the results are compared with the time integration results and first harmonic component in the same plot at frequency range of 0-3 Hz (Figure 5.20).

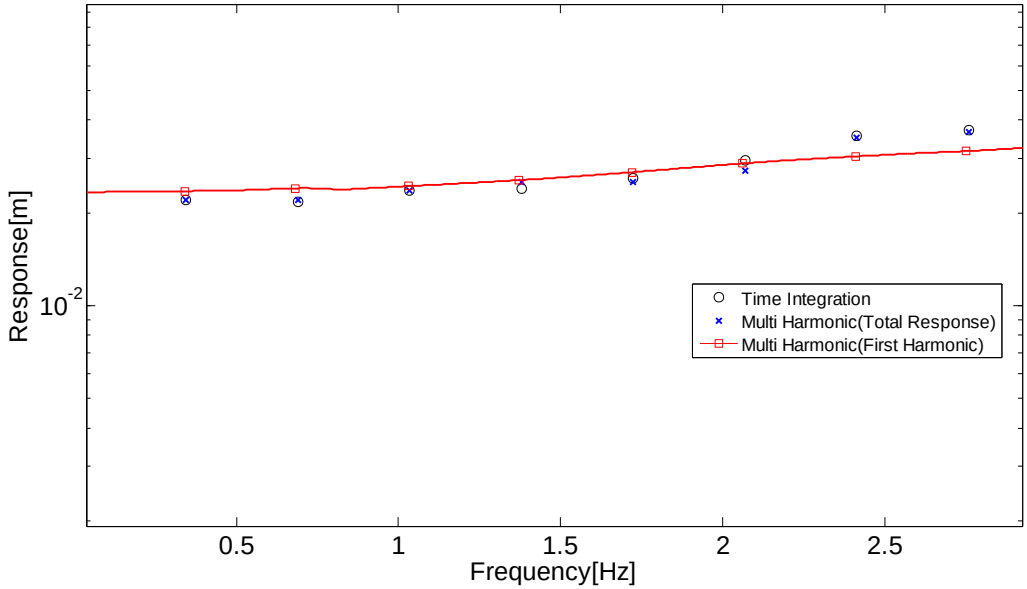

Figure 5.20 Frequency domain and time domain integration results for case study T.2 by considering the phase of the harmonic components

Inconsistency between the time integration and frequency domain solutions, given in Figure 5.19, is an expected result; but it should be stated here that the time integration result follows the same path of high to low sweep of the frequency domain result. The situation can be observed by executing the single harmonic solution and time domain solution and plot them on the same graph (Figure 5.21).

A conflict arises at this point between the results and the information given in [6]. Although, it is claimed by considering Figure 5.22 that, in the interval $[\omega_{low}, \omega_{high}]$ the solution $Y^{(1)}$ and $Y^{(3)}$ are possible with $Y^{(1)} > Y^{(3)}$, the results given in Figure 5.8, 5.9 in Section 5.1.1 and in Figure 5.19 are somewhat different. This differencies are mainly because of the fact that the converged solutions in regions $Y^{(1)}$ and $Y^{(3)}$ are dependent on precise definition of the initial guess in frequency domain analysis and on precise definition of the initial condition in time domain analysis. Coarse frequency increment may cause to an early jump, which prevents accurately observing the correct jumping frequency of the system response.

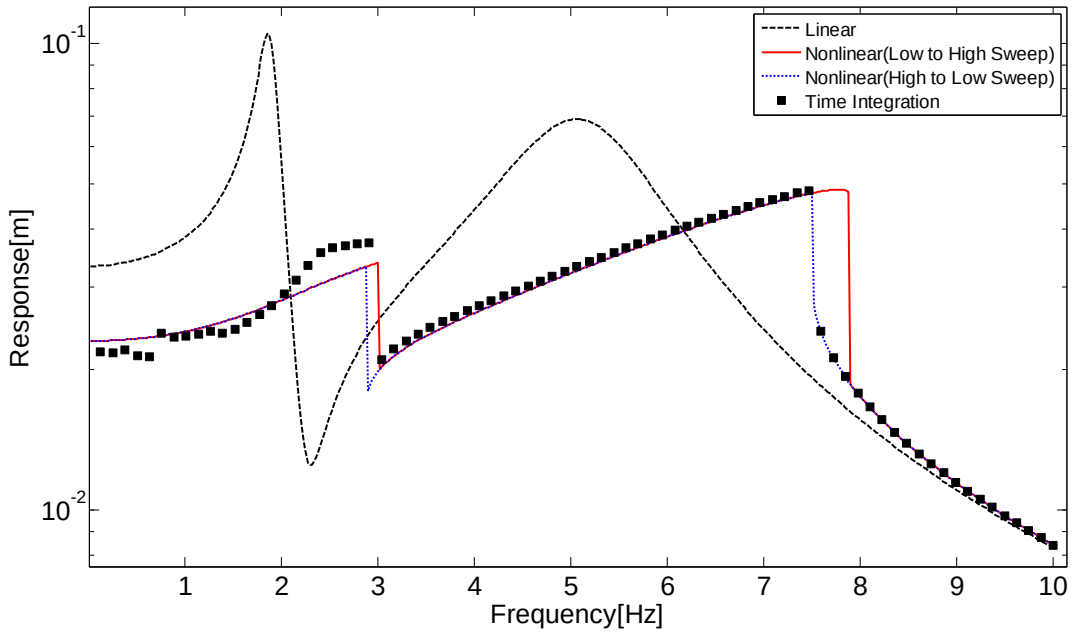

Figure 5.21 Frequency domain (Single Harmonic) and time domain integration results for case study T.2.

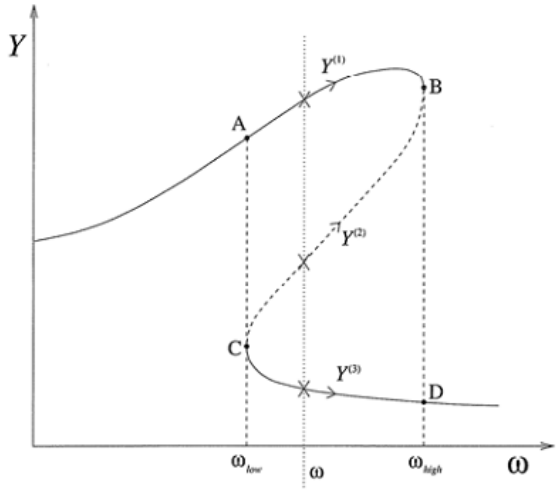

Figure 5.22 Displacement response of a hardening Duffing oscillator [9]

Best way to observe the multiharmonic effects on the solution is to give the results of single and multi harmonic solutions and compare them with time domain solutions on the same figure (Figure 5.23). By considering the plot, it can be concluded that the response can not be represented by the single harmonic component when the system is excited at 0.63 Hz which corresponds to one third of the first natural frequency.

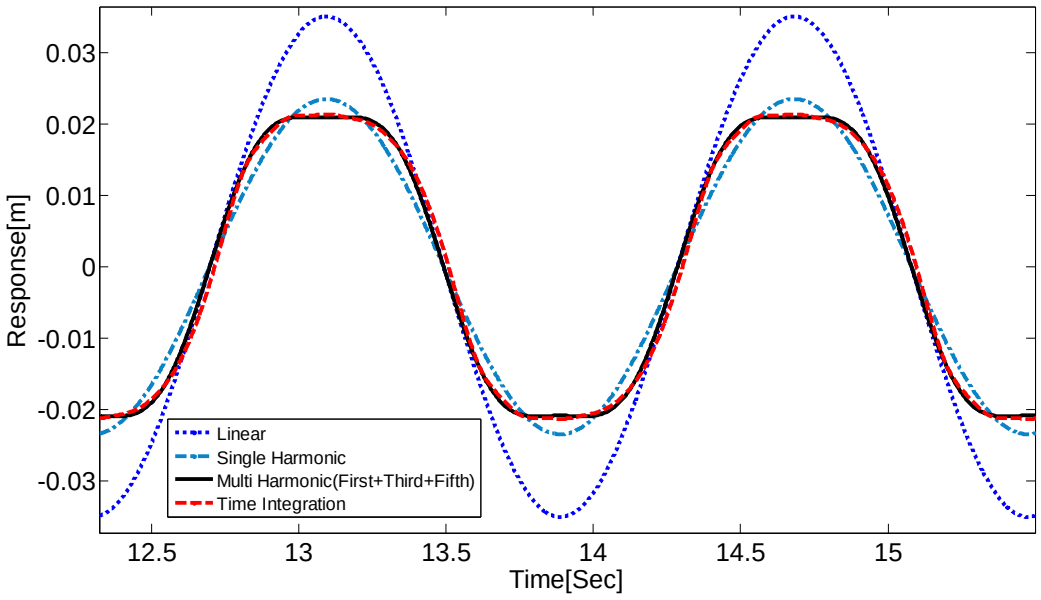

Figure 5.23 Time Domain, Single Harmonic and Multi Harmonic Analyses results for case study T.2 when system is harmonically excited at 0.63 Hz

The solution time comparisons of frequency domain and time domain solutions are given in Table 5.6.

Table 5.6 Solution Time Comparison for Case Study T.2

Solution Method	Frequency Increment [Hz]	Solution Time [s]
Single Harmonic	0.01	6.36
Multi Harmonic by considering 1^{st} and 3^{rd} harmonics	0.01	46.7
Multi Harmonic by considering 1^{st} , 3^{rd} and 5^{th} harmonics	0.01	107
Multi Harmonic by considering 1^{st} , 3^{rd} , 5^{th} and 7^{th} harmonics	0.01	248
Time Integration (30 s run) ODE45	0.4	288
Time Integration (30 s run) ODE45	0.1	1112

5.2.3 Case Study T.3

In this case study again the system shown in Figure 5.12 is considered. The linear parameters are the same as the case study T.1 except for the amplitude of the excitation force. The amplitude of the harmonic forcing in this case is taken as:

$$F_1 = 10 \text{ N}$$

Nonlinearities between coordinates are defined in Table 5.7.

Table 5.7 Nonlinearity definitions for case study T.3

Nonlinear Connections: (DOF1-DOF2)	Nonlinearity Type	Nonlinearity Coefficients
1-1(Ground) (s_1^*)	Coulomb Friction	$F_f = 1.5 \text{ N}$
2-2(Ground) (s_2^*)	Cubic Stiffness	$\beta = 8\text{x}10^5 \text{ N/m}^3$

Figure 5.24 and shows comparison of multi harmonic solution with respect to the time integration result.

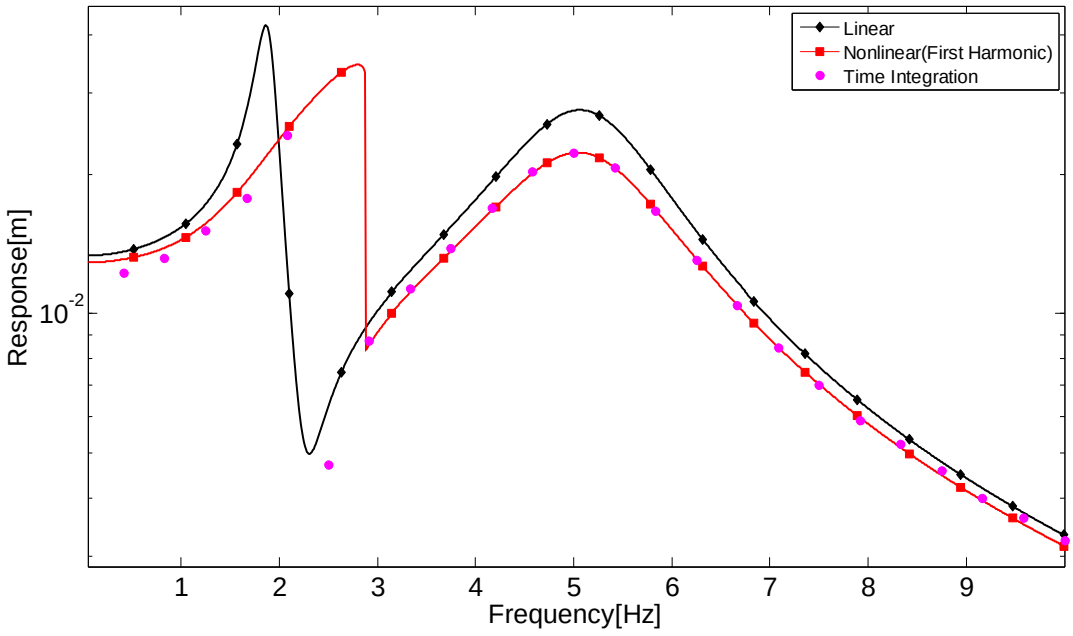

Figure 5.24 First harmonic component of frequency domain (multi harmonic) and time domain integration results for case study T.3.

It can be observed from Figure 5.24 that frequency domain and time domain results are in an agreement except for the frequency range between 0-2 Hz. In this frequency range, multi harmonic components of the solution are pronounced and have to be considered. Moreover, time integration solution is again following the path of the high to low sweep of the frequency domain solution. The multi harmonic effects can be observed from multi harmonic solution results given in Figure 5.25 which concentrates on the frequency range between 0-4 Hz.

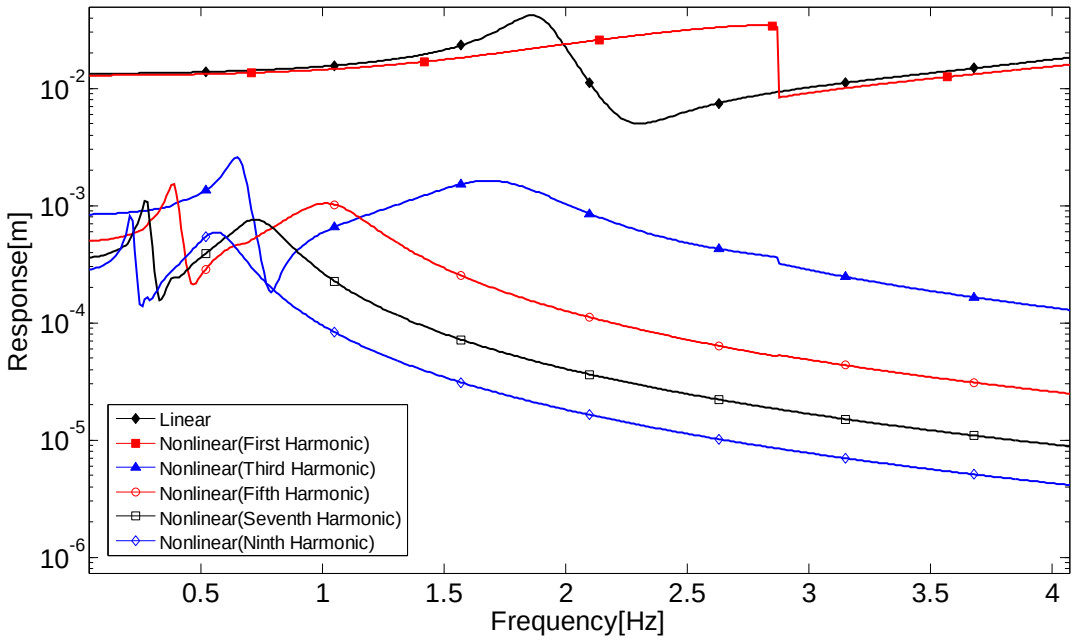

Figure 5.25 Frequency domain (multi harmonic) solutions between 0-4 Hz for case study T.3.

From Figure 5.25, it can be concluded that at ~0.63 Hz, multi harmonic effects should be taken into consideration. The result in Figure 5.26, that shows the multi harmonic and time domain solution, and the spectral density function estimate of the response when the system is excited at 0.63 Hz given in Figure 5.27, verifies that system response at 0.63 Hz can better be represented by addition of first, third, fifth and seventh harmonic components :

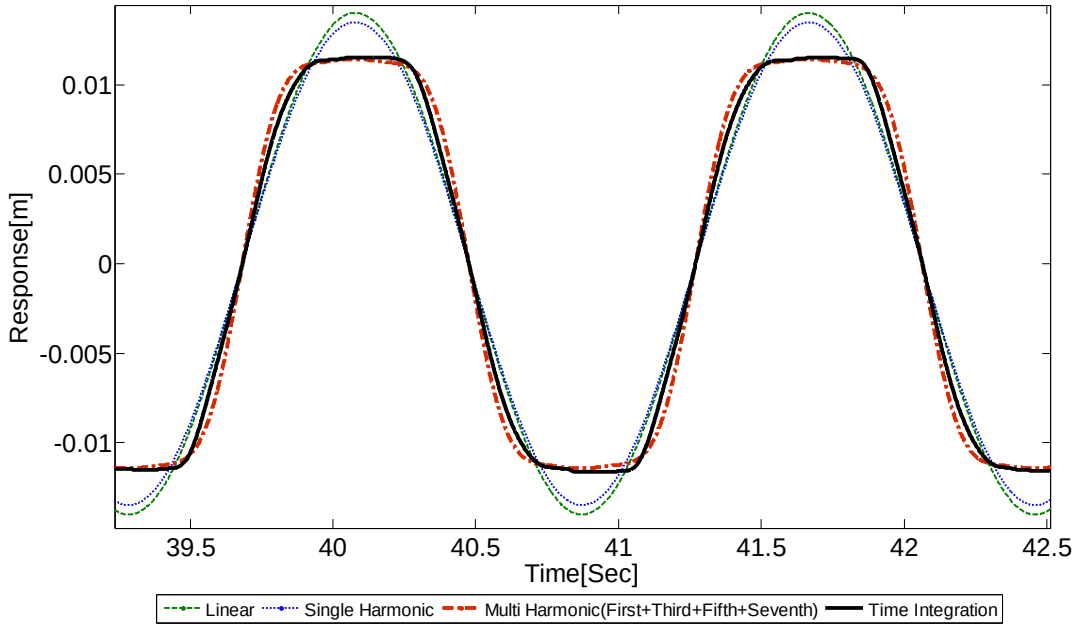

Figure 5.26 Time Domain, Single Harmonic and Multi Harmonic Analyses results for case study T.3 when system is harmonically excited at 0.63 Hz

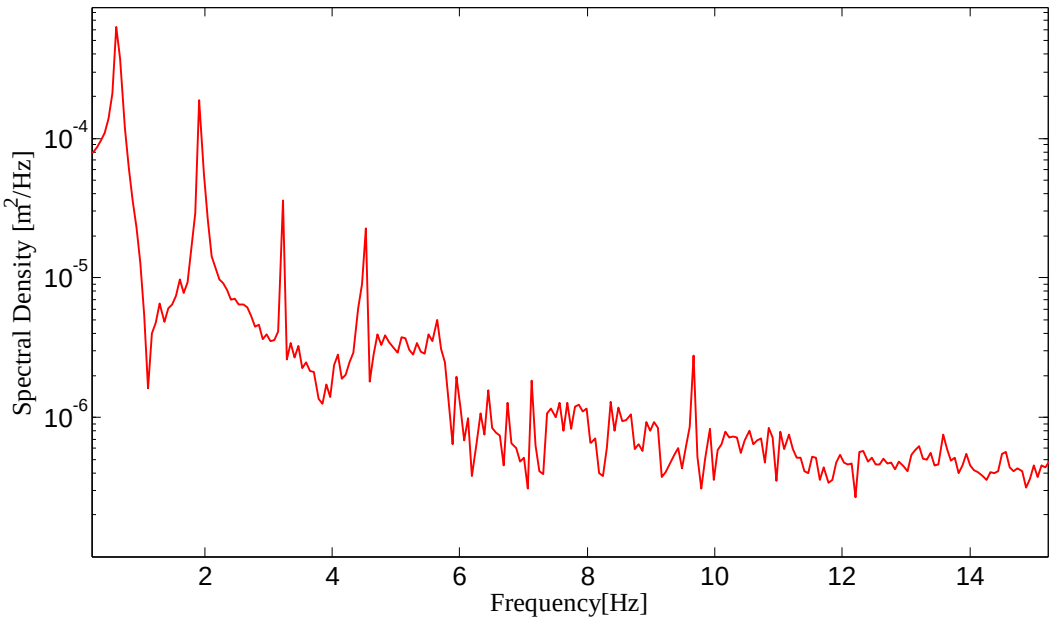

Figure 5.27 Power spectral density function estimate of x_1 for case study T.3 when system is harmonically excited at 0.63 Hz

5.2.4 Case Study T.4

Consider the system given in Figure 5.28.

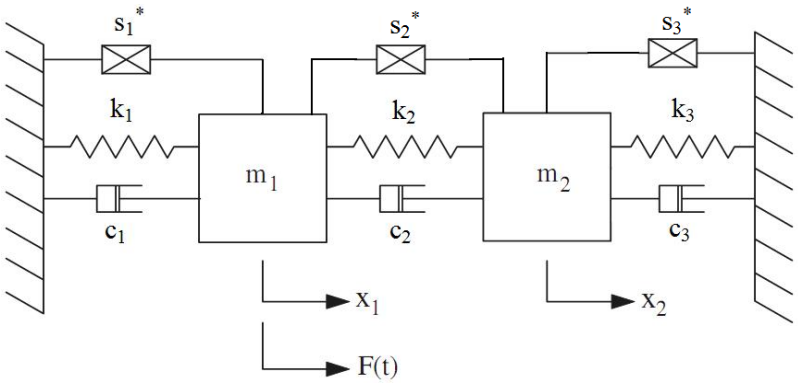

Figure 5.28 2 DOF system with 3 nonlinear elements

The linear parameters and forcing definitions are same as the case study T.1. Nonlinearities between coordinates are defined in Table 5.8.

Table 5.8 Nonlinearity definitions for case study T.4

Nonlinear Connections: (DOF1-DOF2)	Nonlinearity Type	Nonlinearity Coefficients
1-1(Ground) (s_1^*)	Arctan Stiffness	$\rho = 2$
		$\kappa = 600$
1-2 (s_2^*)	Arctan Stiffness	$\rho = 1$
		$\kappa = 500$
2-2(Ground) (s_3^*)	Arctan Stiffness	$\rho = 1$
		$\kappa = 500$

Figure 5.29 shows the variation of multi harmonic solution components of the response (x_1) with respect to the excitation frequency.

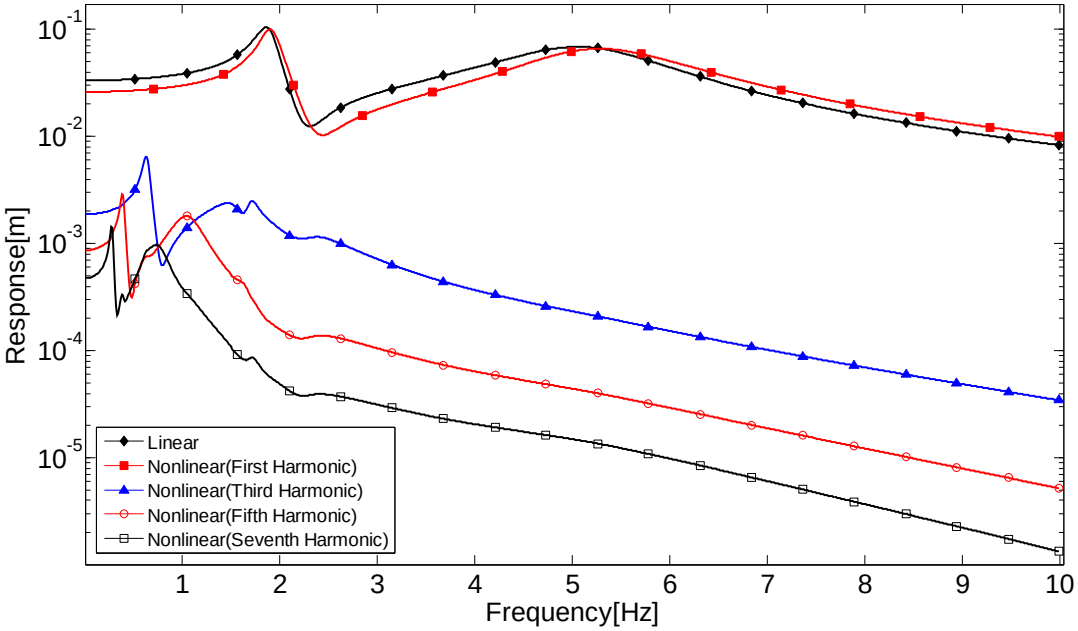

Figure 5.29 Frequency domain (multi harmonic) solutions between 0-10 Hz for case study T.4.

Figure 5.30 and shows comparison of first harmonic solution with respect to the time integration result.

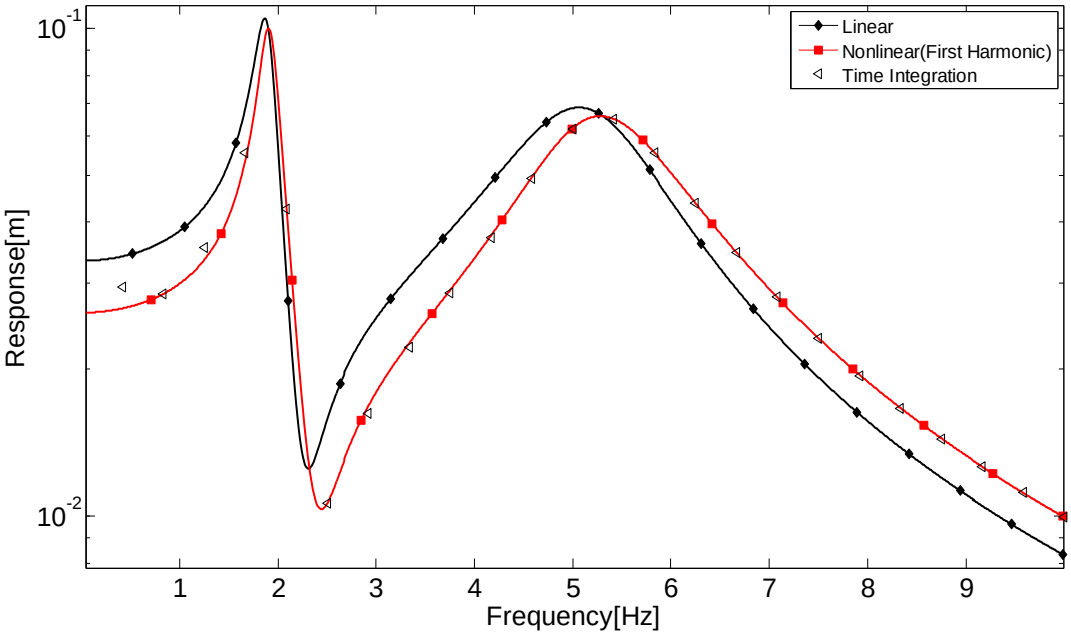

Figure 5.30 First harmonic component of frequency domain (multi harmonic) and time domain integration results for case study T.4.

It can be observed from Figure 5.30 that frequency domain and time domain results are in an agreement except for the frequency range between 0-2 Hz. In this frequency range, multi harmonic components of the solution are significant and have to be considered. The result in Figure 5.31 that shows the spectral density function estimate of the response when the system is excited at 0.63 Hz, verifies that system response at 0.63 Hz can better be represented by addition of first and third harmonic components (Figure 5.32).

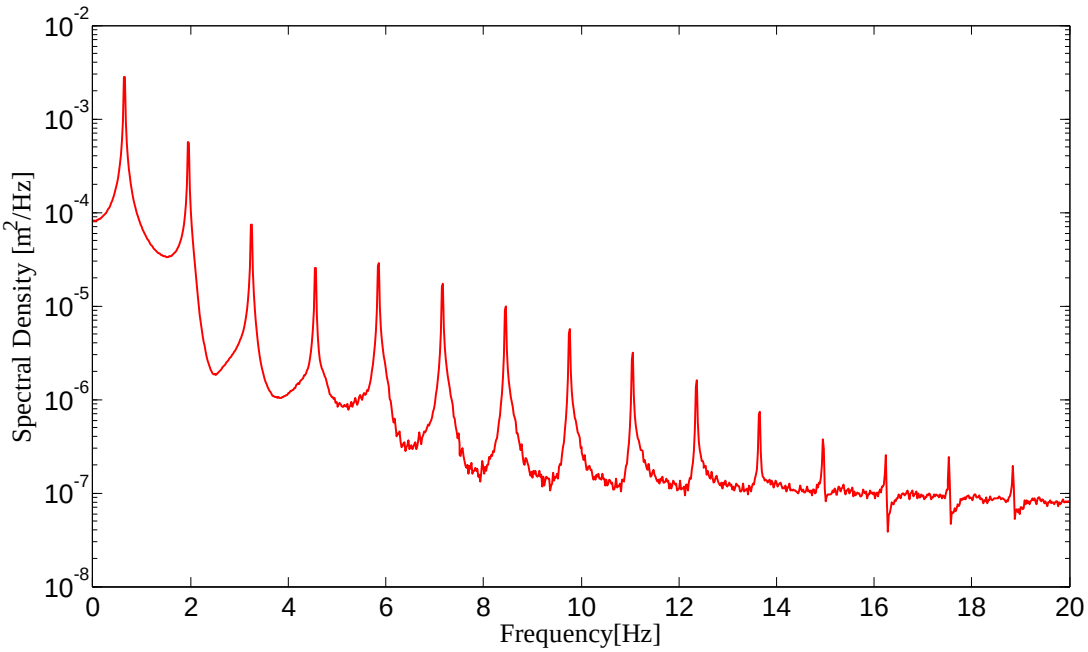

Figure 5.31 Power spectral density function estimate of x_1 for case study T.4 when system is harmonically excited at 0.63 Hz

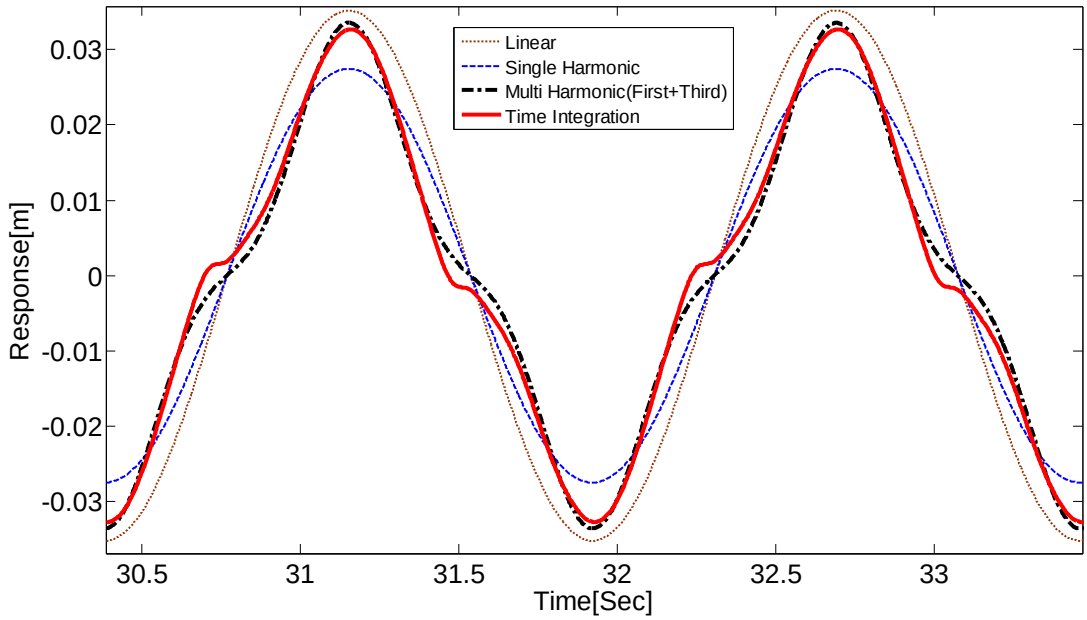

Figure 5.32 Time Domain, Single Harmonic and Multi Harmonic Analyses results for case study T.4 when system is harmonically excited at 0.65 Hz

5.2.5 Case Study T.5

Consider again the system given in Figure 5.28. The linear parameters and forcing definitions are same as the case study T.1. Nonlinearities between coordinates are defined in Table 5.9.

Table 5.9 Nonlinearity definitions for case study T.5

Nonlinear Connections: (DOF1-DOF2)	Nonlinearity Type	Nonlinearity Coefficients
1-1(Ground) (s_1^*)	Preloaded Stiffness	$F_p = 0.5$ N
		$k = 500$ N/m
1-2 (s_2^*)	Preloaded Stiffness	$F_p = 0.3$ N
		$k = 300$ N/m
2-2(Ground) (s_3^*)	Preloaded Stiffness	$F_p = 0.4$ N
		$k = 400$ N/m

Figure 5.33 shows the variation of multi harmonic solution components of the response (x_1) with respect to the excitation frequency. Figure 5.34 shows comparison of first harmonic solution with respect to the time integration result.

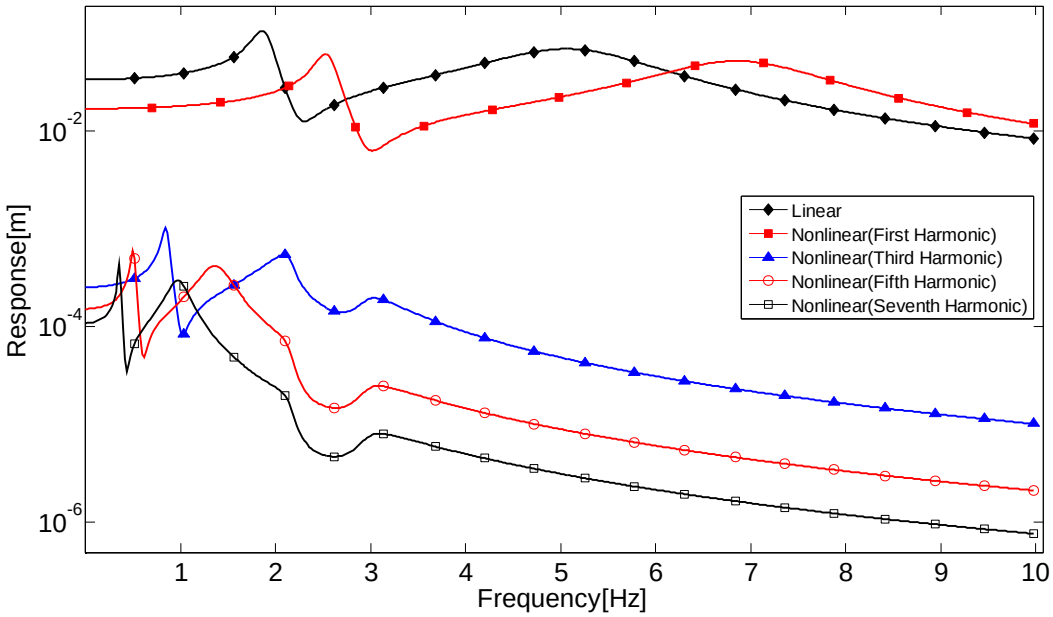

Figure 5.33 Frequency domain (multi harmonic) solutions between 0-10 Hz for case study T.5.

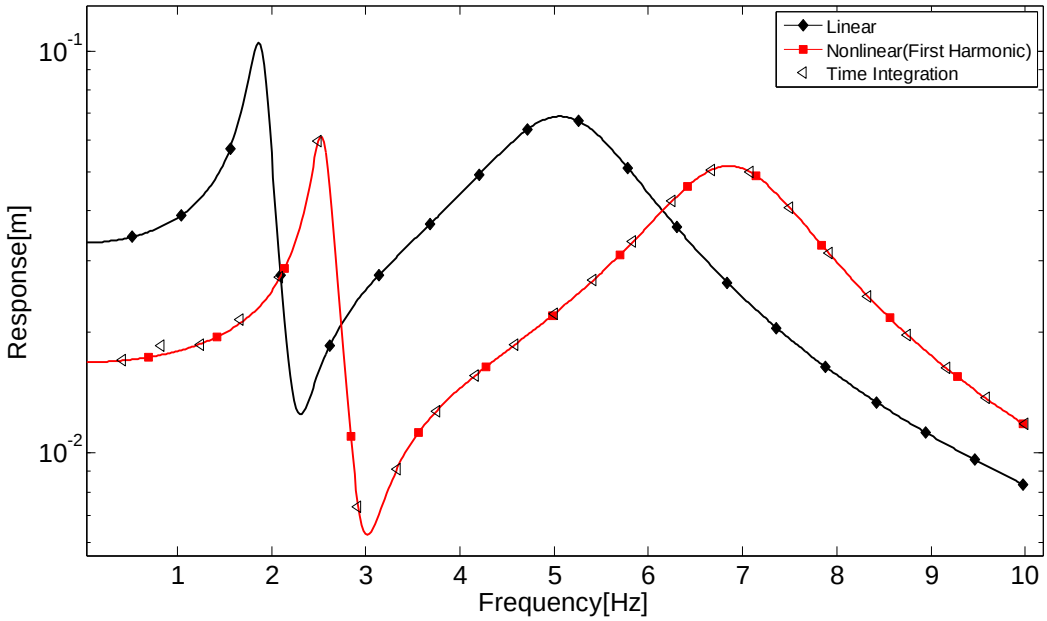

Figure 5.34 First harmonic component of frequency domain (multi harmonic) and time domain integration results for case study T.5.

It can be observed from Figure 5.34 that frequency domain and time domain results are in an agreement except for the frequency value near 0.84 Hz. In this frequency range, multi harmonic components of the solution are effective and have to be considered. The result in Figure 5.35 that shows the spectral density function estimate of the response when the system is harmonically excited at 0.84 Hz, verifies that system response at 0.84 Hz can better be represented by addition of first and third harmonic components (Figure 5.36).

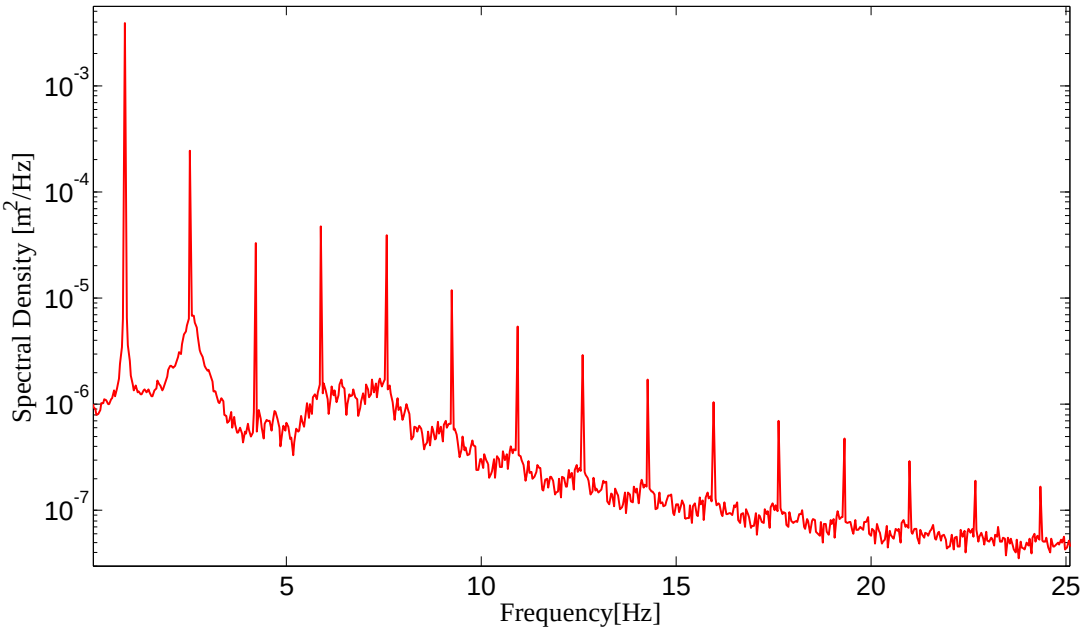

Figure 5.35 Power spectral density function estimate of x_1 for case study T.5 when system is harmonically excited at 0.84 Hz

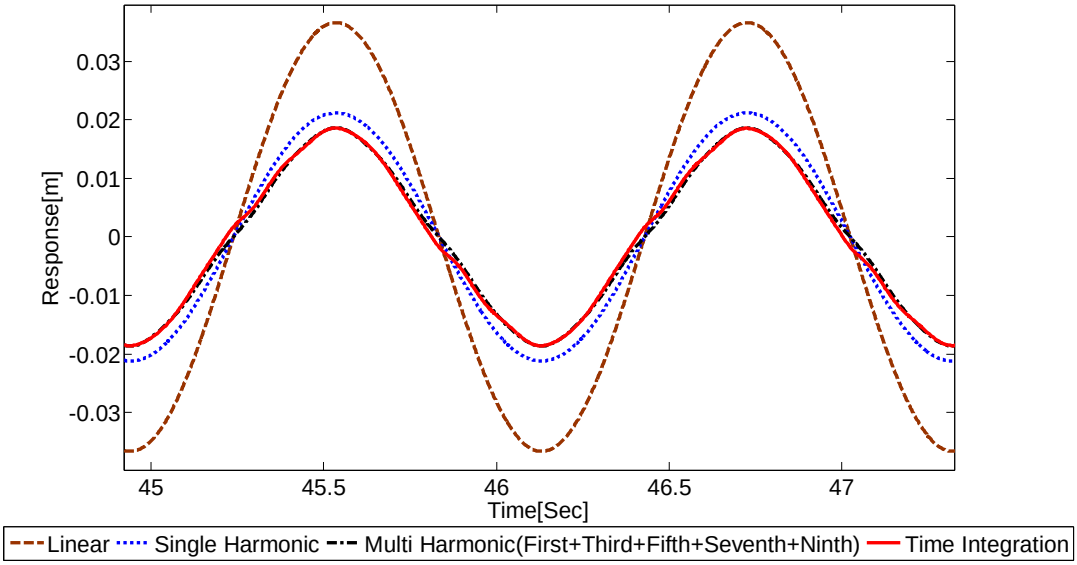

Figure 5.36 Time Domain, Single Harmonic and Multi Harmonic Analyses results for case study T.5 when system is harmonically excited at 0.84 Hz

5.2.6 Case Study T.6

Consider again the system given in Figure 5.28. The linear parameters are the same as the case study T.1 except for the amplitude of the excitation force. The amplitude of the harmonic forcing in this case is taken as:

$$F_1 = 10\,\mathrm{N}$$

Nonlinearities between coordinates are defined in Table 5.10.

Table 5.10 Nonlinearity definitions for case study T.6

Nonlinear Connections: (DOF1-DOF2)	Nonlinearity Type	Nonlinearity Coefficients
1-1(Ground) (s_1^*)	Piecewise Linear Stiffness	$\delta = 0.05$ m
		$k_1 = 100$ N/m
		$k_2 = 150$ N/m
1-2 (s_2^*)	Cubic Stiffness	$\beta = 8\text{x}10^5$ N/m^3
2-2(Ground) (s_3^*)	Coulomb Friction	$F_f = 1\,\mathrm{N}$

Figure 5.37 shows the variation of multi harmonic solution components of the response (x_1) with respect to the excitation frequency and time integration solution at the same plot.

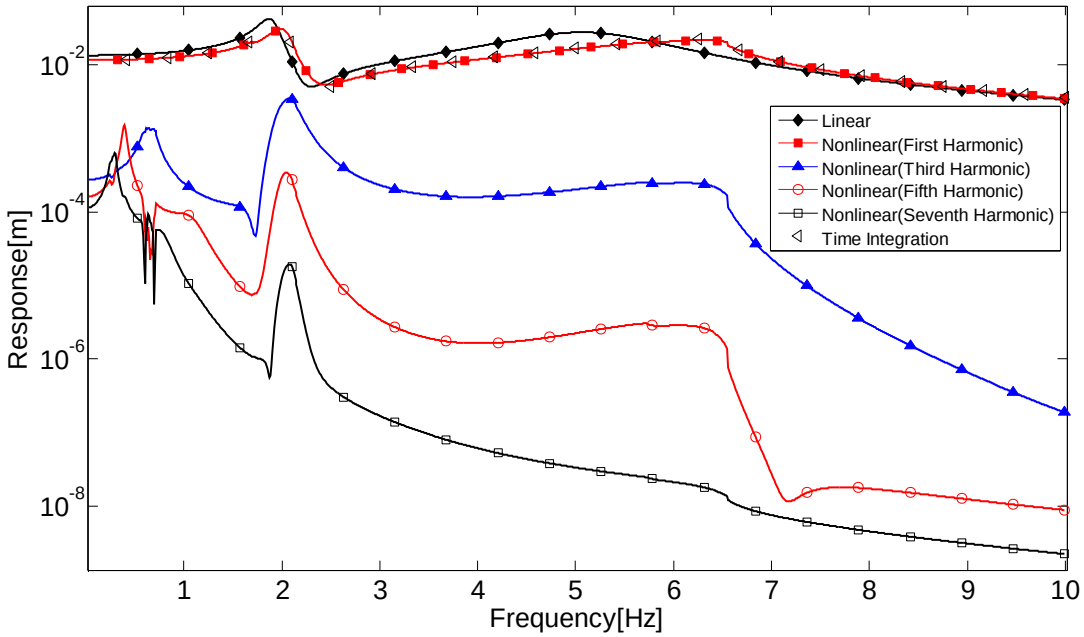

Figure 5.37 Frequency domain (multi harmonic) and Time Domain solutions between 0-10 Hz for case study T.6.

Again it can be observed from Figure 5.37 that frequency domain and time domain results are in an agreement except for the frequency value near ~2 Hz. At frequencies close to this frequency value, multi harmonic components of the solution are effective and have to be considered. The result in Figure 5.38 that shows the spectral density function estimate of the response when the system is excited at 2 Hz, verifies that system response at 2 Hz can better be represented by addition of first, third, fifth and seventh harmonic components (Figure 5.39). Moreover, the discrepancies between the time integration and multi harmonic results in Figure 5.39 is mainly because of the affects of the sub-harmonic components in the response which can be observed in spectral function estimate given in Figure 5.38.

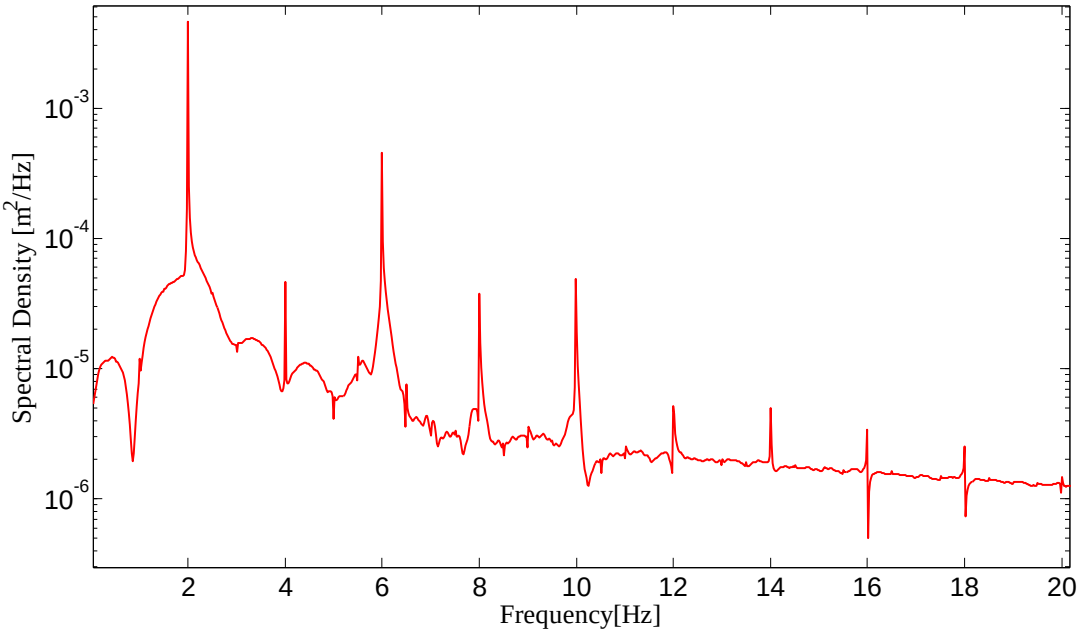

Figure 5.38 Power spectral density function estimate of x_1 for case study T.6 when system is harmonically excited at 2 Hz

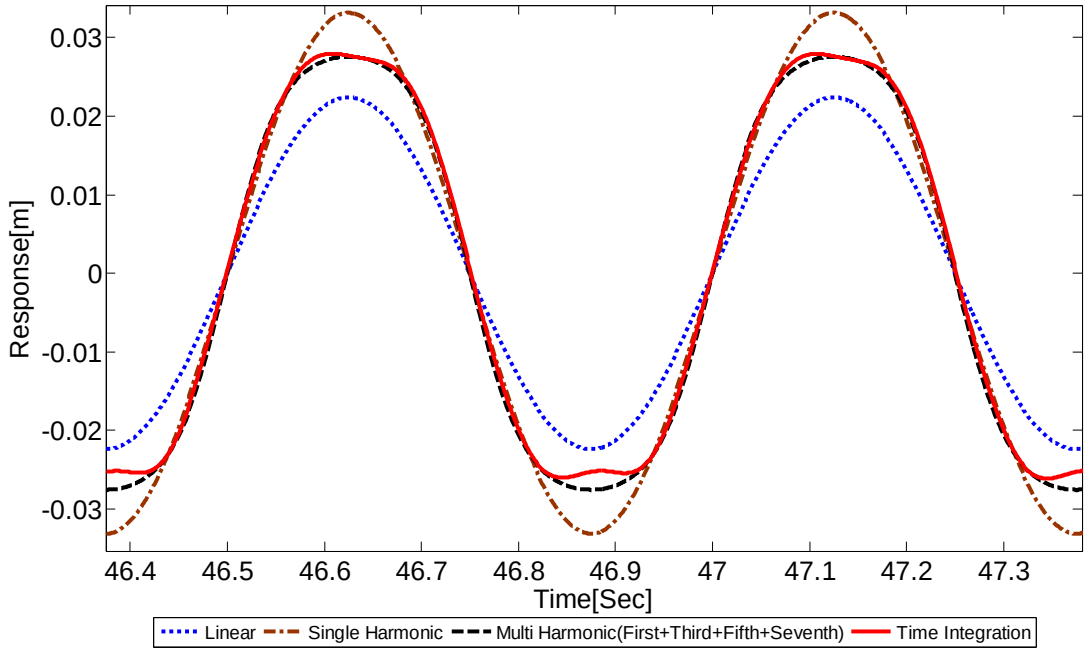

Figure 5.39 Time Domain, Single Harmonic and Multi Harmonic Analyses results for case study T.6 when system is harmonically excited at 2 Hz

CHAPTER 6

CASE STUDIES

In this chapter, several case studies are presented to demonstrate the application of the method and the program for large ordered systems and for various types of nonlinear elements. The discrete models are created by ANSYS® by using the substructuring method described in Appendix B, and the output files are taken as the input for the program MH-NLS.

6.1 Case Study A

Two beam models (Figure 6.1 and 6.2) fixed at one end surfaces and joined through linear and nonlinear elements will be examined (Figure 6.3). The beams are meshed with SOLID 185 [65] elements and joined with four COMBIN 14 2D-3D [65] linear spring type elements through their nearby edges in order to ensure the connection of two beams which is necessary to form common system matrices (Figure 6.4). In the FEM model, each node has 3 DOF's (in x, y and z directions).

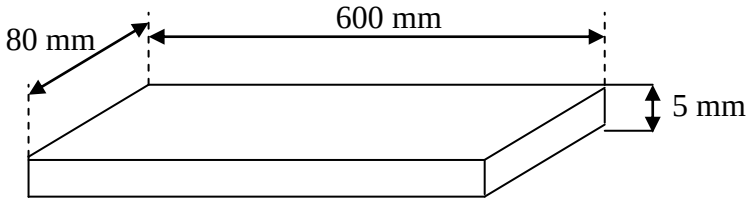

Figure 6.1 Dimensions of the first beam in case study A

The spring constants of the linear spring type elements in three directions (x, y and z) are taken as 5000 N/m.

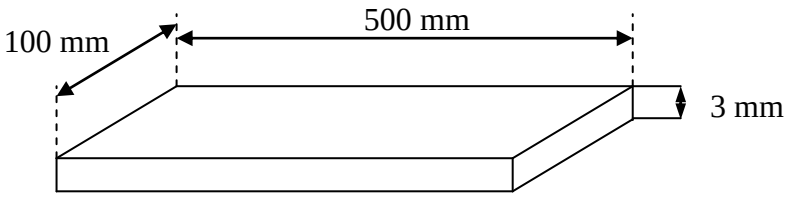

Figure 6.2 Dimensions of the second beam in case study A

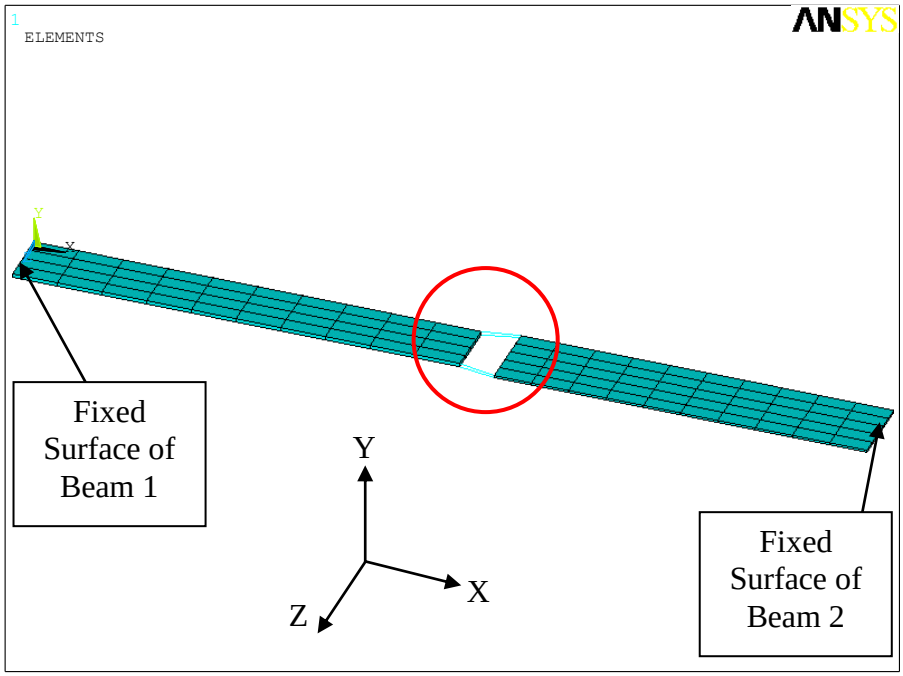

Figure 6.3 The FEM models and fixed surfaces of 2 beams in case study A

The material properties of two beams considered for the analysis are given in Table 6.1 (A typical aluminum material).

Table 6.1 Material properties for case study A

Density	2700 kg/m^3
Modulus of Elasticity	60 GPa
Poisson's Ratio	0.3

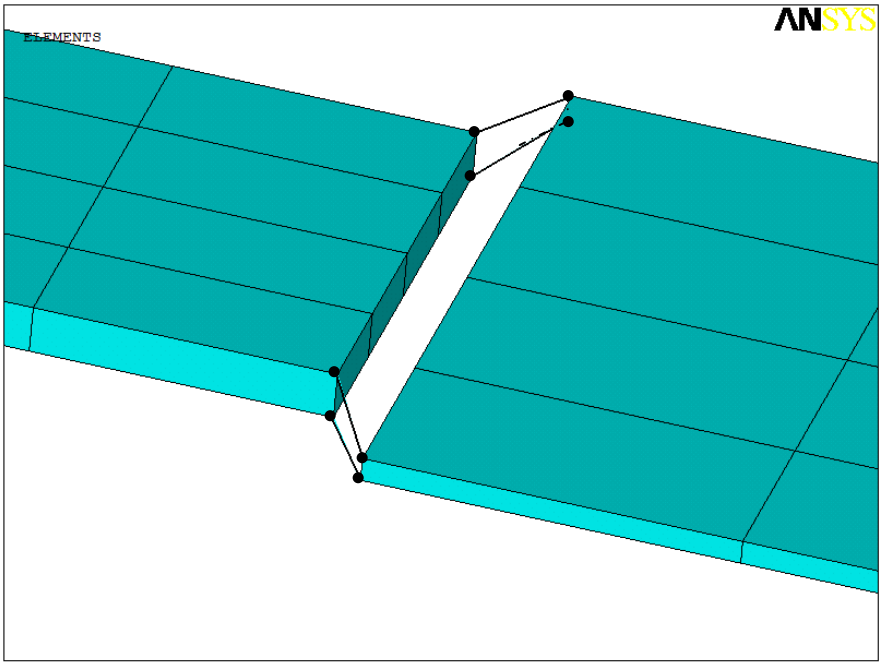

Figure 6.4 Connection of beams through edges with linear spring elements, zoom in circle region in Figure 6.3

The FEM is constituted with 660 DOF after meshing procedure. In order to verify that the system matrices are extracted from ANSYS® correctly, linear modal analysis is made in ANSYS® as well as by using the program developed and the natural frequencies obtained in both analyses are compared (Table 6.2). The results are found to be very close. The mode shapes corresponding to the first three natural frequencies are given in Figure 6.5.

Table 6.2 First 9 natural frequencies of the system obtained by ANSYS® and MH-NLS [Hz]

Program	Natural Frequencies (Hz)								
ANSYS®	78.7	94.2	142.2	182.9	186.4	309.3	487.5	583.9	634.4
MH-NLS	76.9	92.7	141.6	182.6	185.8	309.2	487.3	583.7	634.3

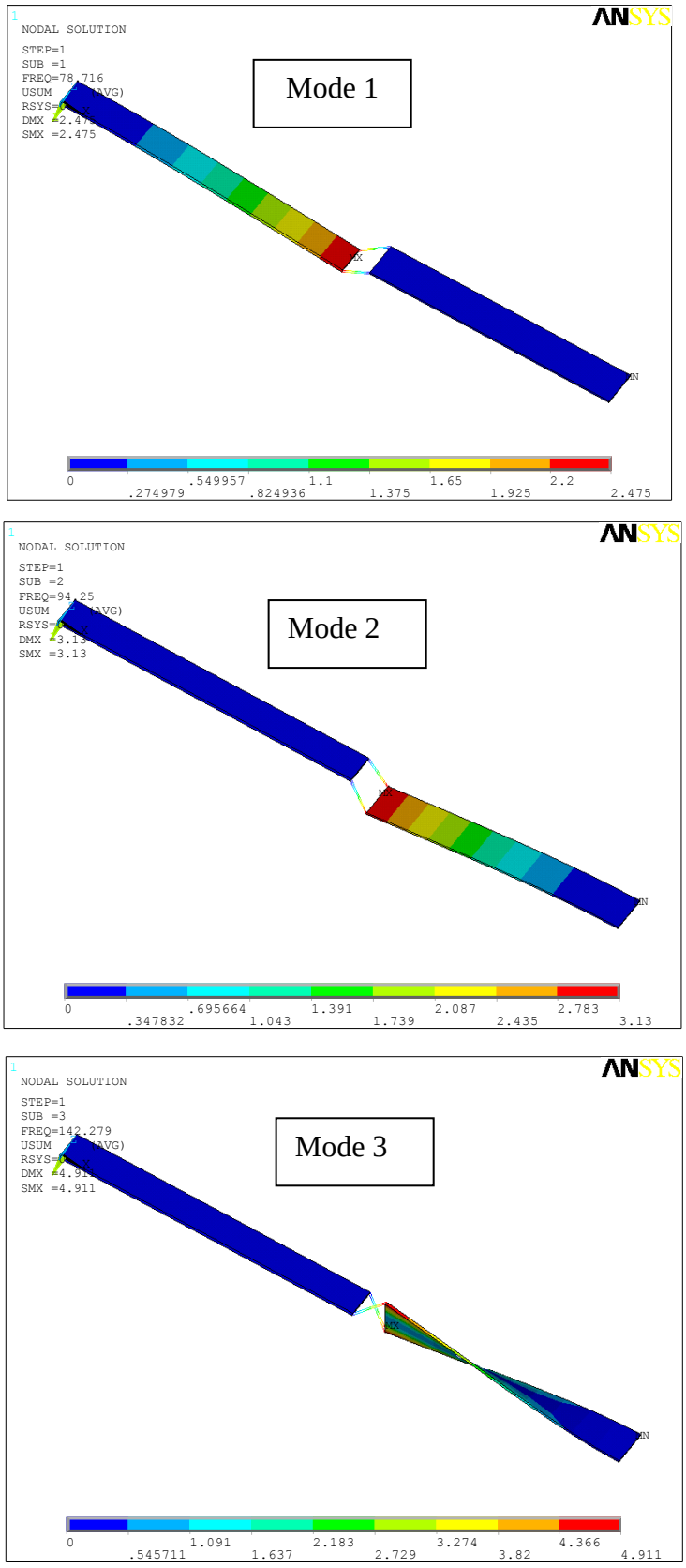

Figure 6.5 Mode shapes of the first three modes for case study A

6.1.1 Case Study A.1

The system introduced in Case Study A is used, and nonlinearity (bold line) is defined between the nodes (points) shown in Figure 6.6 in all three directions, x, y and z (Table 6.3). The forcing, loss factor and number of modes used in FRF calculations are given in Table 6.4.

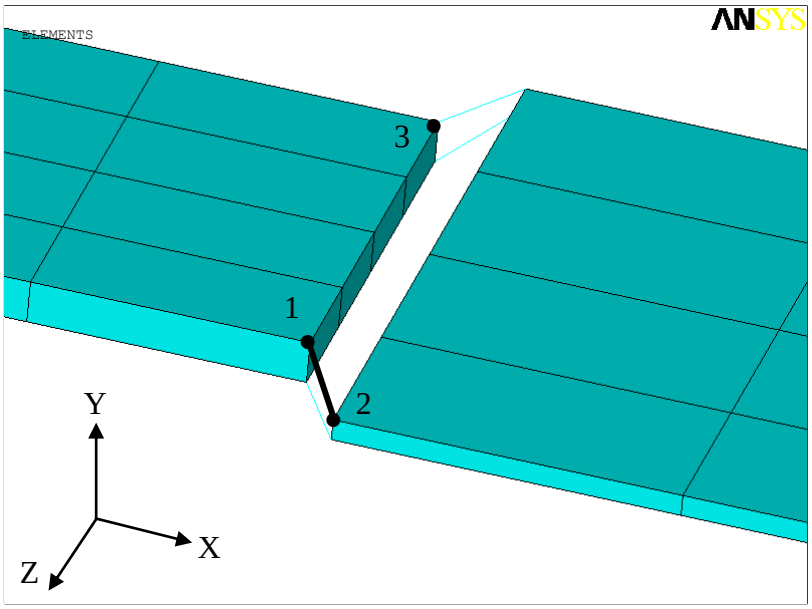

Figure 6.6 Nonlinear connections for case study A.1

Table 6.3 Nonlinearity definitions between nodes for case study A.1

Nonlinear Connections: (Node 1-Node 2)	Nonlinearity Type	Nonlinearity Coefficients
1-2	Cubic Stiffness	$\beta = 5x10^{8}$ N/m^{3}

Table 6.4 Loss factor, forcing and number of modes used in FRF calculation for case study A.1

Loss Factor	Forcing			Number of Modes used in FRF Calculation
	On node	Value (N)	Direction	
0.0012 (% 0.12)	1	10	-Y	15
	3	2	-Y	

The single harmonic response, pseudo receptance and multi harmonic response of node 1 in Y direction is given in Figure 6.7, 6.8 and 6.9 respectively.

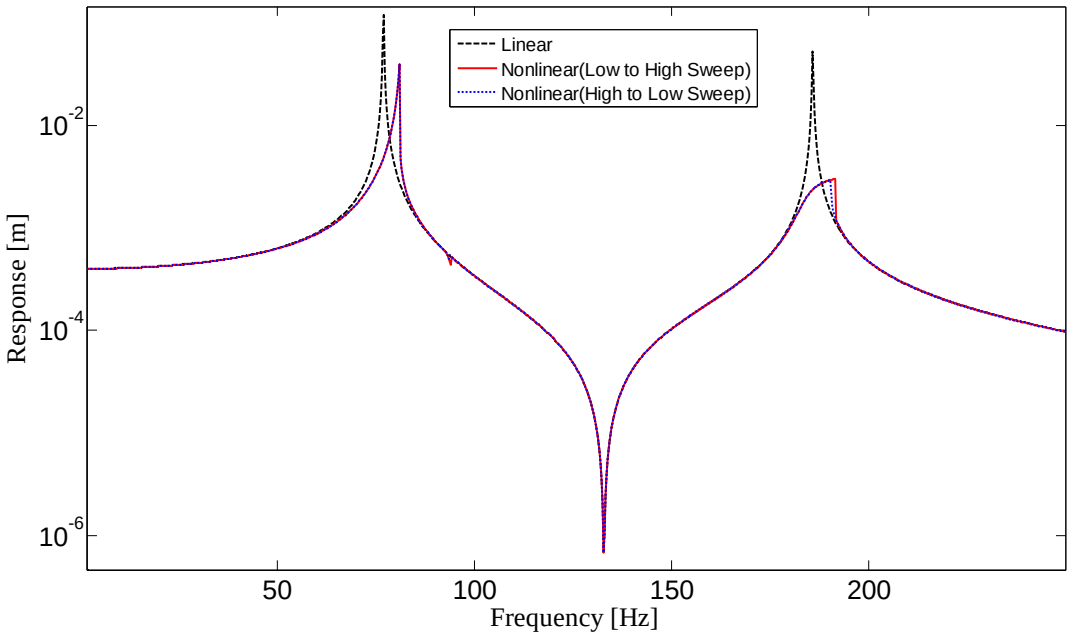

Figure 6.7 Single harmonic response of $\left|X_1\right|_y$ (node 1 in Y direction), case study A.1

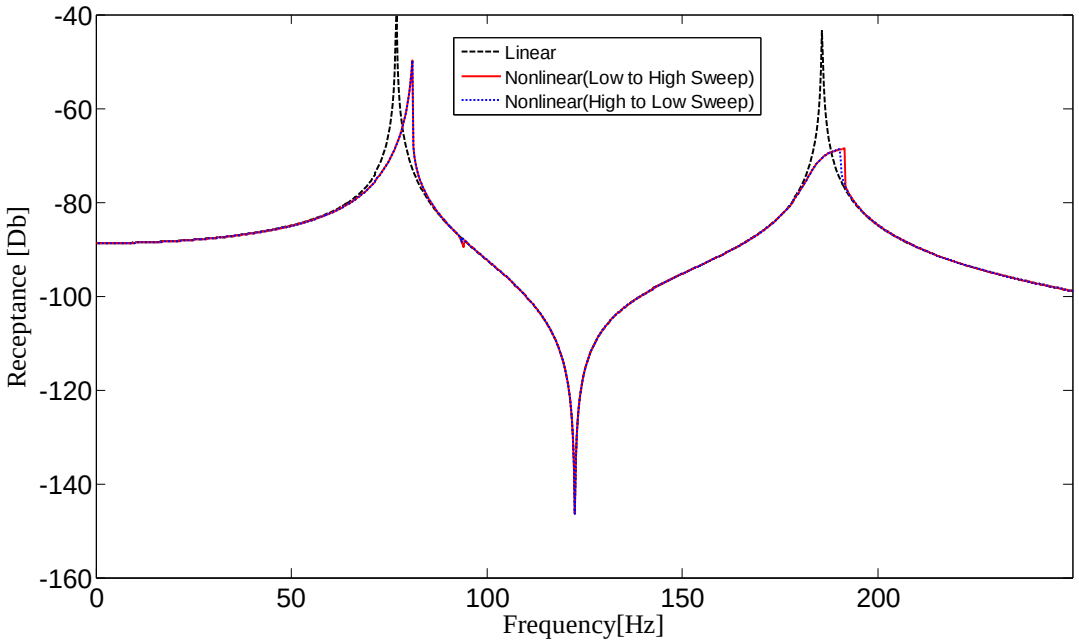

Figure 6.8 Pseudo receptance $\left|\alpha_{11}\right|_y$ (in y direction), case study A.1

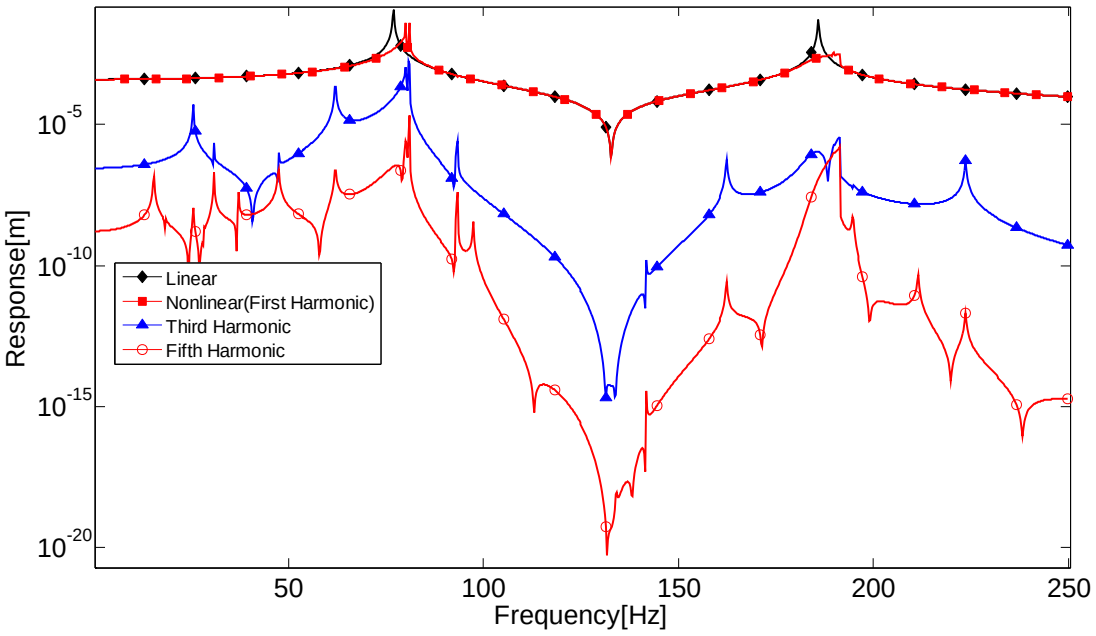

Figure 6.9 Multi harmonic response solution of $\left|X_1\right|_y$ (node 2 in Y direction), case study A.1

Figure 6.10 that shows the modal summation and matrix inversion results, confirming that using only 15 modes is enough to predict the response accurately at this frequency range. Computational time saving is complemented with accurate result.

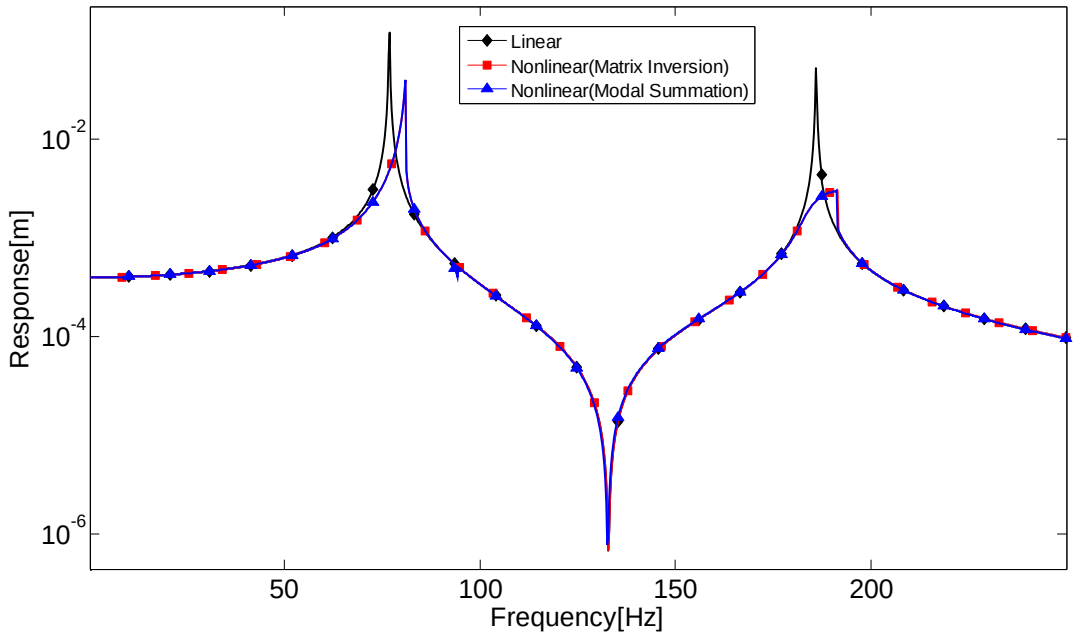

Figure 6.10 Modal summation and matrix inversion solutions comparison, case study A.1

Solution time comparison for single and multi harmonic solutions with matrix inversion counterparts are given in Table 6.5

Table 6.5 Solution Time Comparison for Case Study A.1

Solution Method	Frequency Increment [Hz]	Solution Time [s]
Single Harmonic (Modal Summation-15 Modes)	0.25	33.24
Single Harmonic (Matrix Inversion)	0.25	964.98
Multi Harmonic with 3 harmonic components (Modal Summation-15 Modes)	0.25	291.35
Multi Harmonic with 3 harmonic components (Matrix Inversion)	0.25	>> 7200

6.1.2 Case Study A.2

The system introduced in Case Study A is used and, nonlinearities (bold lines) are defined between the nodes (points) shown in Figure 6.11 in all three directions, x, y and z (Table 6.6). The forcing, loss factor and number of modes used in FRF calculations are given in Table 6.7.

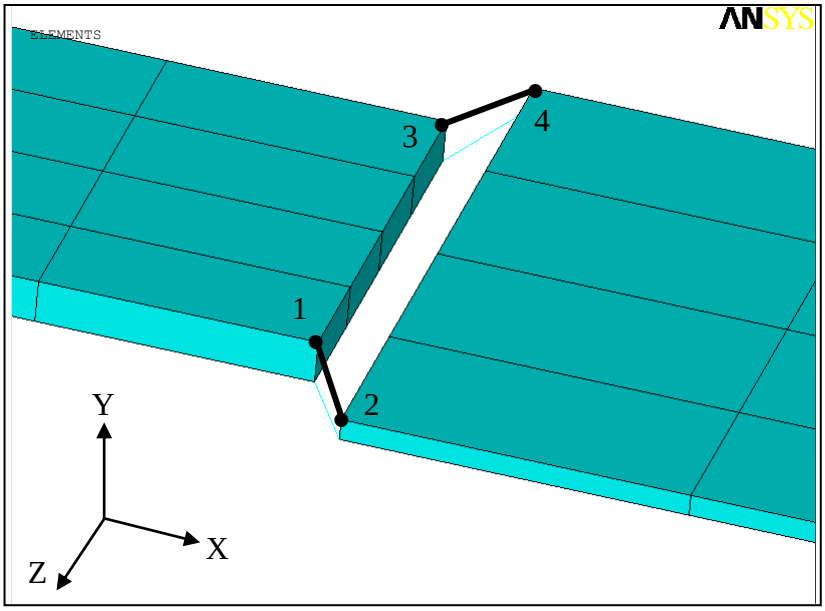

Figure 6.11 Nonlinear connections for case study A.2

Table 6.6 Nonlinearity definitions between nodes for case study A.2

Nonlinear Connections: (Node 1-Node 2)	Nonlinearity Type	Nonlinearity Coefficients
1-2	Cubic Stiffness	$\beta = 5x10^5$ N/m^3
3-4	Arctan Stiffness	$\rho = 10$
		$\kappa = 250$

Table 6.7 Loss factor, forcing and number of modes used in FRF calculation values for case study A.2

Loss Factor	Forcing			Number of Modes used in FRF Calculation
	On node	Value (N)	Direction	
0.0012 (% 0.12)	1	5	-Y	15
	3	1	-Y	

The single harmonic response, pseudo receptance and multi harmonic response of node 1 in Y direction is given in Figure 6.12-13, 6.14 and 6.15 respectively.

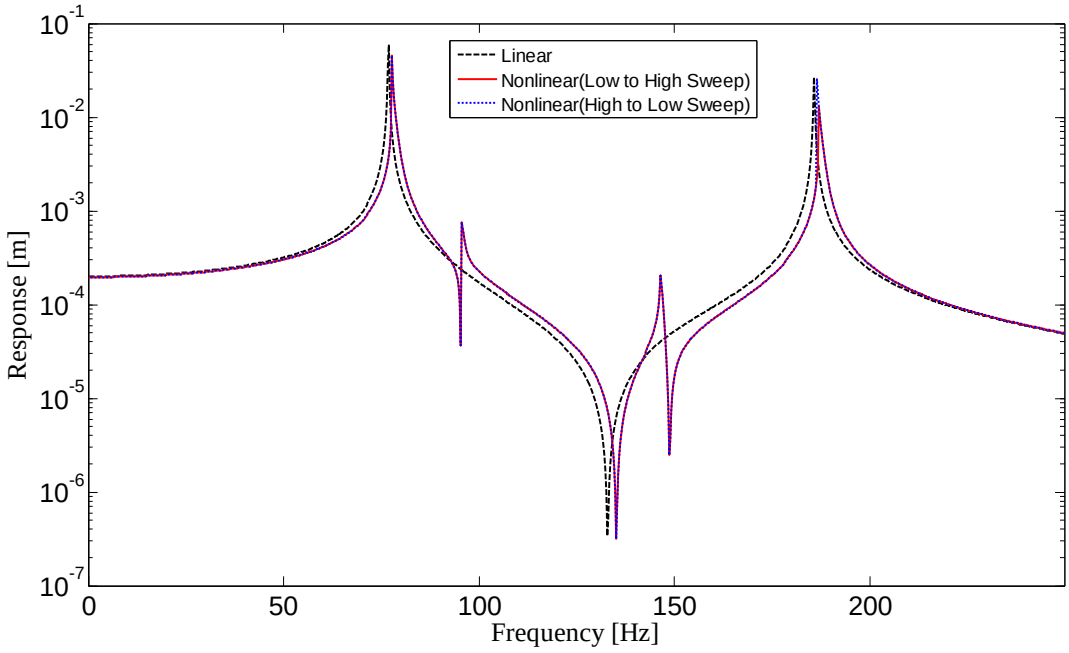

Figure 6.12 Single harmonic response of $|X_1|_y$ (node 1 in Y direction), case study A.2

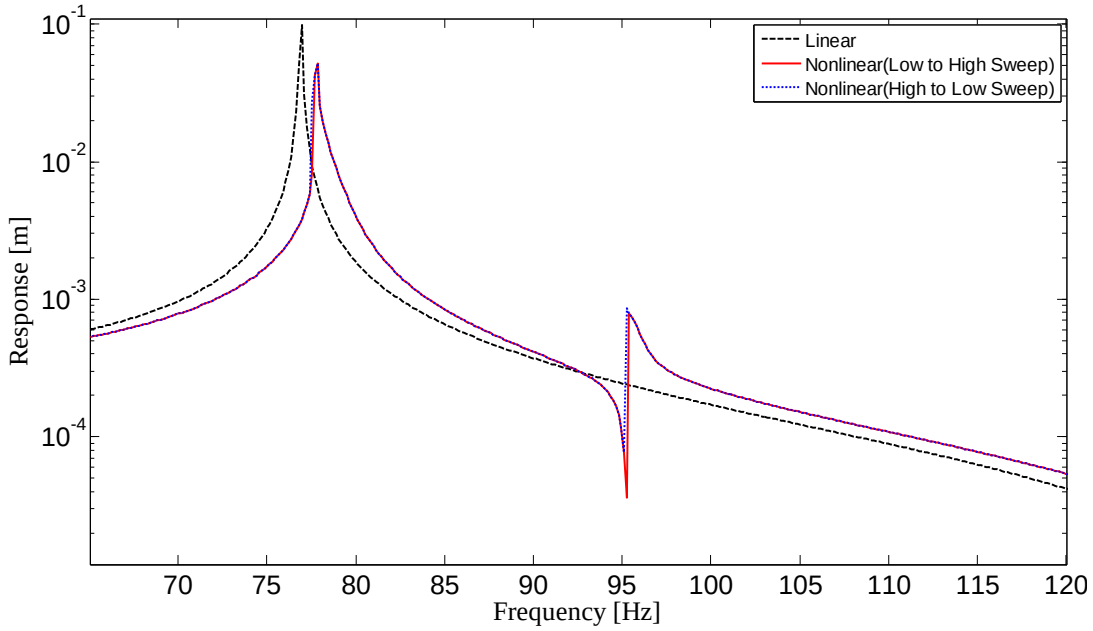

Figure 6.13 Single harmonic response of $\left|X_1\right|_y$ (close-up), case study A.2

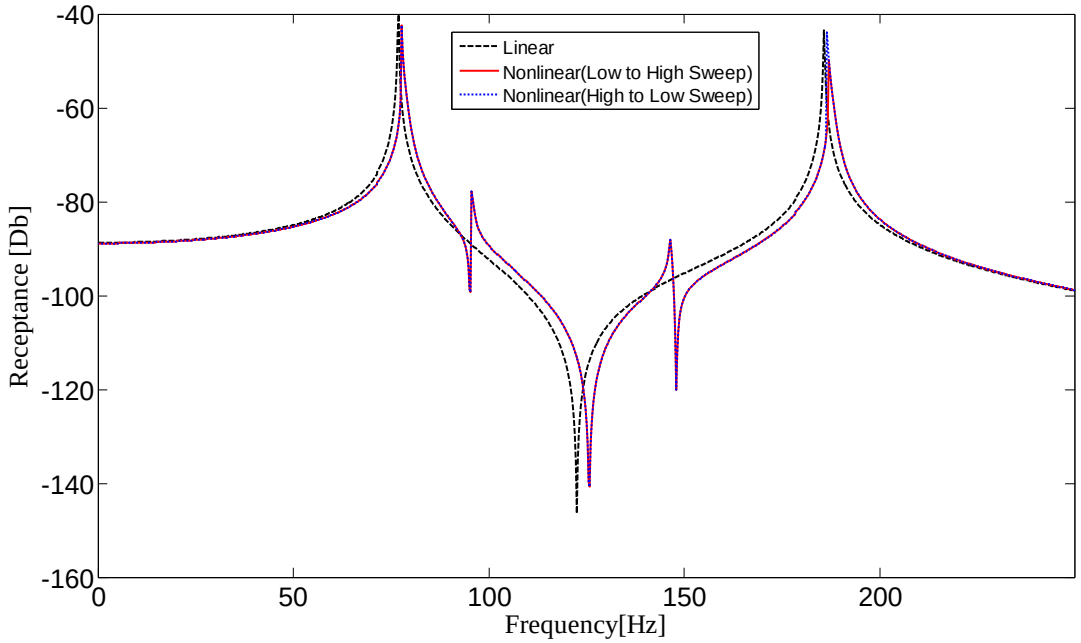

Figure 6.14 Pseudo receptance $\left|\alpha_{11}\right|_y$, case study A.2

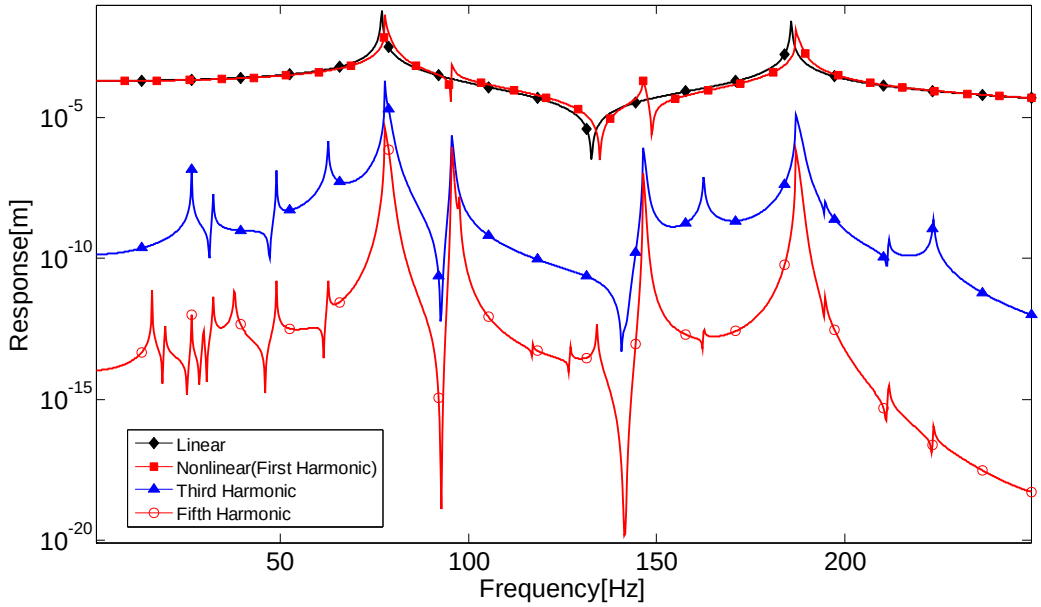

Figure 6.15 Multi harmonic response solution of $\left|X_1\right|_y$ (node 1 in Y direction), case study A.2

Figure 6.16 showing the modal summation and matrix inversion results confirm that using only 10 modes is enough to predict the response accurately. Computational time saving is again complemented with accurate result.

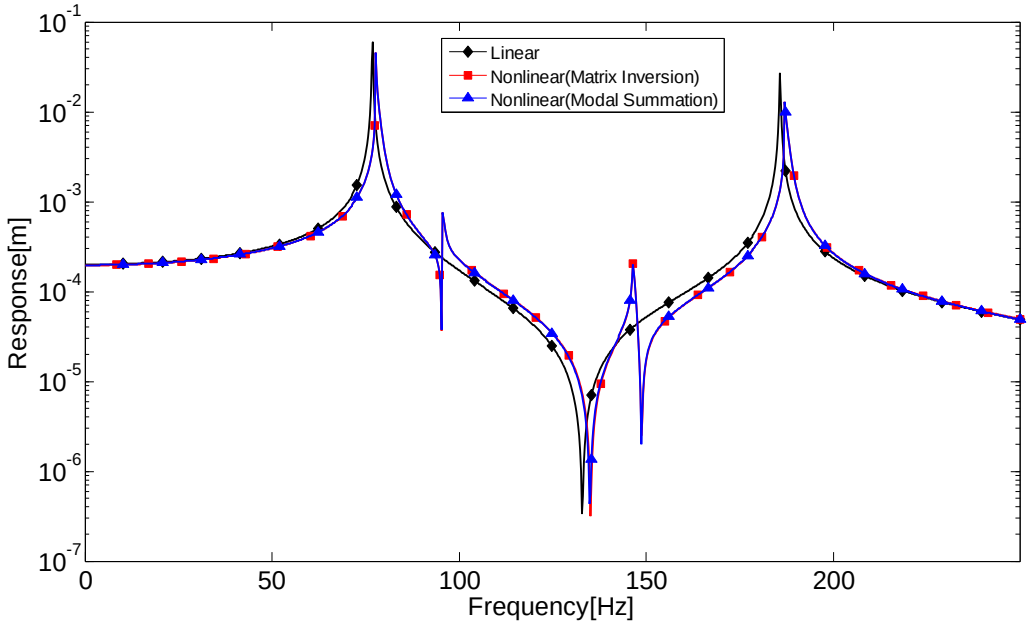

Figure 6.16 Modal summation and matrix inversion solutions comparison, case study A.2

Solution time comparison for single and multi harmonic solutions with matrix inversion counterparts are given in Table 6.8

Table 6.8 Solution Time Comparison for Case Study A.2

Solution Method	Frequency Increment [Hz]	Solution Time [s]
Single Harmonic (Modal Summation-15 Modes)	0.25	29.42
Single Harmonic (Matrix Inversion)	0.25	945
Multi Harmonic with 3 harmonic components (Modal Summation-15 Modes)	0.25	511.22
Multi Harmonic with 3 harmonic components (Matrix Inversion)	0.25	>>7200

6.1.3 Case Study A.3

The system introduced in Case Study A is used, and nonlinearities (bold lines) are defined between the nodes (points) shown in Figure 6.17 in all three directions, x, y and z (Table 6.9). The forcing, loss factor and number of modes used in FRF calculations are given in Table 6.10.

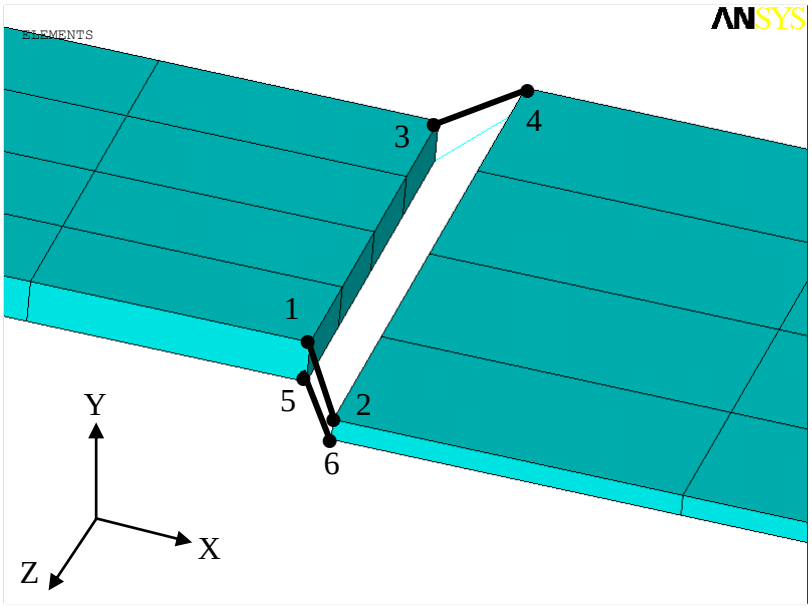

Figure 6.17 Nonlinear connections for case study A.3

Table 6.9 Nonlinearity definitions between nodes for case study A.3

Nonlinear Connections: (Node 1-Node 2)	Nonlinearity Type	Nonlinearity Coefficients
5-6	Cubic Stiffness	$\beta = 5\ N/m^3$
1-2	Preloaded Stiffness	$F_p = 1x10^{-3}\ N$
		$k = 2000\ N/m$
3-4	Preloaded Stiffness	$F_p = 5x10^{-4}\ N$
		$k = 3000\ N/m$

Table 6.10 Loss factor, forcing and number of modes used in FRF calculation values for case study A.3

Loss Factor	Forcing			Number of Modes used in FRF Calculation
	On node	Value (N)	Direction	
0.0012 (% 0.12)	1	5	-Y	15
	3	1	-Y	

The single harmonic response, pseudo receptance and multi harmonic response of node 1 in Y direction is given in Figure 6.18, 6.19 and 6.20 respectively.

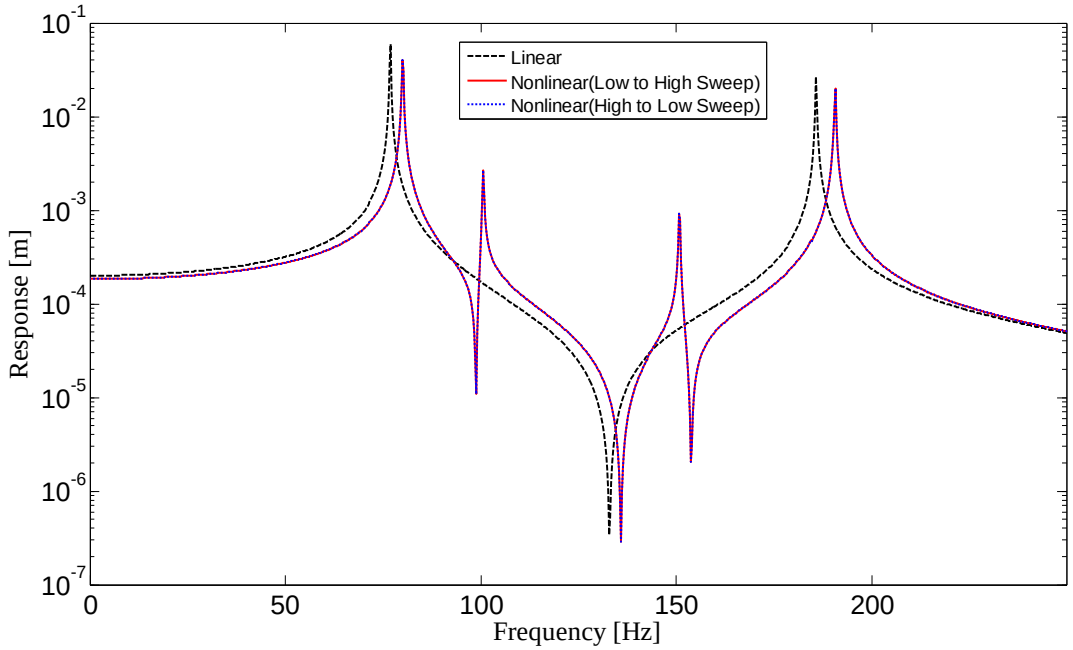

Figure 6.18 Single harmonic response of $\left|X_1\right|_y$ (node 1 in Y direction), case study A.3

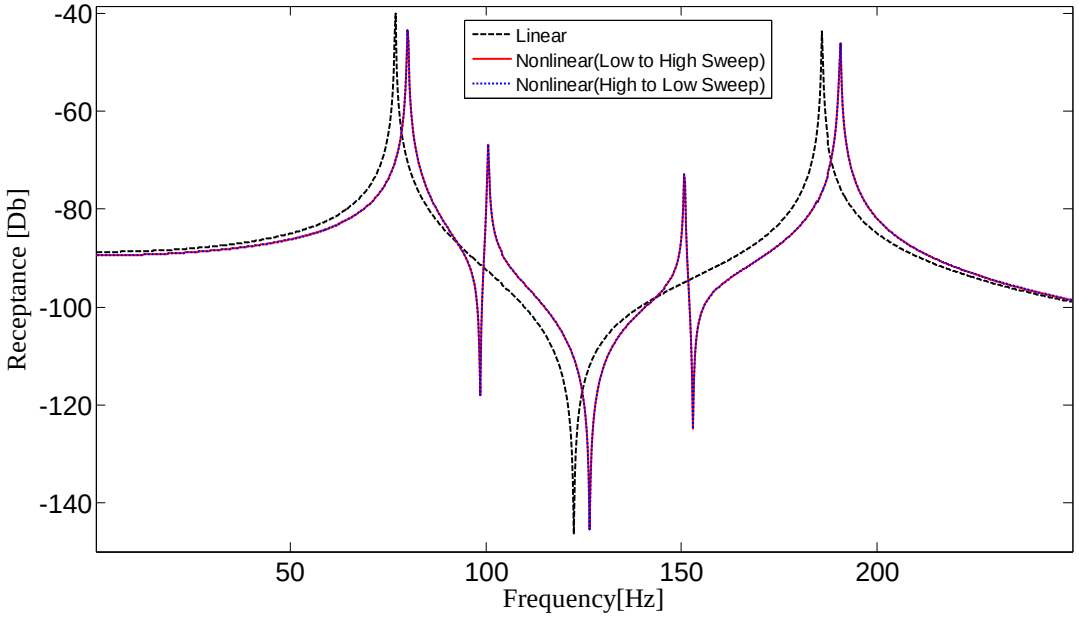

Figure 6.19 Pseudo receptance $\left|\alpha_{11}\right|_y$ (in y direction), case study A.3

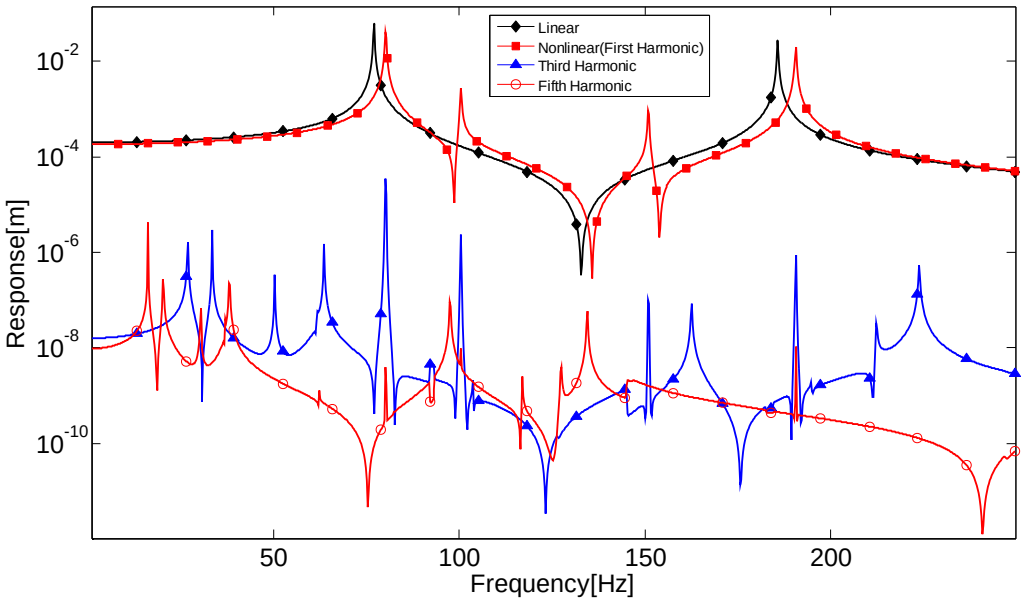

Figure 6.20 Multi harmonic response solution of $\left|X_1\right|_y$ (node 2 in Y direction), case study A.3

Figure 6.21 showing the modal summation and matrix inversion results confirm that using only 15 modes is enough to predict the response accurately. Computational time saving is again complemented with accurate result.

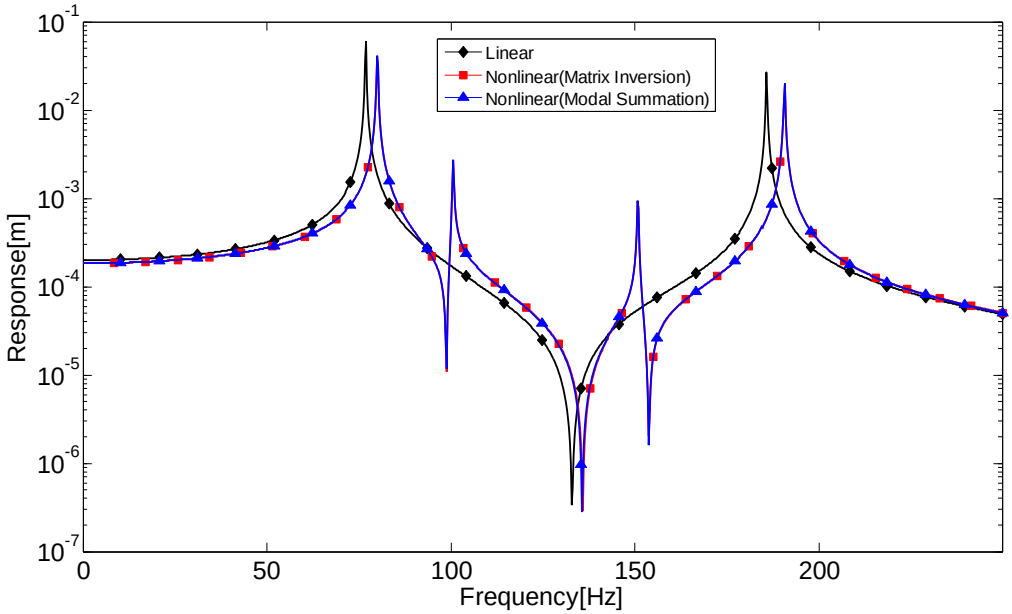

Figure 6.21 Modal summation and matrix inversion solutions comparison, case study A.3

Solution time comparison for single and multi harmonic solutions with matrix inversion counterparts are given in Table 6.11

Table 6.11 Solution Time Comparison for Case Study A.3

Solution Method	Frequency Increment [Hz]	Solution Time [s]
Single Harmonic (Modal Summation-15 Modes)	0.25	56.92
Single Harmonic (Matrix Inversion)	0.25	971.23
Multi Harmonic with 3 harmonic components (Modal Summation-15 Modes)	0.25	860.97
Multi Harmonic with 3 harmonic components (Matrix Inversion)	0.25	>>14400

6.1.4 Case Study A.4

The system introduced in Case Study A is used, and nonlinearities (bold lines) are defined between the nodes (points) shown in Figure 6.22 in all three directions, x, y and z (Table 6.12). The forcing, loss factor and number of modes used in FRF calculations are given in Table 6.13.

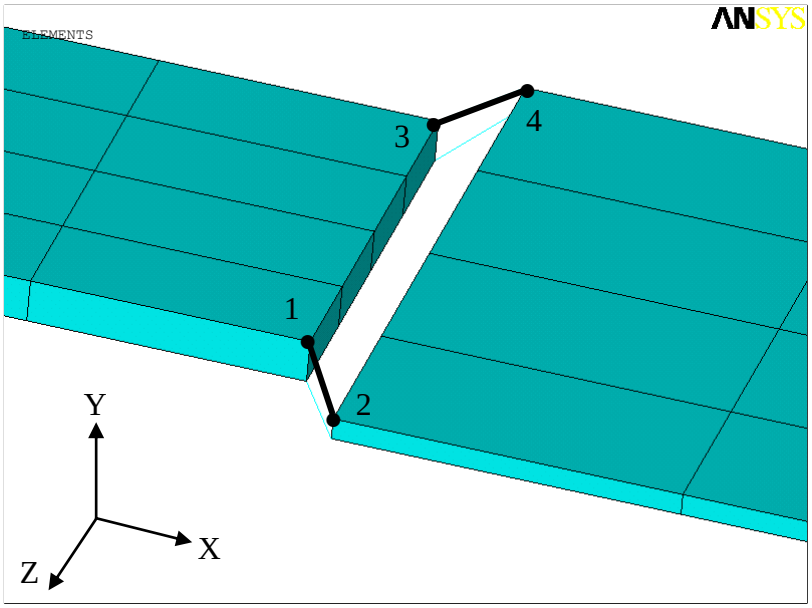

Figure 6.22 Nonlinear connections for case study A.4

Table 6.12 Nonlinearity definitions between nodes for case study A.4

Nonlinear Connections: (Node 1-Node 2)	Nonlinearity Type	Nonlinearity Coefficients
1-2	Piecewise Linear Stiffness	$\delta = 5x10^{-4}$ m
		$k_1 = 1000$ N/m
		$k_2 = 5000$ N/m
3-4	Piecewise Linear Stiffness	$\delta = 10^{-3}$ m
		$k_1 = 5000$ N/m
		$k_2 = 6000$ N/m

Table 6.13 Loss factor, forcing and number of modes used in FRF calculation for case study A.4

Loss Factor	Forcing			Number of Modes used in FRF Calculation
	On node	Value (N)	Direction	
0.0012 (% 0.12)	1	10	-Y	15
	3	5	-Y	

The single harmonic response, pseudo receptance and multi harmonic response of node 1 in Y direction is given in Figure 6.23, 6.24 and 6.25 respectively.

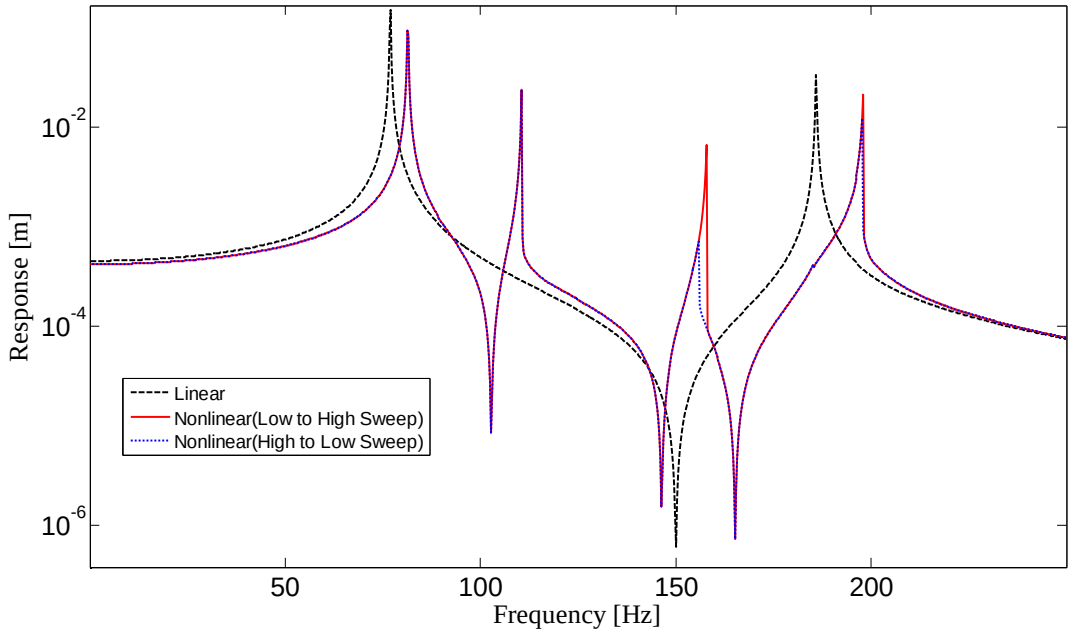

Figure 6.23 Single harmonic response of $\left|X_1\right|_y$ (node 1 in Y direction), case study A.4

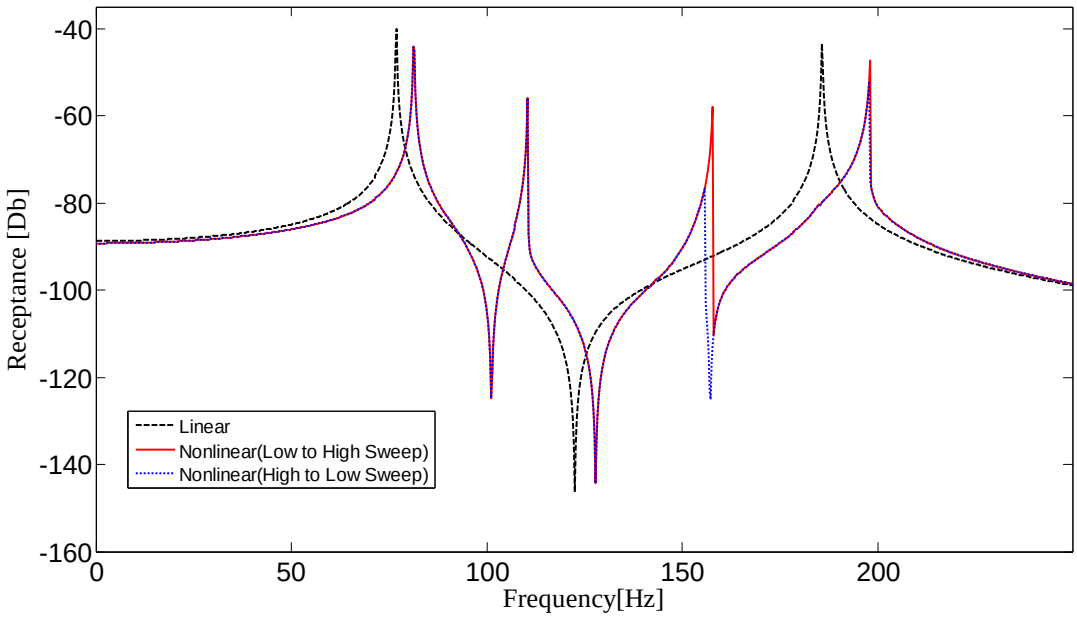

Figure 6.24 Pseudo receptance $\left|\alpha_{11}\right|_y$ (in y direction), case study A.4

Figure 6.25 that shows the modal summation and matrix inversion results confirms that using only 15 modes is enough to predict the response accurately. Computational time saving is again complemented with accurate result.

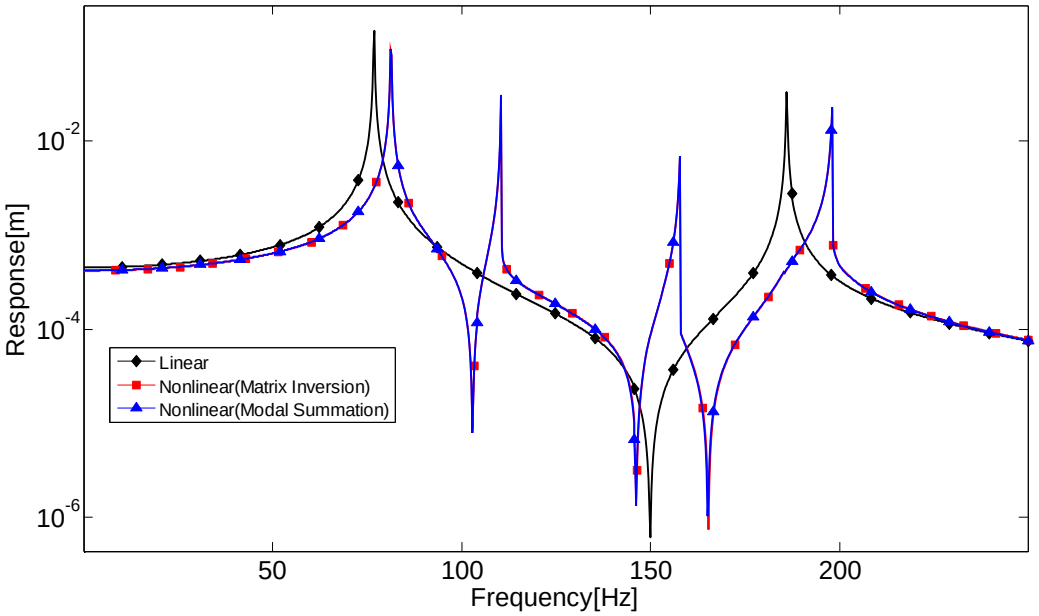

Figure 6.25 Modal summation and matrix inversion solutions comparison, case study A.4

Solution time comparison for single harmonic solution by considering the modal summation and matrix inversion results is given in Table 6.14

Table 6.14 Solution Time Comparison for Case Study A.4

Solution Method	Frequency Increment [Hz]	Solution Time [s]
Single Harmonic (Modal Summation-15 Modes)	0.25	32.54
Single Harmonic (Matrix Inversion)	0.25	939.34

6.2 Case Study B

One punched beam and a hollow cylinder inside the hole of the beam, (Figure 6.26 and 6.27), fixed at one end surfaces and joined through linear and nonlinear elements will be examined (Figure 6.28). The solid beam and cylinder elements are meshed with SOLID 185 [65] elements and joined with four COMBIN 14 2D-3D [65] linear spring type elements through neighbor 8 nodes in order to ensure the connection of two solids which is again necessary to form common system matrices (Figure 6.29). In the FEM model, each node has 3 DOF's (in x, y and z directions).

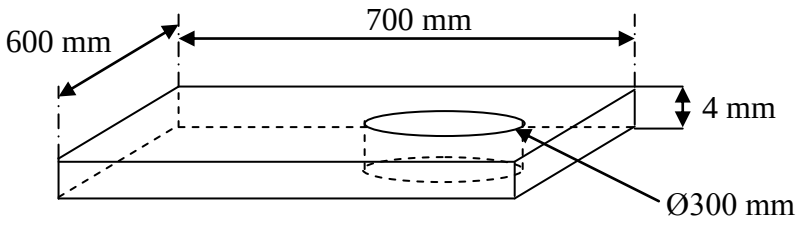

Figure 6.26 Dimensions of the punched beam in case study B

The spring constants of the linear spring type elements in three directions (x, y and z) are taken as 2000 N/m.

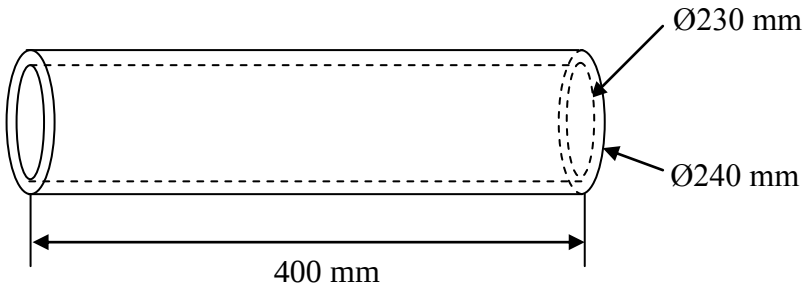

Figure 6.27 Dimensions of the hollow cylinder in case study B

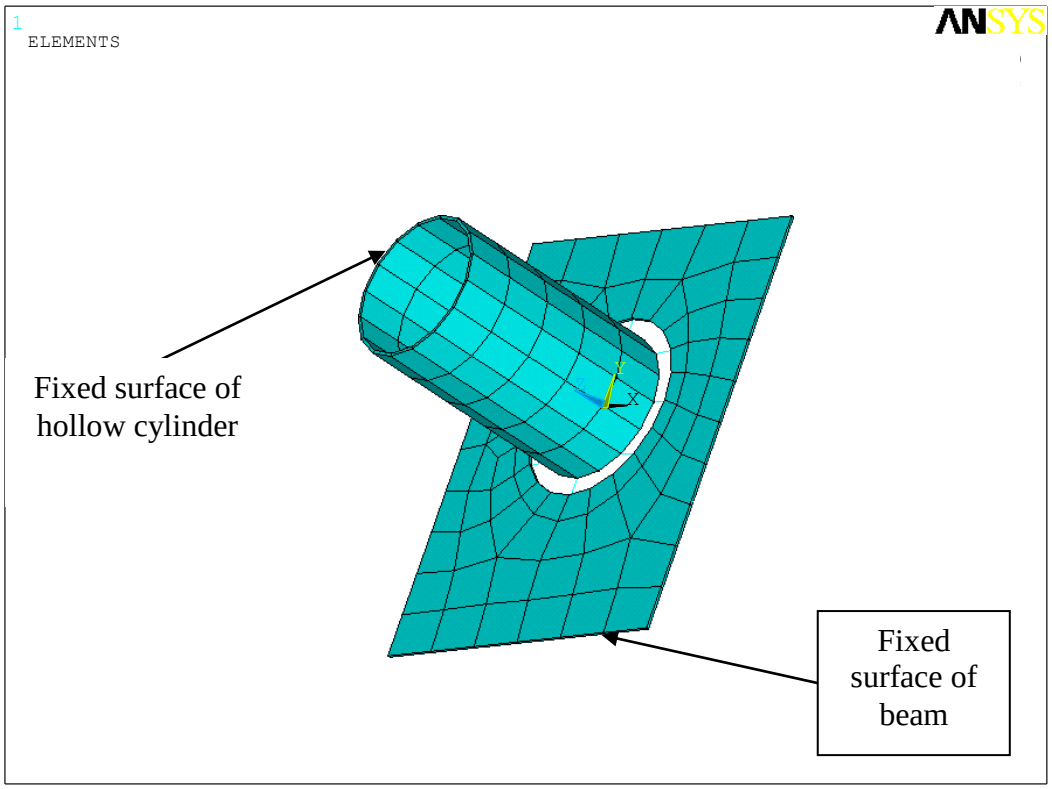

Figure 6.28 The FEM models and fixed surfaces of 2 parts in case study B

The material properties of two parts considered in the analysis are given in Table 6.15.

Table 6.15 Material properties for case study B

Density	5000kg/m^3
Modulus of Elasticity	10 GPa
Poisson's Ratio	0.3

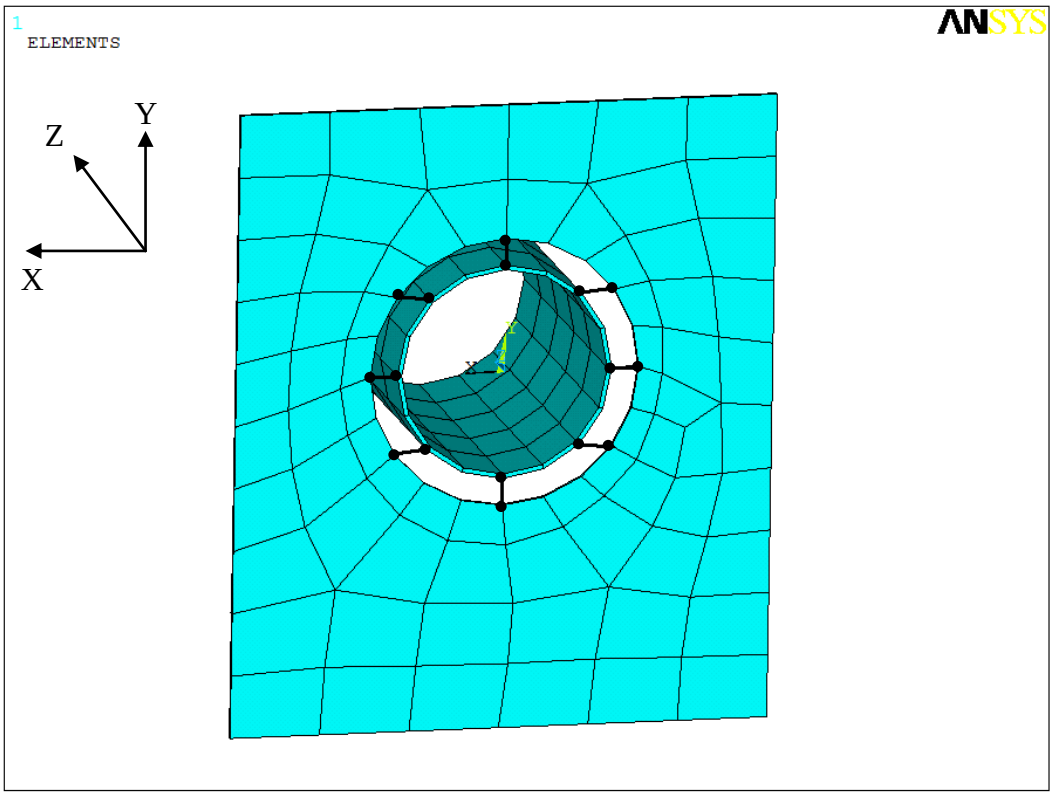

Figure 6.29 Connection of parts through neighboring nodes with linear spring elements and coordinate system definition for case study B

The FEM is constituted with 1032 DOF after meshing procedure. Again linear modal analysis is made in ANSYS® as well as by using the program developed and the natural frequencies obtained in both analyses are compared (Table 6.16). The results are found to be almost the same. The mode shapes corresponding to the first three natural frequencies are given in Figure 6.30.

Table 6.16 First 9 natural frequencies of the system obtained by ANSYS® and MH-NLS [Hz] for case study B

Program	Natural Frequencies (Hz)								
ANSYS®	18.0	26.7	103.8	116.3	153.1	166.2	205.2	224.0	262.6
MH-NLS	17.6	26.6	103.8	116.3	153.1	166.2	205.2	224.0	262.6

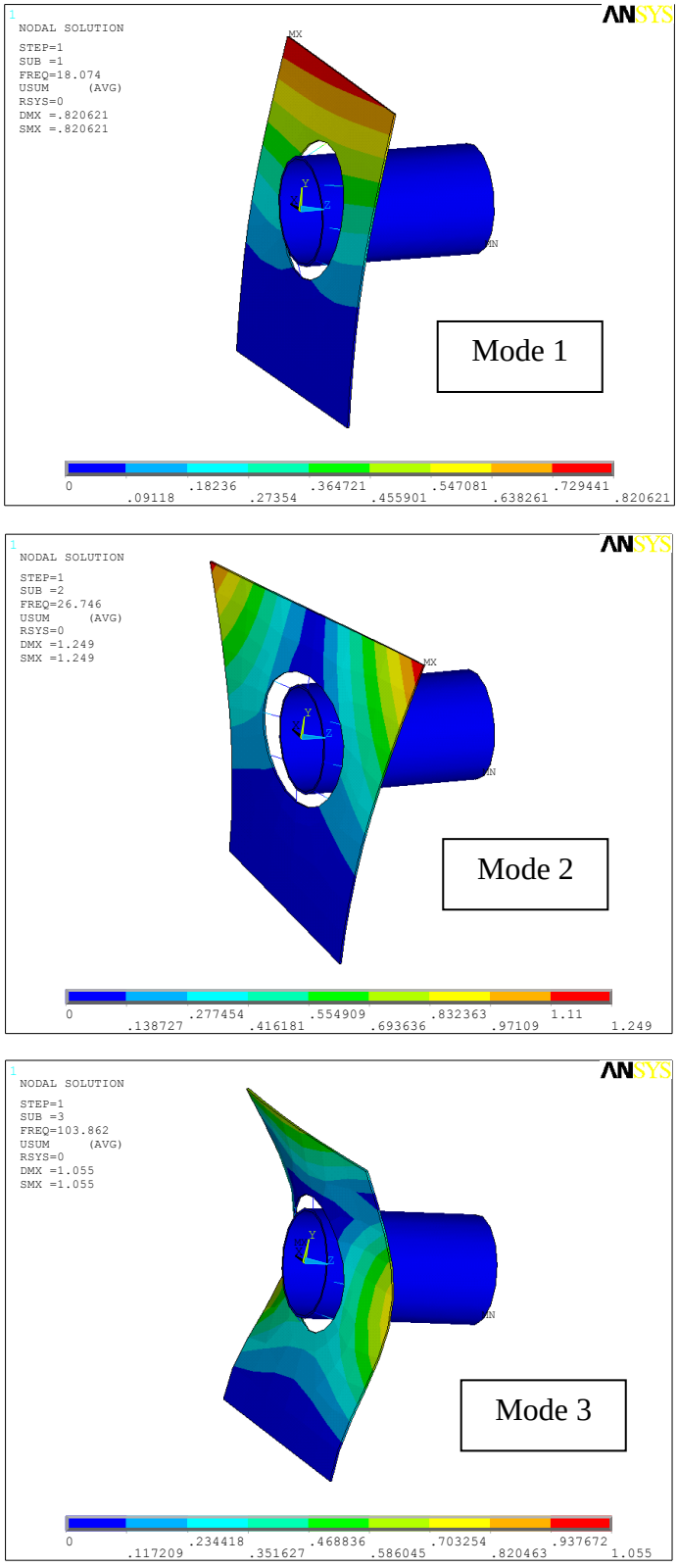

Figure 6.30 Mode shapes of the first three modes for case study B

6.2.1 Case Study B.1

The system introduced in Case Study B is used, and nonlinearities are defined between the nodes (points) with bold lines shown in Figure 6.31 in all three directions, x, y and z (Table 6.17). The forcing, loss factor and number of modes used in FRF calculation is given in Table 6.18.

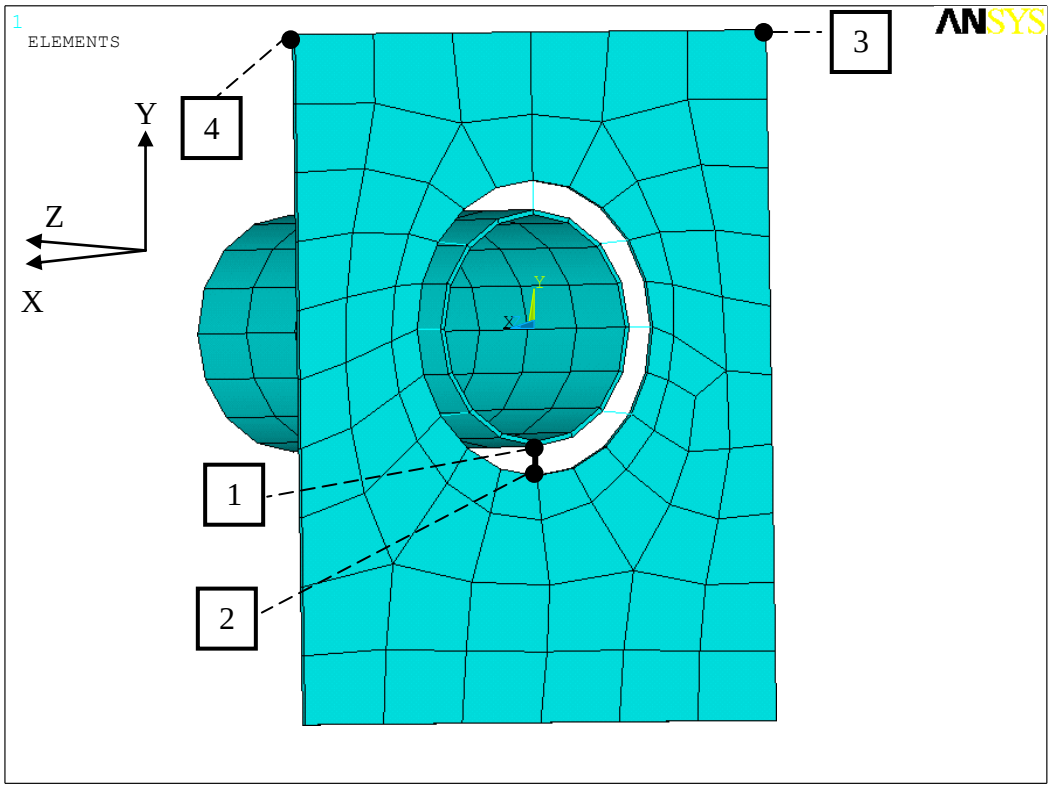

Figure 6.31 Nonlinear connections, excitation and response nodes for case study B.1

Table 6.17 Nonlinearity definitions between nodes for case study B.1

Nonlinear Connections: (Node 1-Node 2)	Nonlinearity Type	Nonlinearity Coefficients
1-2	Cubic Stiffness	$\beta = 10^{14}$ N/m^3

Table 6.18 Loss factor, forcing and number of modes used in FRF calculation values for case study B.1

Loss Factor	Forcing			Number of Modes used in FRF Calculation
	On node	Value (N)	Direction	
0.0012 (% 0.12)	3	2	Z	15
	4	2	Z	

The single harmonic response, pseudo receptance and multi harmonic response of node 4 in Z direction is given in Figure 6.32, 6.33 and 6.34 respectively.

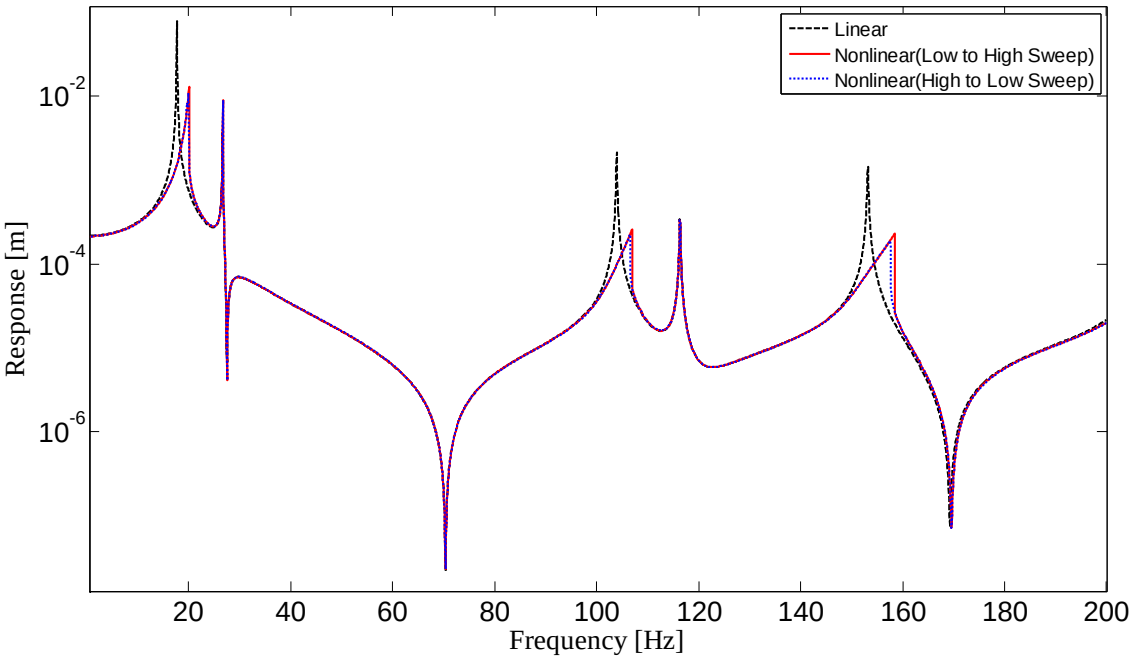

Figure 6.32 Single harmonic response of $\left|X_4\right|_z$ (node 4 in Z direction), case study B.1

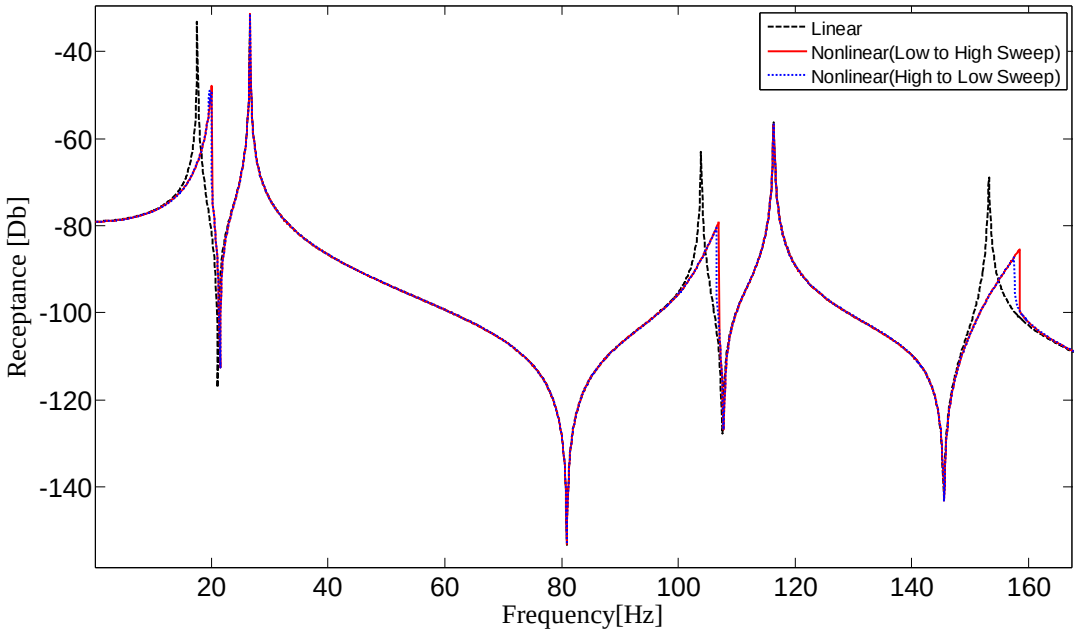

Figure 6.33 Pseudo receptance $\left|\alpha_{44}\right|_z$ (in z direction), case study B.1

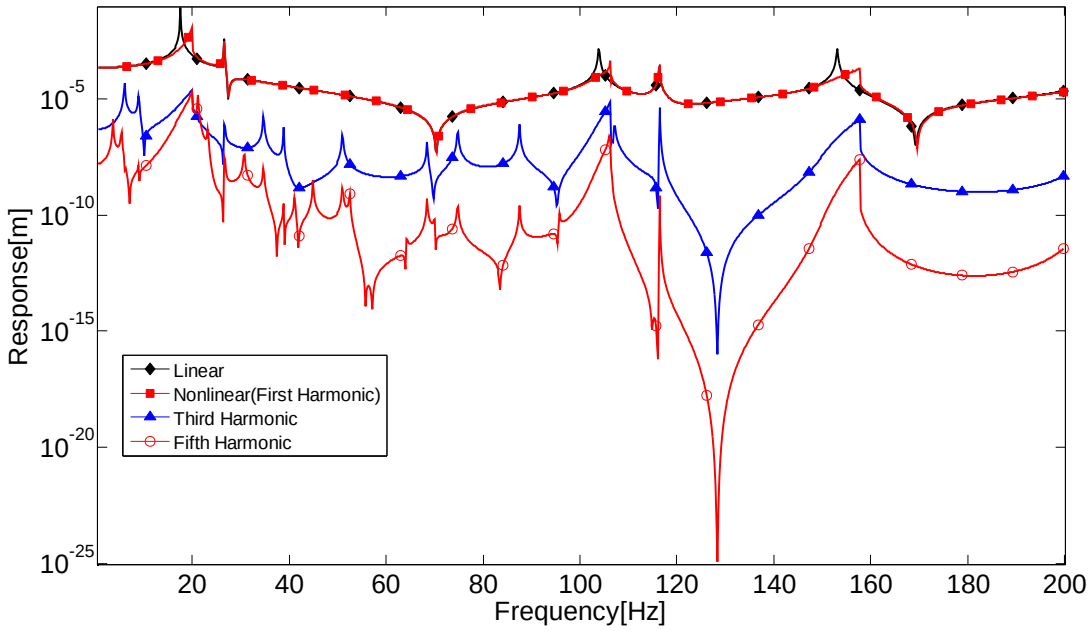

Figure 6.34 Multi harmonic response solution of $\left|X_4\right|_z$ (node 4 in Z direction), case study B.1

Figure 6.35 showing the modal summation and matrix inversion results imply that using only 15 modes is enough to predict the response roughly accurate. But in Figure 6.36 that shows the comparison of the modal summation with 40 modes and matrix inversion results confirms that 40 modes is necessary to predict the response more accurately.

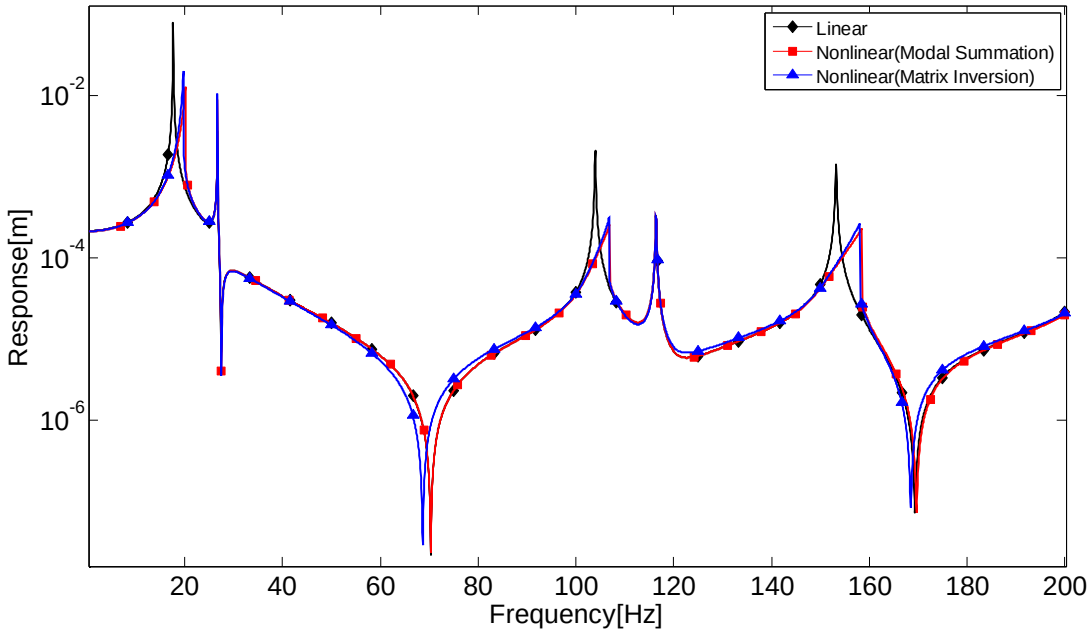

Figure 6.35 Modal summation (using 15 modes) and matrix inversion solutions comparison, case study B.1

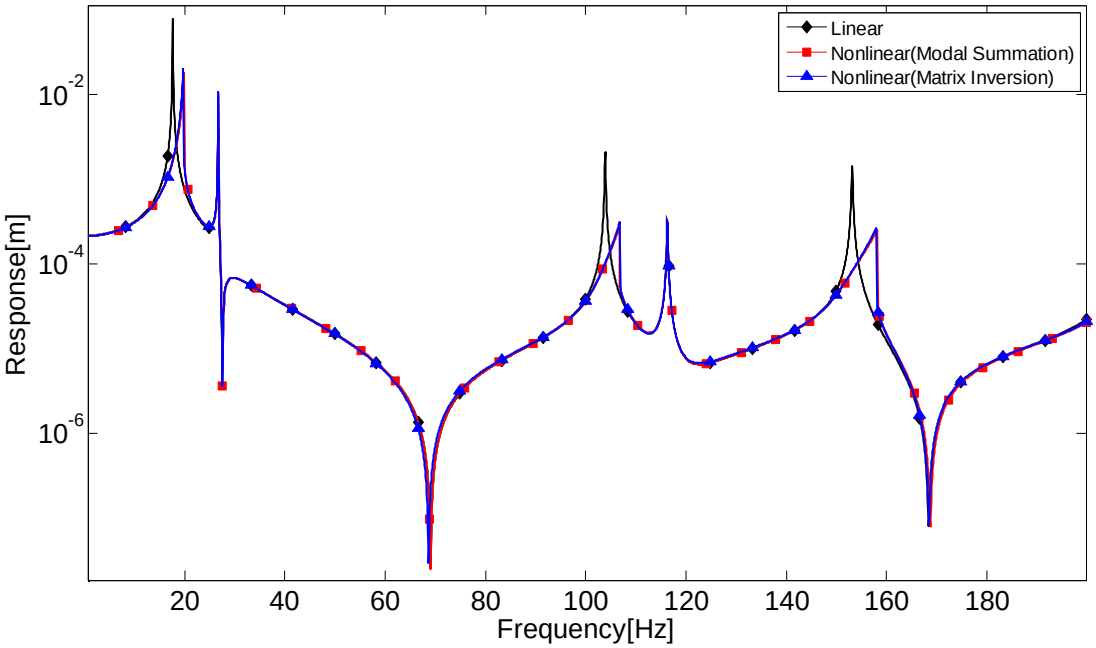

Figure 6.36 Modal summation (using 40 modes) and matrix inversion solutions comparison, case study B.1

Solution time comparison for single and multi harmonic solutions with matrix inversion counterparts are given in Table 6.19

Table 6.19 Solution Time Comparison for Case Study B.1

Solution Method	Frequency Increment [Hz]	Solution Time [s]
Single Harmonic (Modal Summation-15 Modes)	0.1	83.51
Single Harmonic (Modal Summation-20 Modes)	0.1	96.39
Single Harmonic (Modal Summation-30 Modes)	0.1	123.33
Single Harmonic (Modal Summation-40 Modes)	0.1	147.59
Single Harmonic (Matrix Inversion)	0.1	5621.32
Multi Harmonic with 3 harmonic components (Modal Summation-40 Modes)	0.1	847.51
Multi Harmonic with 3 harmonic components (Matrix Inversion)	0.1	>>36000

6.2.2 Case Study B.2

The system introduced in Case Study B is used, and nonlinearities are defined between the nodes (points) with bold lines shown in Figure 6.37 in all three directions, x, y and z (Table 6.20). The forcing, loss factor and number of modes used in FRF calculation is given in Table 6.21.

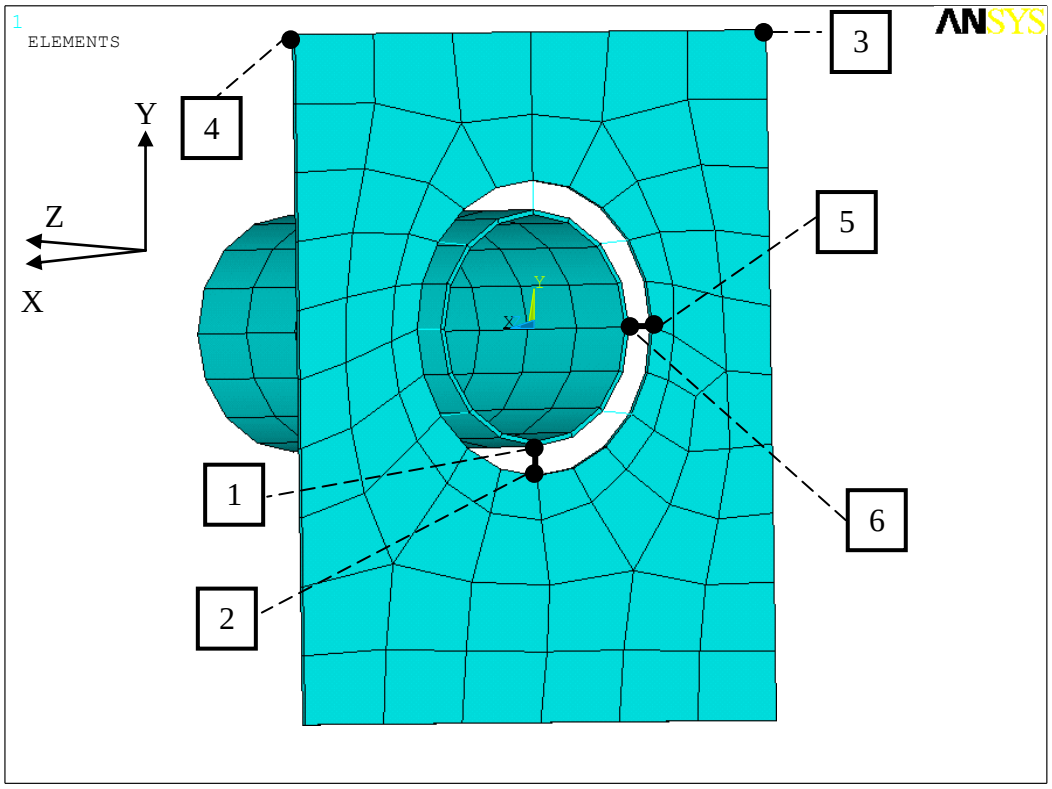

Figure 6.37 Nonlinear connections, excitation and response nodes for case study B.2

Table 6.20 Nonlinearity definitions between nodes for case study B.2

Nonlinear Connections: (Node 1-Node 2)	Nonlinearity Type	Nonlinearity Coefficients
1-2	Arctan Stiffness	$\rho = 10$
		$\kappa = 10000$
5-6	Arctan Stiffness	$\rho = 10$
		$\kappa = 20000$

Table 6.21 Loss factor, forcing and number of modes used in FRF calculation values for case study B.2

Loss Factor	Forcing			Number of Modes used in FRF Calculation
	On node	Value (N)	Direction	
0.0012 (% 0.12)	3	2	Z	40
	4	2	Z	

The single harmonic response, pseudo receptance and multi harmonic response of node 4 in Z direction is given in Figure 6.38, 6.39 and 6.40 respectively.

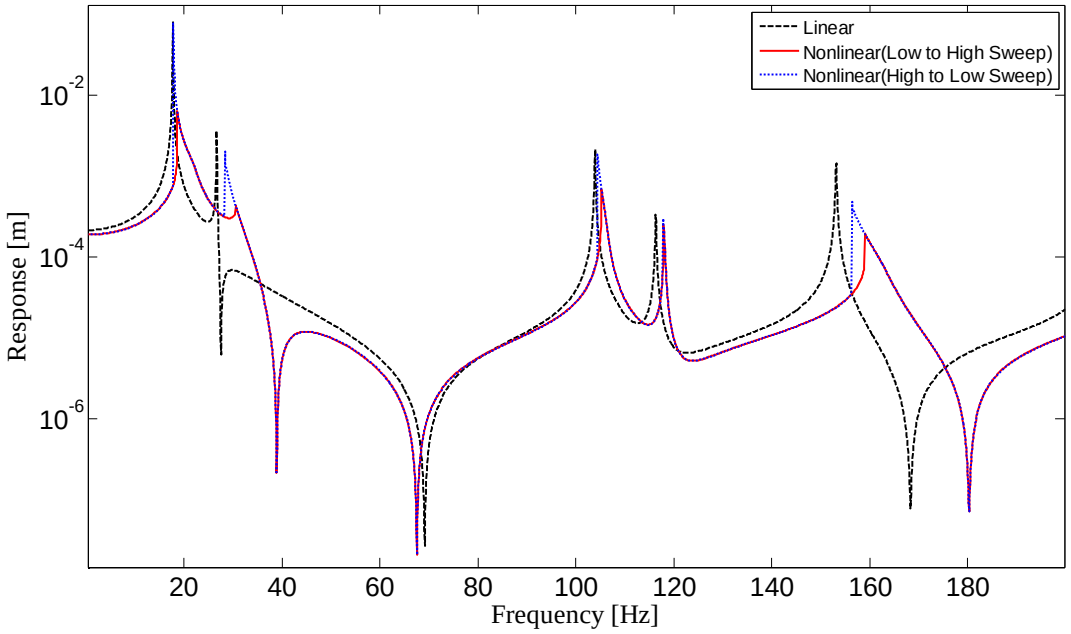

Figure 6.38 Single harmonic response of $|X_4|_z$ (node 4 in Z direction), case study B.2

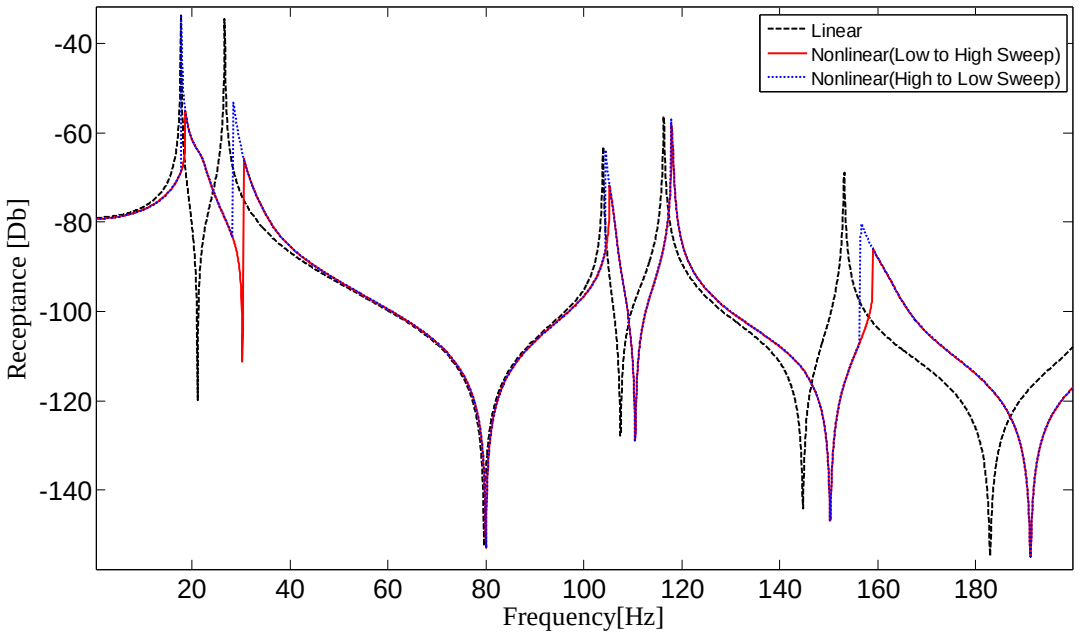

Figure 6.39 Pseudo receptance $\left|\alpha_{44}\right|_z$ (in z direction), case study B.2

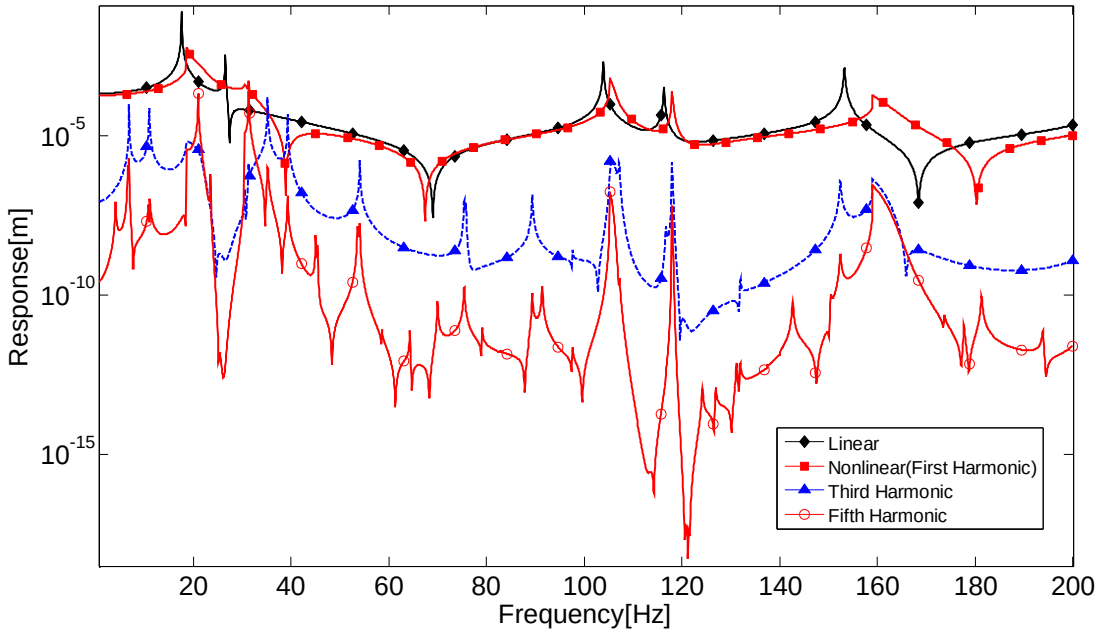

Figure 6.40 Multi harmonic response solution of $\left|X_4\right|_z$ (node 4 in Z direction), case study B.2

Figure 6.41 showing the modal summation and matrix inversion results confirm that using only 40 modes is enough to predict the response accurately. Computational time saving is again complemented with accurate result at this frequency range.

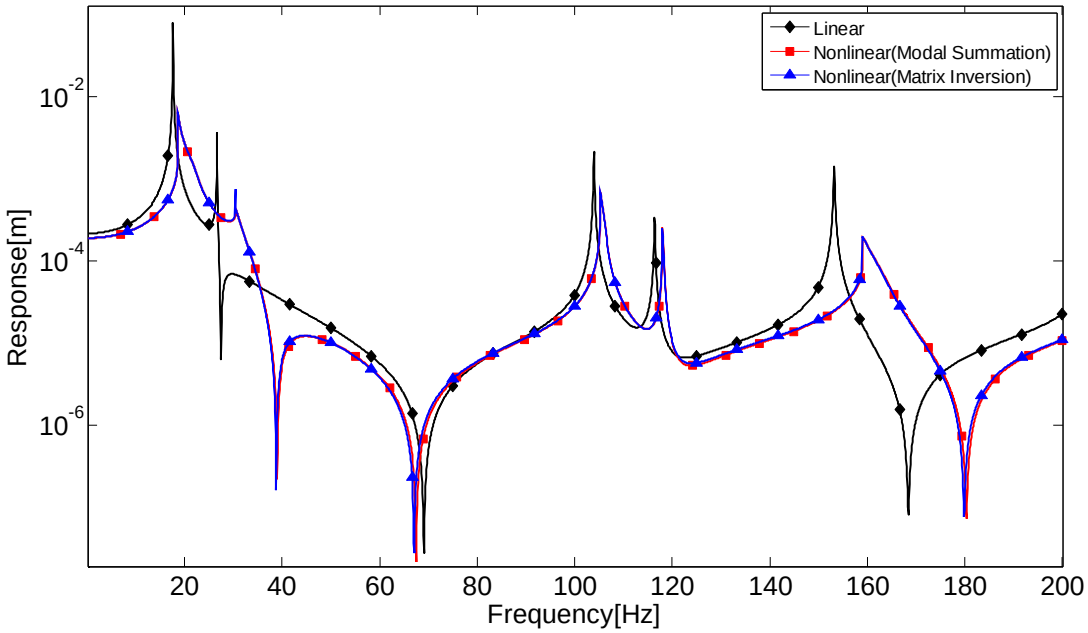

Figure 6.41 Modal summation (using 40 modes) and matrix inversion solutions comparison, case study B.2

Solution time comparison for single and multi harmonic solution is given in Table 6.22

Table 6.22 Solution Time Comparison for Case Study B.2

Solution Method	Frequency Increment [Hz]	Solution Time [s]
Single Harmonic (Modal Summation-40 Modes)	0.1	249.38
Single Harmonic (Matrix Inversion)	0.1	6839.2
Multi Harmonic with 3 harmonic components (Modal Summation-40 Modes)	0.1	860.97
Multi Harmonic with 3 harmonic components (Matrix Inversion)	0.1	>>108000

6.2.3 Case Study B.3

The system introduced in Case Study B is used and nonlinearities are defined between the nodes (points) with bold lines shown in Figure 6.42 in all three directions, x, y and z (Table 6.23). The forcing, loss factor and number of modes used in FRF calculation is given in Table 6.24.

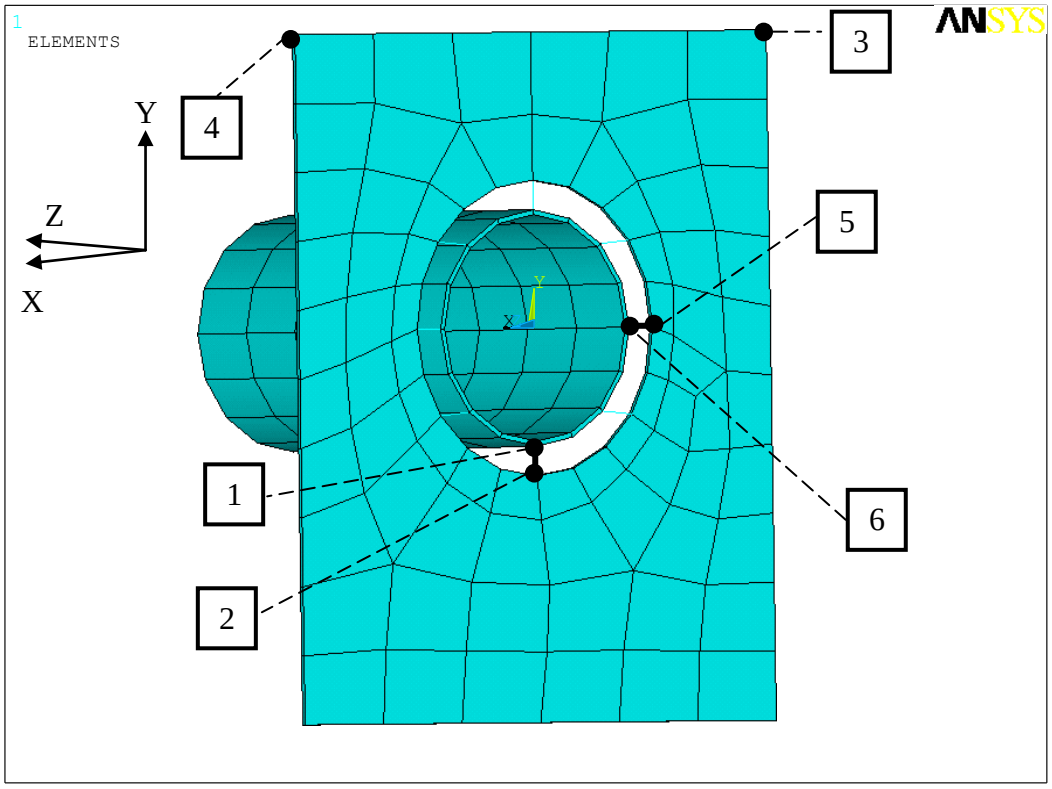

Figure 6.42 Nonlinear connections, excitation and response nodes for case study B.3

Table 6.23 Nonlinearity definitions between nodes for case study B.3

Nonlinear Connections: (Node 1-Node 2)	Nonlinearity Type	Nonlinearity Coefficients
1-2	Preloaded Stiffness	$F_p = 10^{-4}$ N
		$k = 10^{9}$ N/m
5-6	Piecewise Linear Stiffness	$\delta = 10^{-3}$ m
		$k_1 = 10^{7}$ N/m
		$k_1 = 10^{8}$ N/m

Table 6.24 Loss factor, forcing and number of modes used in FRF calculation values for case study B.3

Loss Factor	Forcing			Number of Modes used in FRF Calculation
	On node	Value (N)	Direction	
0.0012 (% 0.12)	3	2	Z	40
	4	2	Z	

The single harmonic response, pseudo receptance and multi harmonic response of node 4 in Z direction is given in Figure 6.43, 6.44 and 6.45 respectively.

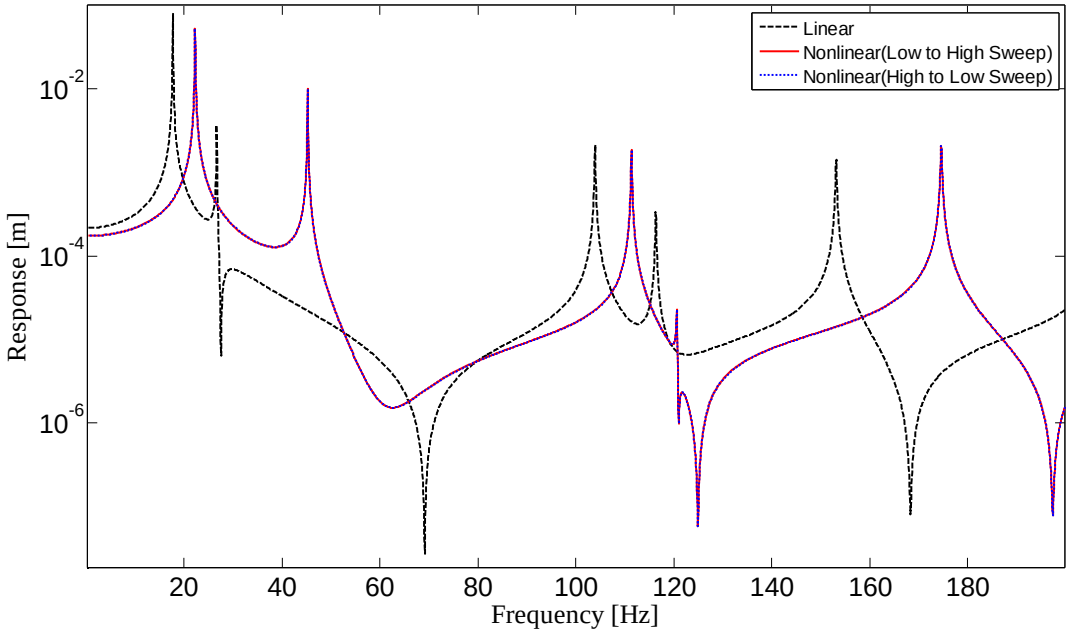

Figure 6.43 Single harmonic response of $\left|X_4\right|_z$ (node 4 in Z direction), case study B.3

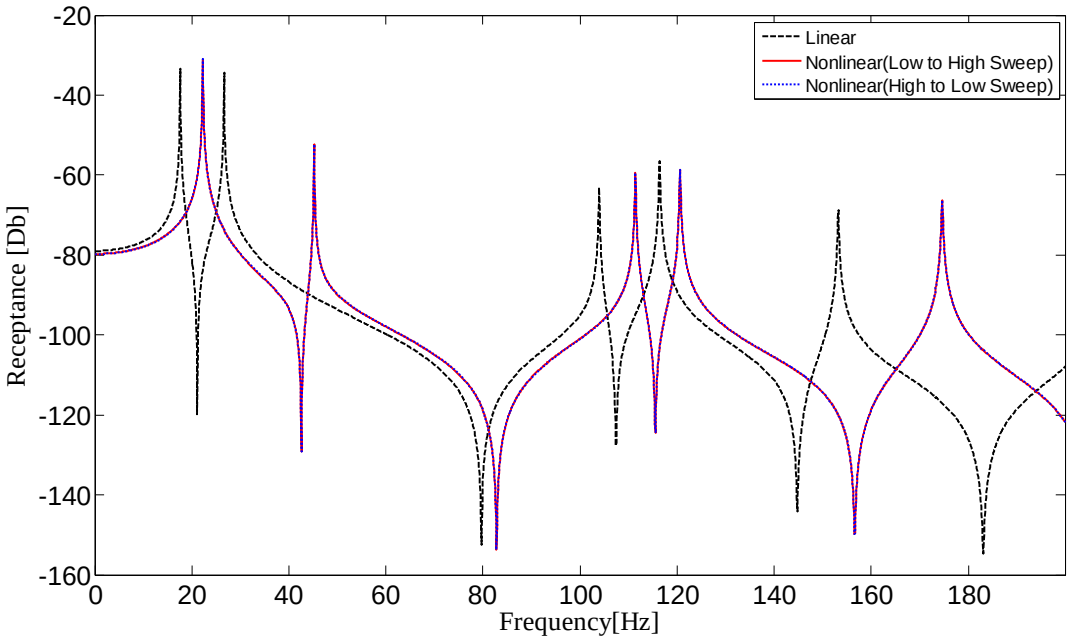

Figure 6.44 Pseudo receptance $\left|\alpha_{44}\right|_z$ (in z direction), case study B.3

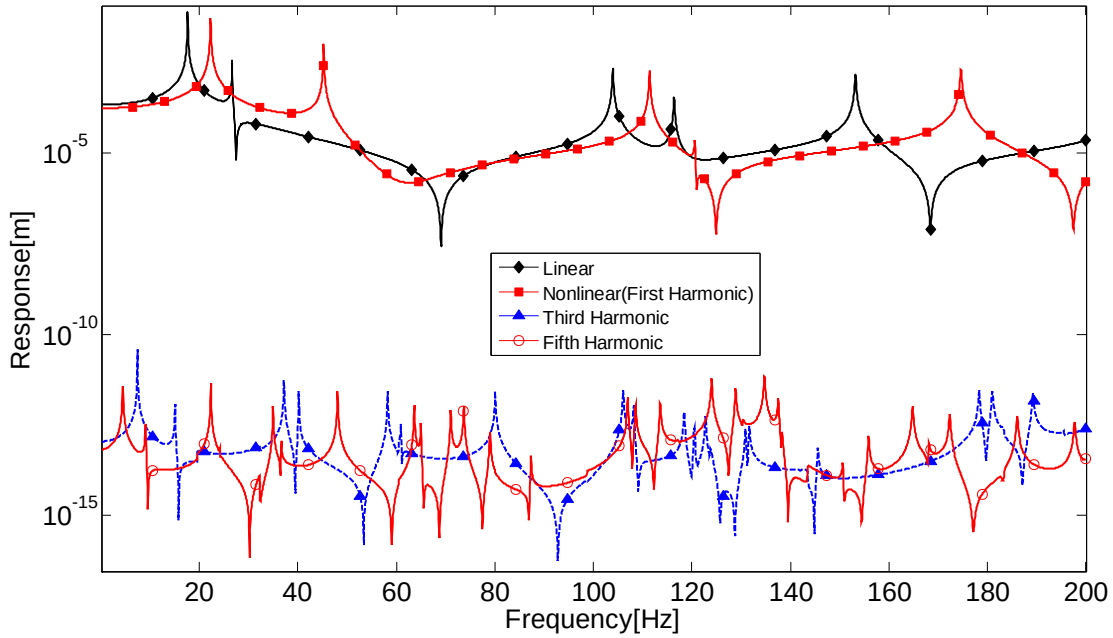

Figure 6.45 Multi harmonic response solution of $\left|X_4\right|_z$ (node 4 in Z direction), case study B.3

Solution time comparison for single and multi harmonic solution is given in Table 6.25

Table 6.25 Solution Time Comparison for Case Study B.3

Solution Method	Frequency Increment [Hz]	Solution Time [s]
Single Harmonic (Modal Summation-40 Modes)	0.1	109.68
Single Harmonic (Matrix Inversion)	0.1	6758.7
Multi Harmonic with 3 harmonic components (Modal Summation-40 Modes)	0.1	1592.41
Multi Harmonic with 3 harmonic components (Matrix Inversion)	0.1	>>72000

CHAPTER 7

DISCUSSIONS, CONCLUSIONS and FUTURE WORK

In this study, the method called “Iterative Receptance Method” which was developed in an earlier study [18] for forced harmonic response analysis of MDOF nonlinear structures is employed to analyze large structures having different types of local nonlinearities. The nonlinearities are quasilinearised using describing function theory. Furthermore, the effect of higher order harmonic terms is considered by using multi harmonic describing function formulation [13]. The mathematical formulations are embedded in a computer program developed in MATLAB® with graphical user interface. The program inputs system matricies from a file which is obtained by using substructuring analysis in a commercial FEM software program, ANSYS®. Different types of nonlinearities in the system can easily be defined through the graphical user interface of the MATLAB® program.

During the verification of the program with time domain solutions, it is shown that frequency domain solution is faster than time domain solution even multi harmonic effects are considered. Although the computational effort for time domain analysis directly depends on the damping and stiffness characteristics of the structure, the computation time for frequency domain analysis depends on modes and harmonics considered.

The results of the case studies imply that ignoring higher order terms can directly effect the accuracy of the results at specific frequency ranges. Elsewhere the effect of higher order terms become negligible, because they have much smaller amplitudes compared to the fundamental harmonic component. Even though the multi harmonic analyses are computationaly costly for large ordered systems, they should be taken

into consideration for frequency ranges where the multiples of the excitation frequency coincide with natural frequencies of the structure.

The solution time comparisons for case studies with large numbers of DOFs show that the formulation, which avoids matrix inversion during the solution, decreases the computation time drastically without affecting the accuracy of the results. It should be noted here that matrix inversion avoided during linear FRF formulation and modal summation is used in comparisons. When the formulation (3.22) which also avoids inversion of a large ordered matrix to find the PRM is used, computational time saving becomes more pronounced.

The program developed benefits from the mathematical background of the method proposed by Özgüven [61] by rearranging matrices so that the nonlinearity and input/output coordinates are collected in a sub-matrix. Hence, the computation of nonlinear response is achieved by evaluating few rows of pseudoreceptance matrix without inverting a matrix of size DOFxDOF.

The frequency increment found to be directly effective on accurately locating the jumping frequency, which also corresponds to the resonance frequency in some systems. To increase the accuracy of the analysis, user tend to decrease the increment which definitly increases the solution time. Especially in large ordered systems this fact needs to be taken into consideration. The adaptable frequency increment can be a remedy for this case, which is one of the suggestions for future work.

The program has no restriction other than the capabilities of the MATLAB® except for the order of the system matrices that can be loaded from the ANSYS® output file. The size of the output file grows violently as the numbers of DOF of the system under investigation increases. In fact, a system greater than 3000 DOF has an output file approximately 500MB which causes loading errors during file loading process. The improvement of the algorithm of file loading process is suggested as a future work.

The most valuable contribution of the program developed is the adaptation of the nonlinear harmonic response theory for a large engineering structure by using a commercial FEM software program for linear part of the vibration analysis. By using this program, the discrete model of a real engineering system can be analyzed by considering several type of nonlinearities in the system. In a future work, the capabilities of the program can be improved by introducing additional nonlinear behaviours.

REFERENCES

[1] S. W. Shaw, B. Balachandran. *A Review of Nonlinear Dynamics of Mechanical Systems in Year 2008.* Special Issue on Nonlinear Dynamics in Mechanical Systems 2(3):611-640, 2008

[2] J. Jerrelind and A. Stensson. *Nonlinear dynamics of parts in engineering systems.* Chaos, Solitons and Fractals, 11:2413-2428, 2000.

[3] D. J. Ewins. *The effect of slight non-linearities on modal testing of helicopter-like structures.* Vertica, 7: 1 – 8, 1983

[4] D. J. Ewins. *Modal Testing: theory, practice and application.* Research Studies Press LTD, London, 2000.

[5] A. Fidlin. *Nonlinear Oscillations in Mechanical Engineering.* Springer-Verlag, Germany, 2006.

[6] K. Worden. G. R. Tomlinson. *Non-linearity in Structural Dynamics: Detection, Identification and Modelling*. Institute of Physics, London, 2001.

[7] M. A. Dokainish and K. Subbaraj. *A survey of direct time-integration methods in computational structural dynamics: I, explicit methods.* International Journal of Computers and Structures, 32:1371-1386, 1989.

[8] M. A. Dokainish and K. Subbaraj. *A survey of direct time-integration methods in computational structural dynamics: Ii, implicit methods.* International Journal of Computers and Structures, 32:1387-1401, 1989.

[9] H. R. E. Siller. *Non-linear Modal Analysis Methods for Engineering Structures.* PhD Thesis, Imperial College London, University of London, 2004.

[10] M. Stylianou and B. Tabarrok. *Finite element analysis of an axially moving beam, part i:time integration*. Journal of Sound and Vibration, 4(178):443-453, 1994.

[11] C. W. Bert, J. D. Stricklin. *Comparative evaluation of six different numerical integration methods for nonlinear dynamic systems.* Journal of Sound and Vibration, 127(2):221–229, 1988

[12] O. A. Bauchau, G. Damilano, and N. J. Theron. *Numerical integration of nonlinear elastic multi-body systems.* International Journal for Numerical Methods in Engineering, 38:2727-2751, 1995.

[13] J. V. Ferreira. *Dynamic response analysis of structures with non-linear components*. PhD thesis, Imperial College London, Department of Mechanical Engineering, Dynamics Section, 1998.

[14] J. H. Taylor. *Describing functions.* In Electrical Engineering Encyclopedia. John Wiley& Sons, New York, 1999.

[15] B. Van der Pol. *Forced oscillations in a circuit with non-linear resistance.* The London, Edinburgh, and Dublin Philosophical Magazine and Journal of Science, 3:65–80, 1927.

[16] N. N. Bogoliubov and J. A. Mitropolsky. *Asymptotic Methods in the Theory of Non-Linear Oscillations.* Hindustan Publishing Company, 1963.

[17] K. Watanabe and H. Sato. *A modal analysis approach to nonlinear multi-degrres-of-freedom system.* ASME Journal of Vibrations, Stress, and Reliability in Design, 110:410-411, 1988.

[18] E. Budak and H. N. Özgüven. *Iterative receptance method for determining harmonic response of structures with symmetrical non-linearities.* Mechanical Systems and Signal Processing, 7:75–87, 1993.

[19] O. Tanrıkulu, B. Kuran, H. N. Özgüven, M. Imregün. *Forced Harmonic Response Analysis of Non-linear Structures Using Describing Functions.* AIAA Journal, Vol. 31(7), 1313-1320, 1993.

[20] B. Kuran and H. N. Özgüven. *A modal superposition method for non-linear structures*. Journal of Sound and Vibration, 189(3):315–339, 1996.

[21] E. Cigeroglu, H. N. Özgüven. *Nonlinear vibration analysis of bladed disks with dry friction dampers.* Journal of Sound and Vibration 295:1028–1043, 2006.

[22] P. Čermelj, M. Boltežar. *Modeling localised nonlinearities using the harmonic nonlinear super model*. Journal of Sound and Vibration, 289:1099-1112, 2006.

[23] H. R. E. Siller, M. Imregun. *An explicit frequency response function formulation for multi-degree-of-freedom non-linear systems*. Mechanical Systems and Signal Processing,20:1867–1882, 2006.

[24] J. V. Ferreira, A. L. Serpa. *Application of the arc-length method in nonlinear frequency response.* Journal of Sound and Vibration 284:133–149, 2005.

[25] R. Maliha, C. U. Dogruer, H. N. Özgüven. *Nonlinear Dynamic Modeling of Gear-Shaft-Disk-Bearing Systems Using Finite Elements and Describing Functions.* Journal of Mechanical Design 126(3):534–541, 2004.

[26] M. B. Ozer, H. N. Özgüven, T. J. Royston. *Identification of structural non-linearities using describing functions and the Sherman–Morrison method.* Mechanical Systems and Signal Processing, 23:30–44, 2007.

[27] P. W. J. M. Nuij, O. H. Bosgra, M. Steinbuch. *Higher-order sinusoidal input describing functions for the analysis of non-linear systems with harmonic responses.* Mech Sys Signal Process 20(8):1883–1904, 2006.

[28] M. Ö. Aydoğan. *Damage detection in dtructures using vibration measurements*. MS thesis, Middle East Technical University Ankara, Department of Mechanical Engineering, Natural and Applied Science, 2003.

[29] R. Majed, J. L. Raynaud. *Analysis of a non-linear structure by considering two non-linear formulations.* Journal of Sound and Vibration 260:847–866, 2003.

[30] F. B. M. Duarte, J. T. Machado. *Describing function of a simple mechanical system with non-linear friction.* ENOC-2008, Saint Petersburg, Russia, June, 30–July, 4 2008

[31] P. A. Atkins, J. R. Wright, K. Worden. *An extension of force appropriation to the identification of non-linear multi-degree of freedom systems.* Journal of Sound and Vibration 237(1): 23–43, 2000

[32] T. C. Kim, T. E. Rook, R. Singh. *Super- and sub-harmonic response calculations for a torsional system with clearance nonlinearity using the harmonic balance method.* Journal of Sound and Vibration 281:965–993, 2005.

[33] S. Kawamura, T. Naito, H. M. Zahid, H. Minamoto. *Analysis of nonlinear steady state vibration of a multi-degree-of-freedom system using component mode synthesis method.* Applied Acoustics 69:624–633, 2008.

[34] C. Duan, R. Singh. *Super-harmonics in a torsional system with dry friction path subject to harmonic excitation under a mean torque*. Journal of Sound and Vibration 285:803–834, 2005.

[35] G. Gloth, M. Sinapius. *Influence and characterisation of weak non-linearities in swept-sine modal testing.* Aerospace Science and Technology 8:111–120, 2004.

[36] K. Y. Sanliturk, D. J. Ewins. *Modelling two-dimensional friction contact and its application using harmonic balance method.* Journal of Sound and Vibration 193(2):511–523, 1995.

[37] S. K. Lai, Y. Xiang, C.W. Lim, X. F. He, Q. C. Zeng. *Higher-order approximate solutions for nonlinear vibration of a constant-tension string.* Journal of Sound and Vibration 317:440–448, 2008.

[38] N. Pugno, C. Surace. *Evaluation of the non-linear dynamic response to harmonic excitation of a beam with several breathing cracks*. Journal of Sound and Vibration 235(5):749–762, 2000.

[39] M. Thothadri, R. A. Casas, F. C. Moon, R. D'Andrea, C. R. Johnson, jr. *Nonlinear System Identification of Multi-Degree-of-Freedom Systems.* Nonlinear Dynamics 32: 307–322, 2003.

[40] D. Göge, M. Sinapius, Ufüllekrug, M. Link. *Detection and description of non-linear phenomena in experimental modal analysis via linearity plots.* International Journal of Non-Linear Mechanics 40: 27 – 48, 2005.

[41] Z. K. Peng, Z. Q. Lang, S. A. Billings. *Non-linear output frequency response functions of MDOF systems with multiple non-linear components* International Journal of Non-Linear Mechanics 42: 941 – 958, 2007.

[42] P. Marzocca, J. M. Nichols, A. Milanese, M. Seaver, S. T. Trickey. *Second-order spectra for quadratic nonlinear systems by Volterra functional series: Analytical description and numerical simulation.* Mechanical Systems and Signal Processing 22: 1882–1895, 2008.

[43] D. Mirri, G. Iuculano , P. A. Traverso, G. Pasini, F. Filicori. *Non-linear dynamic system modelling based on modified Volterra series approaches.* Measurement 33: 9–21, 2003

[44] A. Chatterjee, N. S. Vyas. *Non-linear parameter estimation with Volterra series using the method of recursive iteration through harmonic probing*. Journal of Sound and Vibration 268:657–678, 2003.

[45] A. Chatterjee, N. S. Vyas. *Non-linear parameter estimation in multi-degree-of-freedom systems using multi-input Volterra series.* Mechanical Systems and Signal Processing 18:457–489, 2004.

[46] R. Ying. *The analysis and identification of friction joint parameters in the dynamic response of structures.* PhD thesis, Imperial College London, Department of Mechanical Engineering, 1992.

[47] C. J. Hartwigsen. *Dynamics of jointed beam structures: Computational and experimental studies.* Master Thesis, University of Illinois at Urbana-Champaign, Department of Mechanical Engineering, 2002.

[48] D. J. Segalman. *An initial overview of Iwan Modeling for mechanical joints.* Technical Documentary Report No. SAND2001-0811, Sandia National Laboratories, Albuquerque-New Mexico and Livermore-California, 2001.

[49] H. Ouyang, M. J. Oldfield, J. E. Mottershead. *Experimental and theoretical studies of a bolted joint excited by a torsional dynamic load*. International Journal of Mechanical Sciences 48:1447–1455, 2006.

[50] H. Ahmadian, H. Jalali. *Identification of bolted lap joints parameters in assembled structures.* Mechanical Systems and Signal Processing 21:1041–1050, 2007.

[51] D. J. Segalman. *Modelling joint friction in structural dynamics.* Structural control and health monitoring 13:430–453, 2006.

[52] H. Ouyang, M. J. Oldfield, J. E. Mottershead. *Simplified models of bolted joints under harmonic loading.* Computers and Structures 84:25–33, 2005.

[53] Ö. Arslan. *Modal identification of nonlinear substructures and implementation in structural coupling analysis.* MS thesis, Middle East Technical University Ankara, Department of Mechanical Engineering, Natural and Applied Science, 2008.

[54] R. S. Barbosa and J. A. Tenreiro Machado. *Describing Function Analysis of Systems with Impacts and Backlash.* Nonlinear Dynamics 29: 235–250, 2002.

[55] Ying-Jeh Huang and Yuan-Jaywang. *Steady-State Analysis for a Class of Sliding Mode Controlled Systems Using Describing Function Method.* Nonlinear Dynamics 30: 223–241, 2002.

[56] J. G. Graver. *Underwater gliders: dynamics, control and design*. PhD thesis, Princeton University, Department of Mechanical and Aerospace Engineering, 2005.

[57] A. Narimani, M. F. Golnaraghi, G. N. Jazar. *Frequency response of a piecewise linear vibration absorber.* Journal of Vibration and Control 10:1775–1794, 2004.

[58] C. Duan, R. Singh. *Dynamic analysis of preload nonlinearity in a mechanical oscillator.* Journal of Sound and Vibration 301:963–978, 2007.

[59] A. Gelb, W. E. Van der Velde, *Multiple-input Describing Functions and Nonlinear System Design*, McGraw-Hill, New York, 1968.

[60] J. A. de Marchi. *Modeling of dynamic friction, impact backlash and elastic compliance nonlinearities in machine tools, with applications to asymmetric viscous*

and kinetic friction identification. PhD thesis, Rensselær Polytechnic Institute, Department of Mechanical Engineering, 1998.

[61] H. N. Özgüven. *A new method for hamonic response of non-proportionally damped structures using undamped modal data.* Journal of Sound and Vibration 117: 313 - 328, 1987.

[62] G. Orbay. *Nonlinear vibration of mistuned bladed disk assemblies*. MS thesis, Middle East Technical University Ankara, Department of Mechanical Engineering, Natural and Applied Science, 2008.

[63] B. Kuran. *Dynamic Analysis of harmonically excited non-linear structures by using iterative modal method*. MS thesis, Middle East Technical University Ankara, Department of Mechanical Engineering, Natural and Applied Science, 1992.

[64] MATLAB R2007b Help Manual.

[65] ANSYS Classic 11.0 Help Manual

[66] J. Baker. *A method for obtaining the stiffness matrix and load vector from ANSYS.* www.engr.uky.edu/~jrbake01/ANSYS-Stiffness_Matrix-v8p1.pdf, 11/21/08. (Last visiting date: 15/03/2009)

APPENDIX A

USER MANUEL OF THE PROGRAM: MH-NLS

A.1 Layout of the Program

The Figure 1 shows the typical layout of the program when the program is executed.

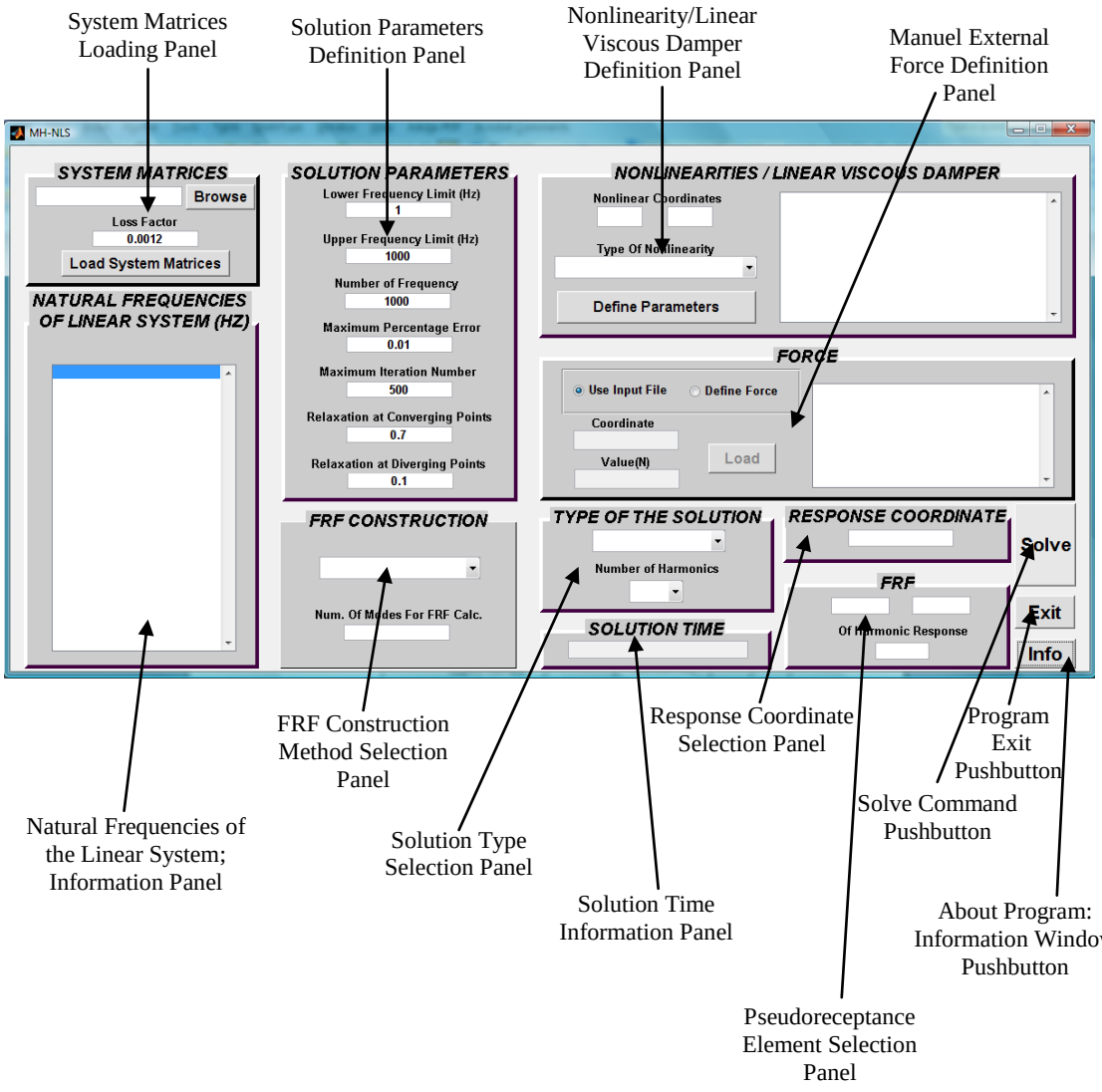

Figure A.1 Layout of the program

A.2 Loading of the System File

After making the substructuring analysis explained in Appendix B, in ANSYS® to the system to be analyzed, change the format of the output file to text file which is created by ANSYS®. This can simply be done by adding an extension of ".txt" to the file (Figure 2).

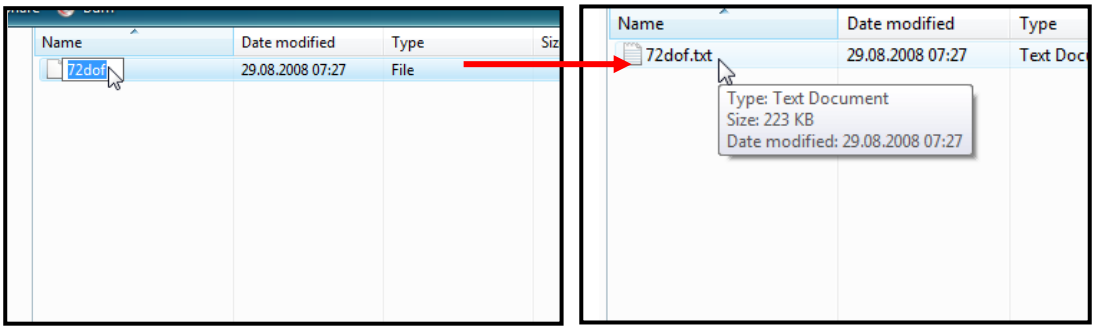

Figure A.2 Changing the extension of the file

After executing the program, first browse for that file (Figure A.3), by the system matrices loading panel introduced in Figure A.1.

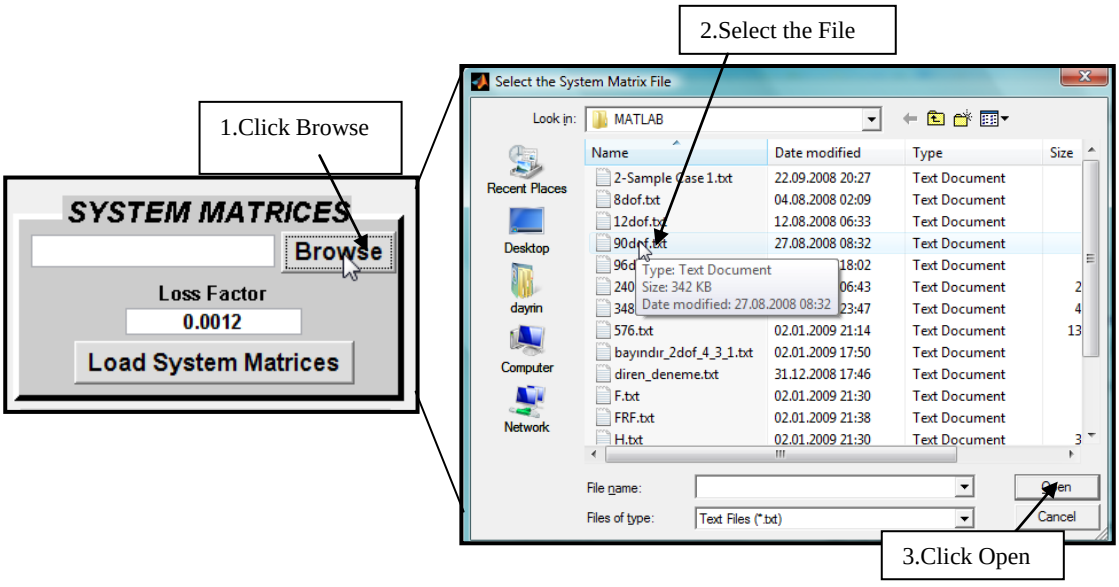

Figure A.3 Selecting the ANSYS® output file

After selecting the file and before loading operation, enter the loss factor if proportional structural damping exists in the structure. If not, enter 0. Then load the file (Figure A.4).

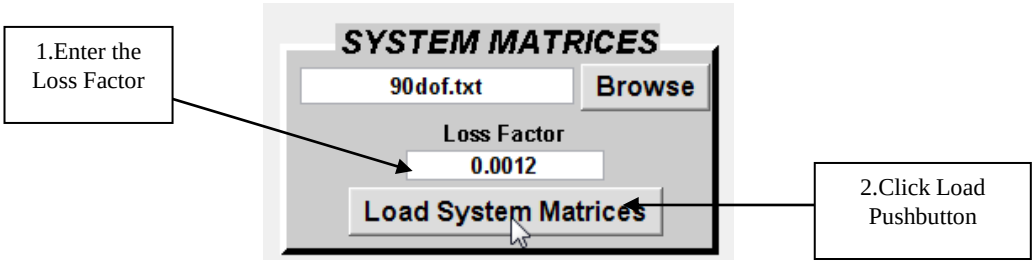

Figure A.4 Loading the system matrices

The program creates a prompt called “system matrices loading status” after loading operation finishes. After clicking “OK” , the linear undamped natural frequencies of the system are printed in the natural frequencies information panel (Figure A.5).

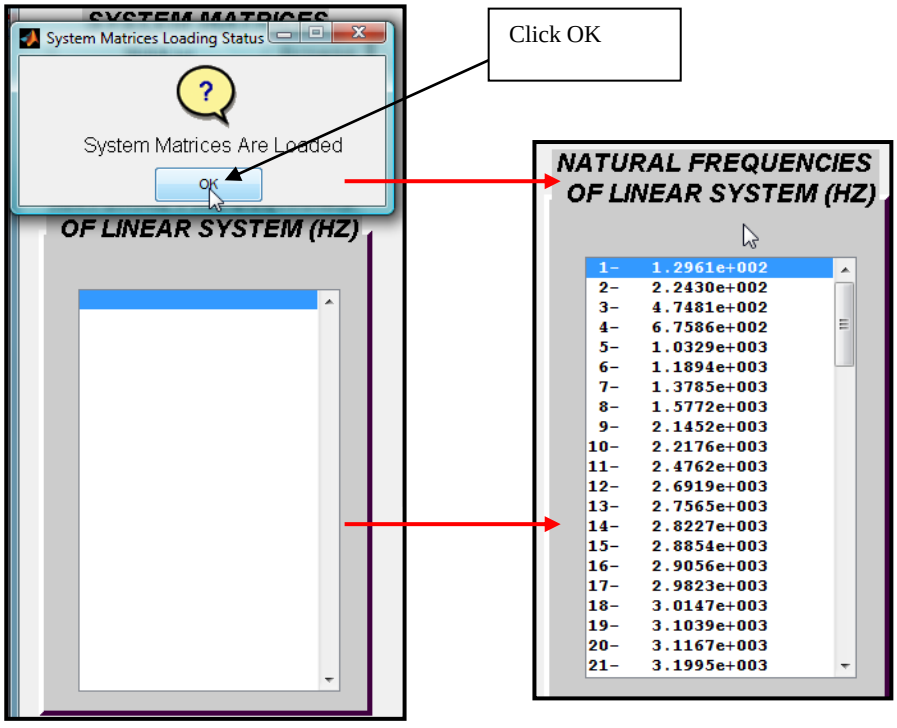

Figure A.5 System matrices loading status prompt, and linear natural frequency information panel

Later, enter the solution parameters (Figure A.6). Program uses some default values for the analysis. Change them if necessary (however, unless necessary avoid changing the relaxation coefficients and percentage error).

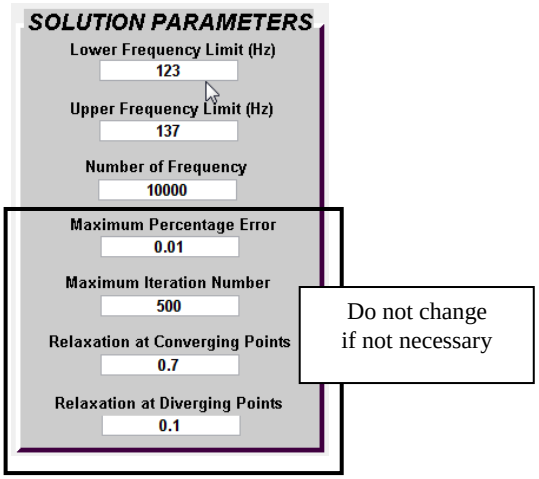

Figure A.6 Solution parameters definition panel

Select FRF matrix construction method. If user selects modal summation method, than he/she must define the number of modes for FRF construction. If the number is greater than the degree of freedom, program will give a warning message when solution button is clicked (Figure A.7).

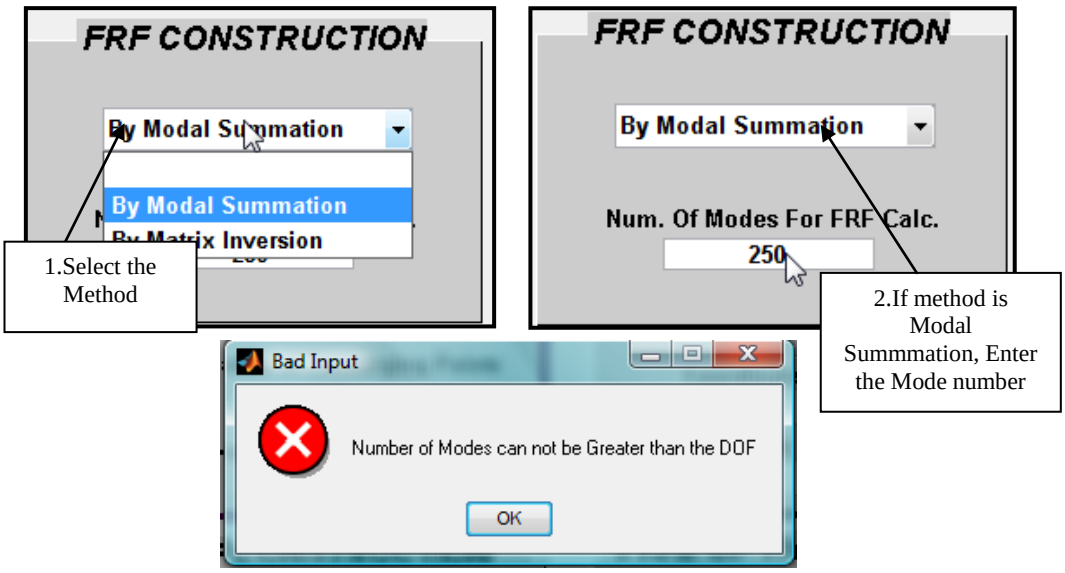

Figure A.7 The FRF construction method selection operation and warning message

Define Nonlinearities/Linear viscous dampers between coordinates. If nonlinearity exists between a coordinate and the ground, enter the same coordinate number. When "define nonlinearity" button is clicked, an input window for the corresponding nonlinearity will be opened (Figure A.8).

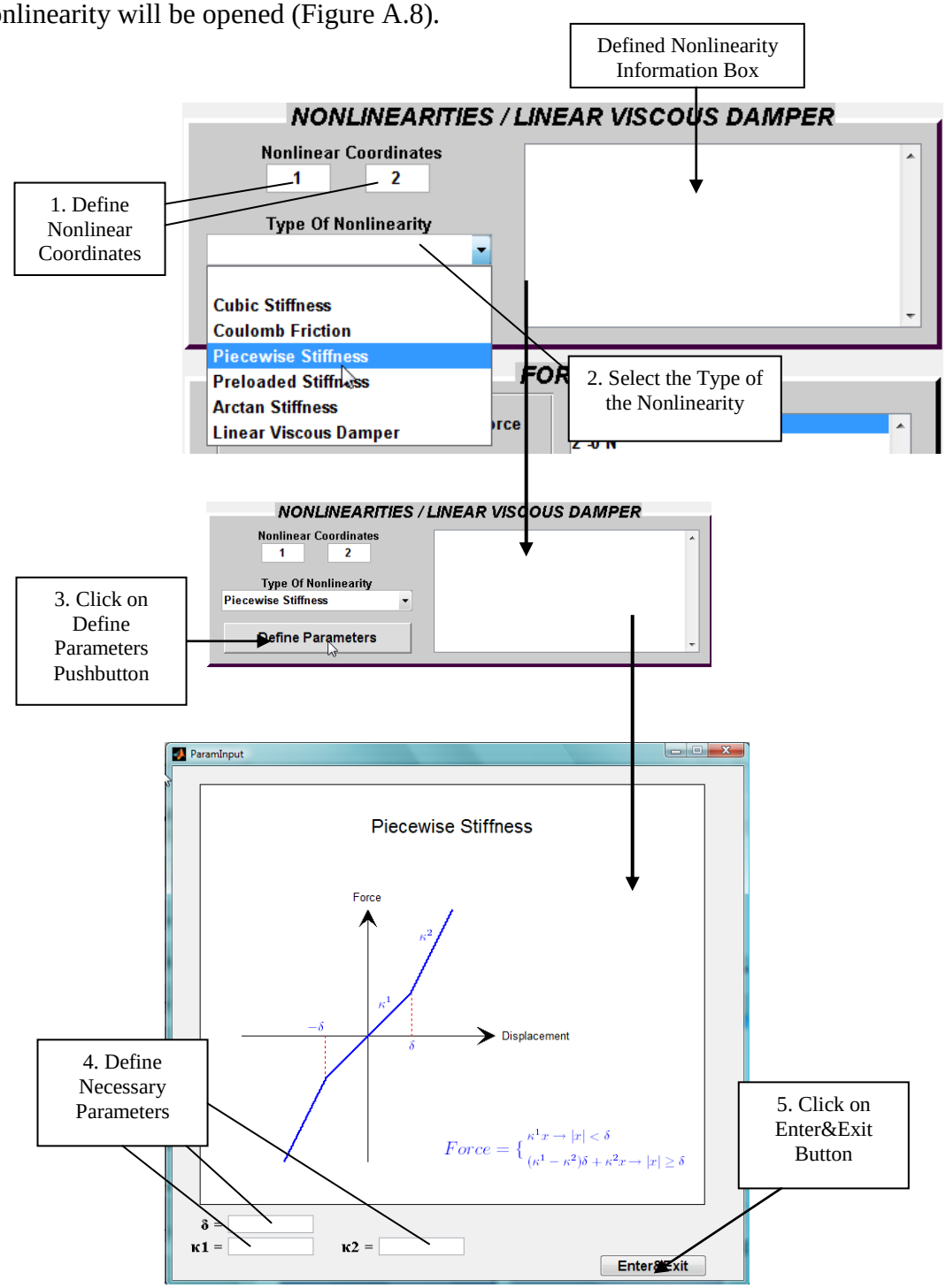

Figure A.8 Defining nonlinearities

The defined nonlinearity can be discareded by simply selecting the corresponding nonlinearity in the nonlinearity information box and after that pressing the “Del” button.

Then, specify the external forcing. User can use the data file which may also contain the external excitation information, or can manually define new external forcing. When input file is selected, the editting boxes will inactive. They will become active when “define force” selection box is selected (Figure A.9).

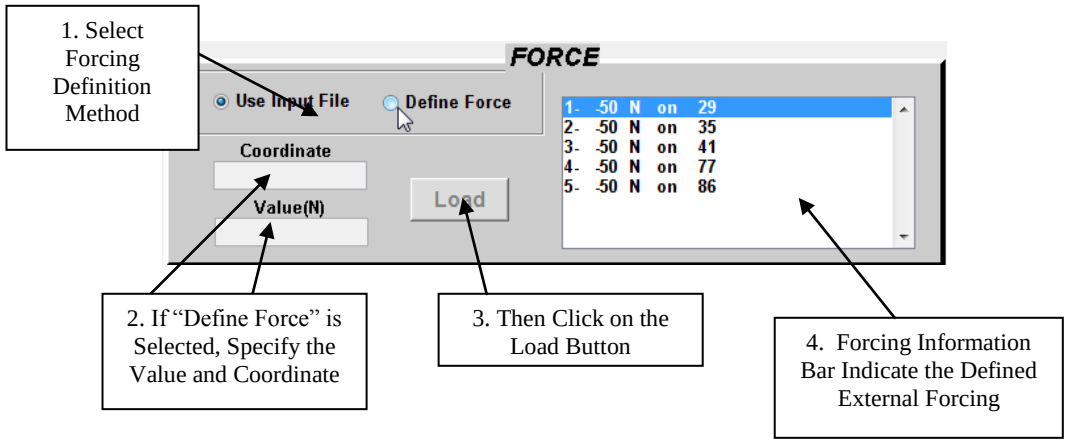

Figure A.8 External forcing definition

Later on, user must specify the type of the solution by the solution type selection panel (Figure A.9).

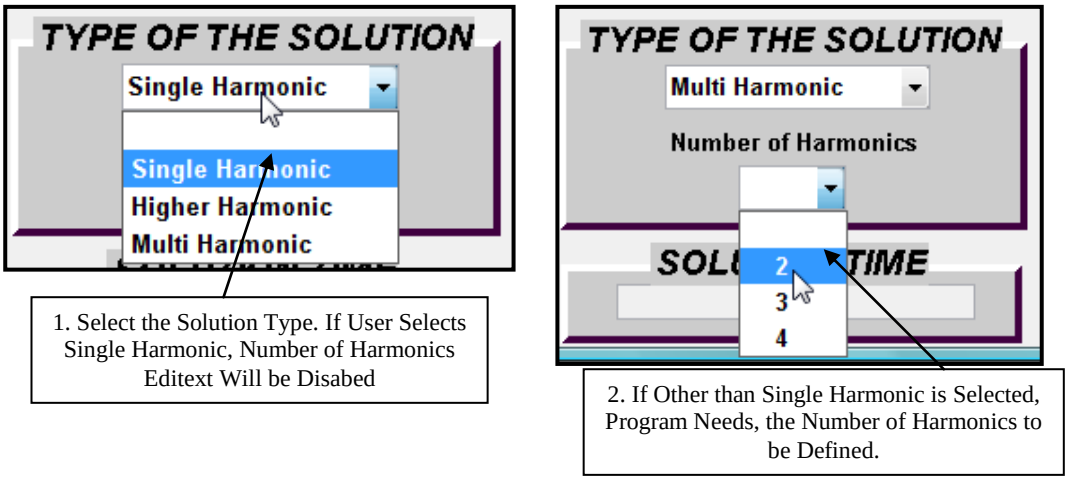

Figure A.9 Solution type selection

The final preprocessing stage is the definition of the response and FRF coordinates to be plotted, which are the main outputs of the program (Figure A.10).

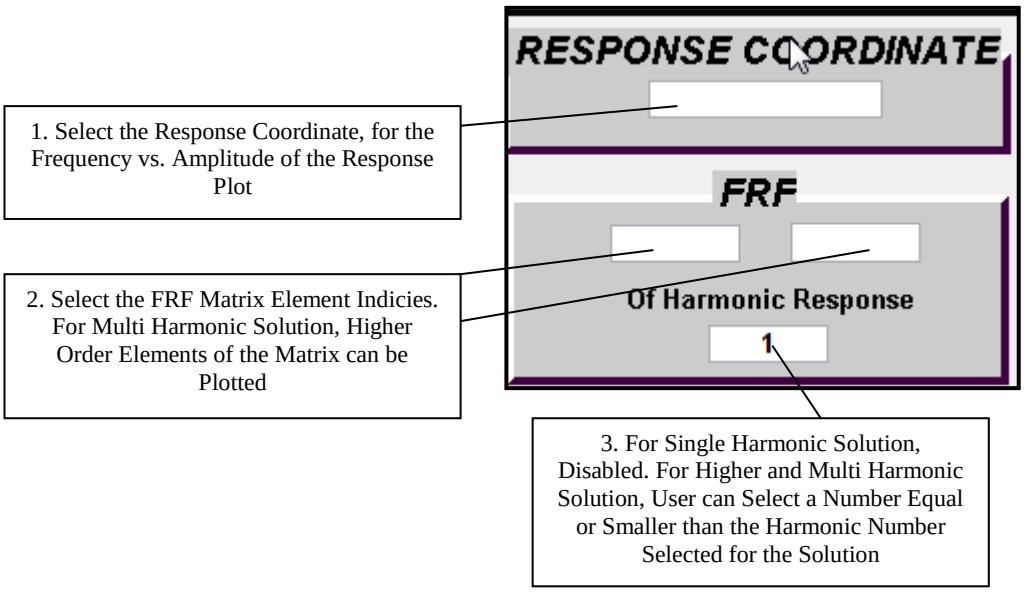

Figure A.10 Response coordinate and FRF matrix indicies selection

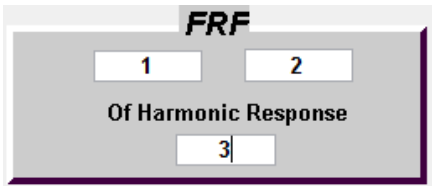

For example, if user inputs the above numbers to the pseudoreceptance element selection panel , the program will evaluate the θ_{12} element of the θ_{33} submatrix of the pseudoreceptance matrix.

$$\theta = \begin{pmatrix} \theta_{11} & \theta_{12} & \cdots & \theta_{1m} \\ \theta_{21} & \theta_{22} & \cdots & \theta_{2m} \\ \vdots & \vdots & \ddots & \vdots \\ \theta_{m1} & \theta_{m2} & \cdots & \theta_{mm} \end{pmatrix}^{-1}$$

m: number of harmonics

Now user can click on the solution button. Results will be created as plots and output files. The solution time will be printed in the program window. User can exit the program after the process is completed (Figure A.11).

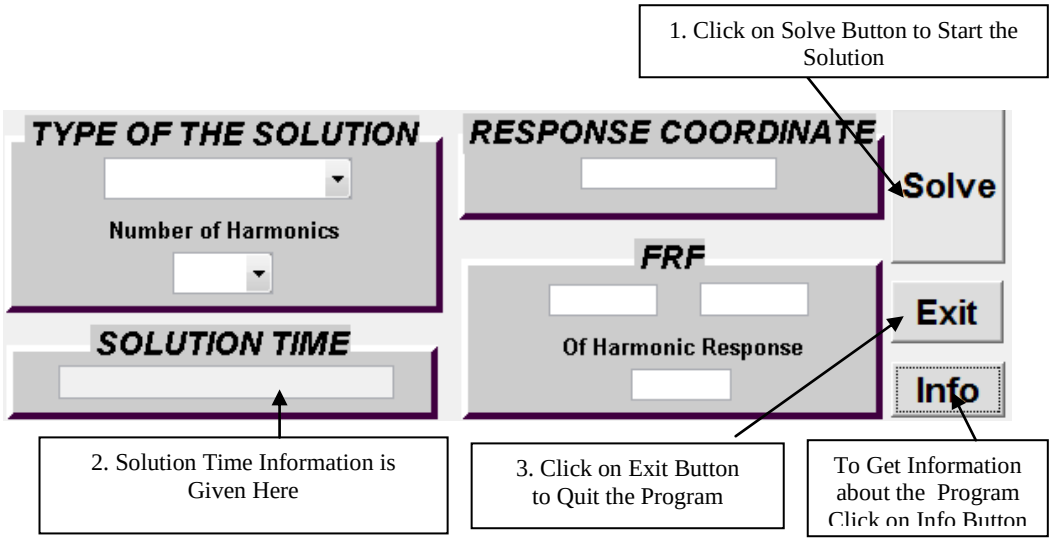

Figure A.11 Solve, exit and info buttons

APPENDIX B

OBTAINING A LISTING OF THE STIFFNESS and MASS MATRIX / LOAD VECTOR FROM ANSYS®, VERSION 11

In order to obtain a listing of the stiffness, mass matrix and forcing vector from an ANSYS model, use the "Substructuring" option in the solution processor, and solve it. The GUI and command line options are given seperately.

GUI Option [66]:

1. Create the model, including all required real constants, material properties, constraints, and applied loads.
2. Enter the solution processor. On the ANSYS Main Menu, select "Solution".
3. On the "Solution" menu, select "Analysis Type", then "New Analysis".
4. On the "New Analysis" menu, select "Substructuring/CMS", and click "OK".
5. On the "Solution" menu, under "Analysis Type", select "Analysis Options".
6. On the box that opens, verify that "Substructuring" is selected, then click "OK".
7. On the "Substructuring Analysis" menu, there is a "SEMATR Matrices to be generated" option. For this option, select "Stiffness+Mass".
8. On the same menu, there is a "SEPR Items to be printed" option. For this option, select "LoadVect+Matrix", then click "OK".
9. On the same menu, there is a "[LUMPM] Use lumped mass approx?" option. For this option, select "Yes" option.

10. Select master degrees of freedom. Assuming you wish to include all unconstrained degrees of freedom in your printed matrices, then select all dof in the model as master dof. To do this, at the ANSYS command prompt, type the command: m,all,all
11. Direct the ANSYS output to an output file. At the ANSYS command prompt, type the command: /output,filename (where filename is any name the user chooses).
12. Solve. On the "Solutions" menu, under the "Solve" heading, select "Current LS", then click "OK". Upon solving, you may get warnings, such as: Node 2 UY master is superseded by a specified constraint. This is simply because some of the master dof selected were constrained to zero displacement. These warnings are not a problem.
13. Redirect the ANSYS output back to the output window. At the ANSYS command prompt, type: /output

Command Line Option:

First, create the model, including all required real constants, meshes, material properties, constraints, and applied loads. Then, enter the commands below at the ANSYS command line.

```
/SOL
ANTYPE,7
SEOPT,sfgf2,2,1,0,0
LUMPM,1
EQSLV,FRONT
SEGEN,OFF
M,ALL,ALL
/OUTPUT, filename                    (where filename is defined by the user)
```

SOLVE
/OUTPUT

“After the above steps, whether the GUI option or command line option is used, an ASCII text file will be stored under the filename chosen (see Step 11 of the GUI Option instructions) in your ANSYS working directory. This file will contain the load vector and stiffness matrix listing. It can be viewed with any text editor, such as Notepad, or any word processing program, such as Microsoft Word. The listing may be preceded by other information, so you may have to scroll through the file some to find it. Using Notepad, if desired, this information can be cut and pasted into another file” [66].

APPENDIX C

AN EXAMPLE OUTPUT FILE CREATED BY ANSYS®

***** ANSYS SOLVE COMMAND *****

TRANSFER SOLID MODEL BOUNDARY CONDITIONS TO FINITE ELEMENT MODEL

CONSTRAINTS TRANSFERRED FROM LINES = 4

*** NOTE *** CP = 12.719 TIME= 16:19:22

There is no title defined for this analysis.

S O L U T I O N O P T I O N S

PROBLEM DIMENSIONALITY. 2-D
DEGREES OF FREEDOM. . . . . UX UY
ANALYSIS TYPE . . . . . .SUBSTRUCTURE
SUPERELEMENT FILE NAME 2d
LUMPED MASS MATRICES. . . . . .ON
MATRICES TO GENERATE. . . . . .K AND M
SUPERELEMENT PRINT OPTIONS. . . . . .PRINT ALL
STRESS STIFFNESS MATRIX SPACE KEY . . . . . .OFF
NUMBER OF MASTER DOF. 12
GLOBALLY ASSEMBLED MATRIX . . . . . .SYMMETRIC

L O A D S T E P O P T I O N S

LOAD STEP NUMBER. 1

**** CENTER OF MASS, MASS, AND MASS MOMENTS OF INERTIA ****

CALCULATIONS ASSUME ELEMENT MASS AT ELEMENT CENTROID

TOTAL MASS = 54.000

CENTER OF MASS	MOM. OF INERTIA ABOUT ORIGIN	MOM. OF INERTIA ABOUT CENTER OF MASS
XC = 0.10000	IXX = 0.1350	IXX = 0.000
YC = 0.50000E-01	IYY = 0.6750	IYY = 0.1350
ZC = 0.0000	IZZ = 0.8100	IZZ = 0.1350
	IXY = -0.2700	IXY = 0.000
	IYZ = 0.000	IYZ = 0.000
	IZX = 0.000	IZX = 0.000

*** MASS SUMMARY BY ELEMENT TYPE ***

TYPE	MASS
1	54.0000

Range of element maximum matrix coefficients in global coordinates
Maximum= 3.144791667E-08 at element 2.
Minimum= 3.144791667E-08 at element 2.

*** ELEMENT MATRIX FORMULATION TIMES

TYPE	NUMBER	ENAME	TOTAL CP	AVE CP
1	2	PLANE42	0.000	0.000000

Time at end of element matrix formulation CP= 12.734375.

*** WARNING *** CP = 12.734 TIME= 16:19:22

Node 1 UX master is superseded by a specified constraint.

*** WARNING *** CP = 12.734 TIME= 16:19:22
Node 1 UY master is superseded by a specified constraint.

*** WARNING *** CP = 12.734 TIME= 16:19:22
Node 5 UX master is superseded by a specified constraint.
*** WARNING *** CP = 12.734 TIME= 16:19:22
Node 5 UY master is superseded by a specified constraint.

Estimated number of active DOF= 8.
Maximum wavefront= 9.
Number of Master DOF= 12.

Time at end of matrix triangularization CP= 12.734375.
1
***** ANSYS - ENGINEERING ANALYSIS SYSTEM RELEASE 11.0 *****
ANSYS Multiphysics
00265231 VERSION=INTEL NT 16:19:22 AUG 03, 2008 CP= 12.734

***** LOAD VECTOR NUMBER 1 *****

ROW NODE DIR VALUE

1 2 UX 10
2 3 UX 0.000000

***** STIFFNESS MATRIX *****

ROW 1 NODE 2 DEG. OF. FR. = UX

1 1000 2-500

```
 ROW   2   NODE     2     DEG. OF. FR. =  UY

  1-500     2 1000

   ***** MASS MATRIX *****

 ROW   1   NODE     2     DEG. OF. FR. =  UX

  1 1    2 0.00000000E+00

 ROW   2   NODE     2     DEG. OF. FR. =  UY

  1 0.00000000E+00    2 5

*** NOTE ***                        CP =      12.734   TIME= 16:19:22
Solution is done!

  *** PROBLEM STATISTICS
 ACTUAL NO. OF ACTIVE DEGREES OF FREEDOM =      1
 R.M.S. WAVEFRONT SIZE =     0.0
 NUMBER OF MASTER DEGREES OF FREEDOM =     8
*** ANSYS BINARY FILE STATISTICS
 BUFFER SIZE USED= 16384
       0.063 MB WRITTEN ON TRIANGULARIZED MATRIX FILE: file.tri
       0.063 MB WRITTEN ON SUBSTRUCTURE MATRIX FILE: 2d.sub
```

APPENDIX D

CODE FOR LOADING SYSTEM MATRICES FROM THE FILE CREATED BY ANSYS®

```
function [F,M,K,N]=Read_Ansys(Filename)

HFile=fopen(Filename,'r');

   Str=fscanf(HFile,'%c');

   fclose(HFile);

   T1Start=strfind(Str,'  ROW    NODE    DIR      VALUE')+...
      length('  ROW    NODE    DIR      VALUE');

   T1End=strfind(Str,'     ***** STIFFNESS MATRIX *****');

   T1=textscan(Str(T1Start:T1End),'%f %f %s %f');

   T1{3}=char(T1{3});

   T1{3}(T1{3}=='U')=[];

   T1{3}=T1{3}';

   F=T1{4};

   N=length(T1{1});

   N2=N^2;

   T2Start=T1End+length('     ***** STIFFNESS MATRIX *****')+2;

   T2End=strfind(Str,' Solution is done!')-2-...
      length(' *** NOTE ***                    CP =       5.312   TIME= 21:43:06');

   Headers=strfind(Str(T2Start:T2End),'   ROW')-1+T2Start;
```

```
    L=length('   ROW 240   NODE    96     DEG. OF. FR. =  UZ  ');

    I=repmat(Headers,[L,1])+repmat((0:L-1)',[1,length(Headers)]);

    Str(I)=' ';

    Str=strrep(strrep(strrep(strrep(Str(T2Start:T2End),'E-','QQQ'),'-',' -'),'QQQ','E-'),...
       '***** MASS MATRIX *****','                    ');

    T2=textscan(Str,'%f %f');

    M=reshape(T2{2}(N2+1:2*N2)',[N,N]);

    K=reshape(T2{2}(1:N2)',[N,N]);

    Data=struct('Node',T1{2},'Dir',T1{3},'Force',F,'Stiff',K,'Mass',M);
FF=fopen('F.txt','w');

KK=fopen('K.txt','w');

MM=fopen('M.txt','w');

fprintf(FF,['%0.4e',repmat('\t%0.4e',[1,size(F,2)-1]),'\r\n'],F');

fprintf(KK,['%0.4e',repmat('\t%0.4e',[1,size(K,2)-1]),'\r\n'],K');

fprintf(MM,['%0.4e',repmat('\t%0.4e',[1,size(M,2)-1]),'\r\n'],M');

fclose(FF);

fclose(KK);

fclose(MM);
```